EVALUATION OF SEISMIC DESIGN CRITERIA FOR ROCKING OBJECTS IN NUCLEAR FACILITIES

EVALUATION OF SEISMIC DESIGN CRITERIA FOR ROCKING OBJECTS IN NUCLEAR FACILITIES

By

AMITABH DAR, **P.Eng.**

B.Eng., M.M.S. (Birla Institute of Technology and Science, Pilani, India)
SCE, MEERI, MCSCE

A Thesis Submitted to the School of Graduate Studies in Partial Fulfillment of the Requirements for the Degree of Master of Applied Science

McMaster University

McMaster University MASTER OF APPLIED SCIENCE (2014) Hamilton, Ontario (Civil Engineering)

Title: Evaluation of seismic design criteria for rocking objects in nuclear facilities

AUTHOR: Amitabh Dar, B. Eng. (Hons), MMS, P.Eng. MEERI, MCSCE

SUPERVISORS: Dr Wael W. El-Dakhakhni and Dr Dimitrios Konstantinidis

NUMBER OF PAGES: xii, 107

ABSTRACT

Seismic response of free standing un-anchored objects is required to be studied in Nuclear Power Plants (NPPs) for their own integrity and potential interaction with the surrounding seismically qualified safety systems. Rocking response of a rigid body subject to seismic excitation is not very well covered in the nuclear standards except for an approximate method given in ASCE 43-05 where the design basis earthquake (DBE) response spectrum for the NPPs given in the United States Nuclear Regulatory Commission (USNRC) regulatory guide 1.60 (known as NBK spectrum developed by Newmark, Blume and Kapur (1973)) is considered as seismic input. This study evaluates existing seismic design criteria for unanchored objects that are vulnerable to rocking and overturning inside nuclear power plants. The original work of Newmark et al (1973) is revisited in order to obtain the NBK spectra at unusual damping (8.4% for example), required in order to follow the ASCE 43-05 method. Eight earthquake records are selected from Newmark et al (1973) with varying Peak Ground Accelerations (PGAs) representing strong to moderate ground motions. Rocking response of rigid bodies to various earthquakes is determined by three methods: 1. The ASCE 43-05 method utilizing the NBK spectrum, 2. The ASCE 43-05 method utilizing the response spectrum of the earthquake records, and 3. solving the equations of motion of a rigid body for the earthquake records. Rocking spectra by these three methods created for eight earthquake records are compared with one another. It is concluded that the ASCE 43-05 method provides inaccurate predictions of the response. Considering the significant level of effort required to implement the ASCE 43-05 method, its inherent contradictions, and its inconsistent conservatism in estimating the seismic demands on rocking objects, it is concluded that the results obtained by nonlinear time history analysis are more accurate, reliable and less time consuming than those by the ASCE 43-05 method. The use of nonlinear dynamic analysis is recommended to obtain the pure planar rocking response of unanchored objects in nuclear facilities.

ACKNOWLEDGEMENTS

It has been a great experience to get back to academics, starting my master's program in 2009, after 25 years of completing my undergraduate degree in civil engineering. This was possible only due to the encouragement from my supervisors Dr Wael El-Dakhakhni and Dr Dimitrios Konstantinidis whose constant support made it possible for me to complete seven half-courses and four quarter courses, and write ten conference papers during the past five years. I sincerely thank both of them. I am also thankful to all the professors with whom I completed my courses. Education at McMaster University has been a great experience.

Thanks are due to Bruce Power, for supporting my education program at McMaster University. I sincerely acknowledge the constant inspiration by my colleague Jim Hanna and invaluable support from Section Manager Rob Dunn. I am indebted to Cathy Sprague, Executive Vice President (Human Resources), Gary Newman, Chief Engineer and Senior Vice President (Engineering), and Gord Kozak, Divisional Manager, Plant Design, Bruce Power for their approval of my education program.

I sincerely appreciate the support, love and affection from my wife Anuradha and thank her for the lost weekends, taking care of the home and family and her patience on my challenges in completing several honey-do lists. I am also thankful to my daughters Apoorva and Arpita for being proud of their dad whose education was concurrent with their own. I dedicate this thesis to my late parents, both of whom had careers in the field of education.

Table of Contents

FIGURES

TABLES

LIST OF ABBREVIATIONS AND ACRONYMS

BDB	Beyond Design Basis
CNSC	Canadian Nuclear Safety Commission
DBE	Design Basis Earthquake
EPRI	Electric Power Research Institute
NBK	Newmark, Blume and Kapur
NLTH	Non-Linear Time History Analysis
NPP	Nuclear Power Plant
PGA	Peak Ground Acceleration
PSA	Peak Spectral Acceleration
RB	Rigid Body
RM	Rocking Motion
SDOF	Single Degree of Freedom
SMA	Seismic Margin Assessment
SPRA	Seismic Probabilistic Risk Assessment
SSC	Structures, Systems and Components
URM	Unreinforced Masonry
USNRC	United States Nuclear Regulatory Commission

LIST OF SYMBOLS

a_{eq}	Equivalent acceleration of SDOF oscillator
a_r	Acceleration required to cause uplift
b	Half-width of the rectangular rocking block
f_{eq}	Equivalent frequency of SDOF oscillator
g	Gravitational acceleration
h	Half-height of the rectangular rocking block
I_o	Moment of inertia of rocking block about its pivot
m	Mass of rectangular rigid block
p	Frequency parameter of a rigid rectangular block $= \sqrt{\frac{3g}{4R}}$
PGA_{CAP}	Peak ground acceleration capacity
R	$\sqrt{(b^2 + h^2)}$
SAH	Horizontal spectral acceleration
SAH_{CAP}	Horizontal spectral acceleration capacity
SAV	Vertical spectral acceleration
SAH_{DEM}	Horizontal demand spectral acceleration
T_H	Housner's period of a rigid rectangular block
$\ddot{x}$	Horizontal Ground acceleration or base acceleration
$\ddot{y}$	Vertical Ground acceleration or base acceleration
α	Angle between the diagonal and vertical side of rectangular rigid block, "stockiness"
β	Damping as percentage of critical damping
γ	Damping exponent
θ	Angle of rotation of rigid block in rocking motion
θ_o	Maximum angle of rotation of rigid block in rocking motion
θ_{om}	Minimum of maximum angle of rotation of rigid block in rocking motion
ω_e	Equivalent angular frequency of a single degree of freedom oscillator

CHAPTER 1 INTRODUCTION

1.1 Introduction

Nuclear Power Plants (NPPs) consist of combinations of many Structures, Systems and Components (SSC) ranging from large concrete containment structures (such as the reactor building, vacuum building, fuel bays, etc.) to the complex mechanical and electrical systems (such as piping, valves, electrical cabinets, fire protection systems, etc.), including small instrumentation and control components (such as pressure transmitters, switches, etc.). Many of these systems and components are parts of *success path*, defined as a set of systems and components essential to bring a reactor to and maintain its safe shut down state up to 72 hours after a seismic event in accordance with the Electric Power Research Institute (EPRI) report NP-6041 (1991). Systems and components on the success path are included in Safe Shut Down Equipment List requiring seismic qualification. Since such systems or components may be located at any floor, at any height from the ground level, in-structure response spectra are required at every floor as well as specific points of interest (e.g., at the top of a crane bracket on the fifth floor of a building) in order to qualify them for a seismic event known as the Design Basis Earthquake (DBE) in Canada and Safe Shut Down Earthquake (SSE) in the United States (Dar et al. 2014). Small instrumentation components (e.g., switches, circuit breakers) installed inside an electrical cabinet anchored to a floor experience much higher accelerations in comparison to the base of the cabinet and

hence the floor response spectrum is amplified three to seven times in order to obtain the test response spectrum for such components (EPRI report NP-6041, 1991). Seismic design, qualification and evaluation of SSC in a NPP are subject to stringent rules and regulations aimed at protecting the public and environment from any radiological release. The safe operation of a NPP depends on the design of various SSCs for the multiple combinations of operational, environmental and other load categories including seismic given in the standard CSA N291 (2008).

The NPPs in Canada are required by the regulator, the Canadian Nuclear Safety Commission (CNSC), to carry out periodic Seismic Probabilistic Risk Assessment (SPRA) studies in accordance with the regulation S-294 (CNSC, 2005). In order to establish seismic risk, it is essential to know the seismic weak links detrimental to nuclear safety. The seismic risk depends on the seismic capacity of various SSCs. Introducing conservatism in design results in redundant capacity. However, incorporating conservatism in risk calculation by lowering the capacity results in higher and hence artificial risk. As a consequence of this artificially amplified risk, financial, technical and other resources of an organization are diverted from high risk components to the low risk ones. In order to know true risk, removal of unnecessary conservatism from capacity calculation is warranted. Since rocking response is often required in risk calculation, it should be studied with minimum conservatism and hence methods of analyses with least conservatism are required to be employed in this regard. In a recent SPRA study (Kinectrics, 2014), fragilities

based on rocking analysis of unanchored transformers have been established based on the prevalent industry practice.

Although most systems and components in a NPP are anchored to the supporting structures, there are many of them, such as monitors, carts, storage bins, etc., which cannot be fastened to the floor because of their frequent movement from one place to the other. Apart from these, there are several other large objects (such

Figure 1-1: Examples of unanchored objects that are vulnerable to rocking and overturning inside a NPP. (Clockwise from top left: idle turbine rotor, vessel in storage, hand cart, dry storage container (fuel cask), scaffold, radiation protection masonry, storage bin. (Photo courtesy: Bruce Power, and Western Used Fuel Dry Storage Facility (Ontario Power Generation), Ontario, Canada)

as turbine rotors, large empty pressure vessels in storage etc.) whose rocking response is required to be evaluated in order to calculate the seismic risk. According to the standard ASCE 43-05 *Seismic Design Criteria for Structures, Systems, and Components in Nuclear Facilities*, anchored components are generally preferred in order to avoid rocking and sliding, but unanchored components are acceptable if

they satisfy the requirements of ASCE 43-05. Examples of some unanchored objects are shown in Figure 1-1, including components such as scaffolds and unreinforced masonry (URM). Although modern standards (e.g., CSA N291, 2008) do not allow any URM inside a NPP in seismically qualified areas, the relatively older plants have existing URM inside the containment (EPRI report NP-6041, 1991). This is typically found in older plants designed almost thirty years ago with limited seismic capability (Dar and Hanna, 2012). Such NPPs were assessed later in accordance with the seismic margin assessment methodology outlined in EPRI report NP-6041 (1991). According to this report, rocking response of unreinforced masonry is required to be evaluated for its seismic interaction with other objects in its neighborhood. URM inside a NPP has been identified as one of the major contributors to seismic risk (Reed and Kennedy, 1994).

Response of unanchored objects to a given ground motion is required to be analyzed in order to seismically qualify them for their own integrity and to prevent their possible interaction with a seismically qualified safety system or component inside a NPP. There have been numerous studies on various aspects of the rocking and sliding response of an unanchored body, as described below. However, there is very limited guidance available in the nuclear industry with regard to the rocking response of a rigid body to a seismic event. The standard ASCE 43-05 *Seismic Design Criteria for Structures, Systems, and Components in Nuclear Facilities* (2005), applicable to NPPs, refers to and recommends a method similar to what is given by Wesley et al. (1980), which is itself based on a reserve energy technique

introduced by Blume (1960), considering a rigid rocking body as an 'equivalent' Single-Degree-of-Freedom (SDOF) oscillator. Canadian nuclear standards do not contain any discussion on rocking (Dar et al. 2013).

1.2 Literature review

The focus of this thesis is on pure planar rocking response of a rigid rectangular block on a rigid foundation.

An unanchored rigid body (RB) subjected to base excitation may rock, slide or slide-rock. Criteria for the initiation of these three modes and response were established by Shenton (1996). The problem of sliding objects has been studied at various levels by Shao and Tung (1999), Choi and Tung (2002), Lopez and Soong (2003), Comerio (2005), Chaudhuri and Hutchinson (2005), Hutchinson and Chaudhuri (2006), Konstantinidis and Makris (2005, 2009, 2010), Konstantinidis and Nikfar (2015), and references reported therein.

The first systematic study of a RB in rocking motion (RM) was carried out by Housner (1963), considering it as an inverted pendulum. Housner (1963) obtained the pure planar rocking response of a RB subject to variety of horizontal base excitations, with small angle approximation, as a combination of hyperbolic functions. Yim et al. (1980) conducted dynamic analyses using simulated ground motions to examine the sensitivity of the rocking and overturning response of a RB to system parameters. Hogan (1989) studied the dynamic response of RB in RM subject to harmonic excitation. Makris and Roussos (2000) obtained the response

of rigid blocks subject to ground motions near the source of an earthquake. The response of a RB in RM subject to cycloidal pulses was obtained by Zhang and Makris (2001). All these studies indicated that the response of a RB in RM (in its linearized form) consists of hyperbolic functions. In contrast, it is well known that the response of a linear SDOF oscillator is governed by trigonometric functions. For this reason, in this thesis, a subtle distinction in terminology is made: the term *oscillation* is used for the response of a SDOF oscillator, whereas the term *vibration* is used for the response of a rocking block.

Despite various studies on RB in RM indicating that its behavior is different from that of a SDOF oscillator, attempts have been made to consider a RB as an equivalent SDOF oscillator. Priestley et al. (1978) developed a method to obtain the displacement of a RB at its center of gravity based on response spectrum assuming that a RB in RM can be represented by an 'equivalent' SDOF oscillator with constant damping whose period depends on the amplitude of rocking. Wesley et al. (1980) also considered the RB in RM as a SDOF oscillator and obtained its response based on a reserve energy technique given by Blume (1960). Such efforts were revisited later in the literature. Makris and Konstantinidis (2003) introduced the concept of a *rocking spectrum* and showed it to be a distinct intensity measure for ground motions. The study concluded that the response of a RB in RM cannot be obtained by using an equivalent SDOF oscillator. The standard ASCE 41-06 (2006) refers to their work, cautioning the design professional against the use of a response-spectrum-based approach. Dar et al. (2013) conducted a preliminary

evaluation of the methodology proposed by Wesley et al. (1980) and pointed out that its predictions are inaccurate.

ASCE 43-05 recommends an approximate method to calculate the response of a rigid body by converting the nonlinear equations of motion of the rocking block into the linear equation of motion of an 'equivalent' SDOF oscillator.

In some of the NPPs, used fuel is stored in large pools of water called fuel bays where it remains for a considerable period of time (around 15 years or more) before being sent to a dry storage facility. Storage of spent fuel in unanchored fuel casks in a dry storage facility is another area of application of rocking principles. Luk et al. (2005) used 3D finite element analysis to evaluate the seismic response of freestanding spent fuel dry cask storage systems. The study provided best-fitted power-law curves for estimating the peak rotation or displacement of a cask as a function of various intensity measures (such as, peak ground velocity or pseudo-acceleration at 1Hz) based on selected earthquake records. However, the results of that study are limited to two specific cask designs and are not amenable to generalized application. Furthermore, the data exhibited substantial scatter, and the fitted curves were in some cases of poor quality. The available literature pertaining to nuclear industry applications of rocking and sliding analysis of unanchored objects, ranging from a simplified energy method to detailed time-history methods, including probabilistic analyses, was surveyed by Jensen and Gurbuz (2011). The study provides an overview of new guidance to be adopted in the next edition of ASCE 4 (*ASCE 4 –Rev. 2 Seismic Analysis of Safety-Related Nuclear Structures:*

Standard and Commentary). According to Jensen and Gurbuz (2011), the approximate method in ASCE 43-05, which is based on a reserve energy technique, will be adopted in ASCE 4 Rev. 2. Therefore, evaluation of this methodology is still very relevant.

Comparison between the rocking criteria and methods adopted in the European (EN 1990 and EN 1998), German (KTA 2201.1 and 2201.4) and US (ASCE 43-05) standards was drawn by Schau and Johannes (2013) assuming that an unanchored rigid rocking object can be represented by an SDOF system with a torsional spring. This study found implicit finite element programs to be suitable to study rocking and sliding problems and expressed doubts about the ASCE 43-05 method. No detailed investigation of rocking response obtained by the ASCE 43-05 method was reported.

Since the standard ASCE-43-05 focuses on the pure planar rocking response of a RB in RM (assuming no sliding, which is dealt with separately in the standard), the rocking response obtained by the method suggested in this standard is compared with the rocking response obtained by numerically solving the equations of motion for various earthquake records.

1.3 Research Objective

The objective of this research is to evaluate the ASCE 43-05 seismic design criteria for rocking objects in NPPs. These design criteria provide an approximate method for estimating the maximum uplift rotation in lieu of numerical integration

of the nonlinear equation of motion of the rocking block. The method leans on the assumption that a rocking block can be represented by an 'equivalent' SDOF oscillator with constant damping, but whose period depends on the amplitude of the rocking. Despite the intention to simplify the problem, the ASCE 43-05 procedure (which is described in detail in Chapter 2) is fairly intricate, which leads to the question whether it is preferable to numerically solving the nonlinear equation of motion of the rocking block—even if it could provide reasonable maximum response estimates.

Obtaining the rocking response of a rigid block, subject to the design ground motion, involves piecewise linearization of nonlinear equation of motion which is much more intricate than the dynamic analysis of a linear SDOF oscillator. In want of an analytical tool without involving the use of an expensive software (for this stand-alone purpose) the designer at a nuclear facility tends to look for simpler solutions such as obtaining the maximum rocking response from the design response spectrum. Hence, this thesis also aims at providing a numerical tool for solving the equation of motion of the rocking block, which can be employed in the nuclear industry without involving expensive software and methods requiring high amount of expertise. The software chosen to develop this tool is Mathcad (PTC, 2012) because it is widely used in the nuclear industry.

1.4 Scope

The ASCE 43-05 method requires a response spectrum. The design response spectra for NPPs recommended in the United States Nuclear Regulatory Commission (USNRC) Regulation Guide 1.60 (Revision 1 (1973) and Revision 2 (2014)) is widely known as NBK spectrum named after its creators Newmark, Blume and Kapur (1973). Since the NBK is the design spectrum of many NPPs in United States (McGuire, Silva, and Constantino, 2001) and Canada (Dar and Hanna, 2012), and this spectrum is chosen in ASCE 43-05 to demonstrate an example, it is considered the most suitable response spectrum to carry out this study. This study utilizes, (a) the smoothened design (NBK) response spectrum and (b) response spectra of selected ground motions from the set used by Newmark et al (1973) to derive their smoothened design spectrum. Eight earthquake records are selected from the original study by Newmark et al (1973) with varying PGAs representing strong to moderate ground motions.

The scope of the thesis includes studying the NBK response spectrum and comparing the peak rocking response obtained by the ASCE 43-05 method applied to the two types of response spectra described above with the ones obtained by numerically solving the nonlinear equations of motion subject to the selected earthquake records.

An equivalent damping for an SDOF oscillator, equivalent to a RB in RM, computed by the ASCE 43-05 method turns out to be an atypical number (such as 8.4%), requiring construction of the response spectrum corresponding to that value.

The USNRC Regulation Guide 1.60 (1973, 2014) provides damped response spectra at regular damping values (such as 5%). Obtaining the NBK response spectra at unusual damping values (such as 8.4%), for a designer in the field, requires significantly high level of effort, every time a rocking problem is encountered. The scope of this thesis includes incorporating the construction of the NBK response spectrum as a part of the numerical tool developed to obtain the rocking response.

The scope of this thesis also includes study of the inherent problems in the ASCE 43-05 method. Thus the evaluation of the ASCE 43-05 method consists of highlighting its inherent contradictions and drawing comparison between the rocking response obtained by this method and by solving nonlinear equations of motion of a rigid block

1.5 Thesis Organization

The thesis is organized in four chapters. Chapter 2 provides the contents of the following article:

Dar A, Konstantinidis D, El-Dakhakhni W. W. "Evaluation of ASCE 43-05 seismic design criteria for rocking objects in nuclear facilities". To be submitted to *ASCE Journal of Structural Engineering*.

Chapter 3 presents the conclusions of this study, and Chapter 4 discusses topics for future research.

Although the main contents of the above mentioned article are given in Chapter 2, some parts of this article appear in different chapters with some overlapping information and common references.

There are eight appendices containing the Mathcad 15 (PTC, 2012) worksheets as described below:

1) Appendix A contains the details on NBK spectrum.
2) Appendix B contains the details of the reserve energy method proposed by Wesley et al (1980)
3) Appendix C contains the Mathcad worksheet utilized for creating the NBK spectrum at any damping on logarithmic tripartite scale.
4) Appendix D provides a Mathcad worksheet to obtain the best estimate of maximum rocking angle of a rigid body based on the ASCE 43-05 methods and
5) Appendix E contains a Mathcad worksheet to generate rocking spectrum of a rigid body from the NBK spectrum based on the ASCE 43-05 method.
6) Appendix F provides a worksheet to generate rocking spectrum of a rigid body from the actual response spectrum of an earthquake record based on the ASCE 43-05 method. This worksheet also utilizes the algorithm developed by Nigam and Jennings (1969) to obtain the response spectrum at any damping ratio value.

7) Appendix G provides a Mathcad worksheet to generate rocking spectrum of a rigid body from the equations of motion.

1.6 Bibliography

American Society of Civil Engineers. (2005). *ASCE 43-05 – Seismic Design Criteria for Structures, Systems and Components in Nuclear Facilities.* Reston, Virginia, USA.

American Society of Civil Engineers. (2006). *ASCE 41-06 – Seismic Rehabilitation of Existing Buildings.* Reston, Virginia, USA.

Atkinson, G. M. and Elgohary, M. (2007). Typical uniform hazard spectra for eastern North American sites at low probability levels. *Canadian Journal of Civil Engineering*, **34**, 12-18.

Blume, J. (1960). A reserve energy technique for the earthquake design and rating of structures in the inelastic range. *2nd World Conference on Earthquake Engineering.* Tokyo and Kyoto, Japan.

Chatzis, M. N. and Smyth, A. W. (2012). Modeling of the 3D rocking problem. *International Journal of Non-Linear Mechanics*, **47**(4), 85–98.

Chaudhuri, S. R. and Hutchinson, T. C. (2005). Characterizing frictional behavior for use in predicting the seismic response of unattached equipment. *Soil Dynamics and Earthquake Engineering*, **25**, 591–604.

Choi, B. and Tung, C. D. (2002). Estimating sliding displacement of an unanchrored body subjected to earthquake. *Earthquake Spectra*, **18**(4), 601–613.

CNSC (2005). *Regulatory Standard Probabilistic Safety Assessment (PSA) for Nuclear Power Plants S-294.* Canadian Nuclear Safety Commission.

Comerio, M. C. (editor) (2005). *Testbed study on a laboratory building: exercising seismic performance assessment. Report No. 2005/12.* Berkeley, CA: Pacific Earthquake Engineering Research Center (PEER) University of California, Berkeley.

CSA (2008). *CSA N291.Requirements for Safety-Related Structures for CANDU Nuclear Power Plants.* Rexdale, Ontario, Canada: Canadian Standards Association.

Dar, A. and Hanna, J. D. (2012). Beyond design basis seismic evaluation of nuclear power plants at Bruce site. *Proc. of the 3rd International Structural Specialty Conference*. Edmonton, Alberta: Canadian Society for Civil Engineering.

Dar, A., Konstantinidis, D., and El-Dakhakhni, W. (2013). Requirement of rocking spectrum in Canadian nuclear standards. *Transactions, 22nd International Structural Mechanics in Reactor Technology Conference (SMiRT22).* San Francisco, CA.

Dar, A., Konstantinidis, D., and El-Dakhakhni, W. W. (2014). Station challenges on seismic qualification of structures, systems and components in Canadian nuclear power plants. *Proceedings of the 10th National Conference in Earthquake Engineering.* Earthquake Engineering Research Institute, Anchorage, AK.

EPRI (1991). *NP-6041-SL-Revision 1. A Methodology for Assessment of Nuclear Power Plant Seismic Margin.* Palo Alto, CA: Electric Power Research Institute.

Hogan, S. (1989). On the dynamics of rigid-block motion under harmonic forcing. *Proceedings of the Royal Society of London,* Series A 1989; **425**: 441– 476.

Housner, G. W. (1963). The behavior of inverted pendulum structures during earthquakes. *Bulletin of the Seismological Society of America,* **53**(2), 403–417.

Hutchinson, T. C. and Chaudhuri, S. R. (2006). Bench-shelf system dynamic characteristics and their effects on equipment and contents. *Earthquake Engineering and Structural Dynamics,* **135**(13), 1631–165.

Jensen, S. R. and Gurbuz, O. (2011). Chapter 7.6 ASCE 4 Revision 2. : Sliding and Rocking of Unanchored Components and Structures. *Structures Congress 2011* (pp. 2178-2189). Las Vegas: American Society of Civil Engineers.

Jeong, M. Y., Suzuki, K., and Yim, S. C. (2003). Chaotic rocking behavior of freestanding objects with sliding motion. *Journal of Sound and Vibration,* **262**(5), 1091–1112.

Kinectrics. (2014). *Bruce Nuclear Generating Station Aeismic PRA Level 1 Seismic Fragility Report.* Kinectrics Report No: K-410003-REPT-0065, Rev 00. (Bruce Power Controlled Document).

Konstantinidis, D. and Makris, N. (2005). *Experimental and analytical studies on the seismic response of freestanding and anchored laboratory equipment, Report No. 2005/07.* Berkeley, CA: Pacific Earthquake Engineering Research Center (PEER); University of California, Berkeley.

Konstantinidis, D. and Makris, N. (2007). The dynamics of a rocking block in three dimensions. *Proc. 8th Hellenic Society for Theoretical and Applied Mechanics International Congress on Mechanics.* Patras, Greece.

Konstantinidis, D. and Makris, N. (2009). Experimental and analytical studies on the response of freestanding laboratory equipment to earthquake shaking. *Earthquake Engineering and Structural Dynamics,* **38**(6), 827–848.

Konstantinidis, D. and Makris, N. (2010). Experimental and analytical studies on the response of 1/4-scale models of freestanding laboratory equipment subjected to strong earthquake shaking. *Bulletin of Earthquake Engineering,* **8**(6), 1457–1477.

Konstantinidis, D. and Nikfar, F. (2015). Seismic response of sliding equipment and contents in base-isolated buildings subjected to broad-band ground motions. *Earthquake Engineering and Structural Dynamics*, (in press).

Lopez, G. D. and Soong, T. (2003). Sliding fragility of block-type non-structural components. Part 1: unrestrained components. *Earthquake Engineering and Structural Dynamics,* **32**(1), 111–129.

Luk, V. K., Spencer, B. W., Lam, I. P., and Dameron, R. A. (2005). *NUREG/CR-6865. Parametric evaluation of seismic behavior of freestanding spent fuel dry cask storage systems. Sandia National Laboratories.* U.S. Nuclear Regulatory Commission.

Makris, N. and Konstantinidis, D. (2003). The rocking spectrum and the limitations of practical design methodologies. *Earthquake Engineering and Structural Dynamics,* **32**(2), 265–289.

Makris, N., and Roussos, Y. (2000). 'Rocking response of rigid blocks under near-source ground motions. *Géotechnique,* **50**(3), 243–262.

Makris, N., and Zhang, J. (1999). *Rocking response and overturning of anchored equipment under seismic excitations. Report No. 1999/06.* Berkeley: Pacific Earthquake Engineering Research Center (PEER), University of California.

McGuire, R. K., Silva, W. J., and Constantino, C. J. (2001). *NUREG/CR-6728: Technical Basis for Revision of Regulatory Guidance on Design Ground Motions: Hazard- and Risk-consistent Ground Motion Spectra Guidelines.* United States Regulatory Commission.

Newmark, N. M., Blume, J. H., and Kapur, K. K. (1973). Seismic Design Spectra for Nuclear Power Plants. *Journal of the Power Division, ASCE*, **99**(2), 287-303.

Nigam, S. C. and Jennings, P. C. (1969). Calculation of Response Spectra from Strong-Motion Earthquake Records. *Bulletin of the Seismological Society of America,* **59**(2), 909-922.

Pena, F., Lourenco, P., and Campos-Costa, A. (2008). Experimental dynamic behavior of free-standing multi-block structures under seismic loading. *Journal of Earthquake Engineering*, **12**, 953-979.

Priestley, M., Evison, R., and Carr, A. J. (1978). Seismic response of structures free to rock on their foundations. *Bulletin of the New Zealand National Society for Earthquake Engineering,* **11**(3), 141–150.

PTC. (2012). Mathcad 15.0. Parametric Technology Corporation, 140 Kendrick Street, Needham, MA 02494, USA.

Reed, J. W., and Kennedy, R. P. (1994). *Methodology for Developing Seismic Fragilities EPRI TR-103959.* Palo Alto, California: Electric Power Research Institute.

Schau, H., and Johannes, M. (2013). Rocking and sliding of unanchored bodies subjected to seismic load according to conventional and nuclear rules. *4th ECCOMAS Thematic Conference on Computational Methods in Structural Dynamics and Earthquake Engineering (COMPDYN).* Kos Island, Greece.

Shao, Y. and Tung, C. (1999). Seismic response of unanchored bodies. *Earthquake Spectra*, **15**(3):523–536.

Shenton III, H. W. (1996). Criteria for initiation of slide, rock, and slide-rock rigid-body modes. *Journal of Engineering Mechanics (ASCE),* **122**(7), 690–693.

Taniguchi, T. (2002). Non-linear response analyses of rectangular rigid bodies subjected to horizontal and vertical ground motion. *Earthquake Engineering and Structural Dynamics*, **31**(8), 1481–1500.

USNRC. (1973). *Design Response Spectra for Seismic Design of Nuclear Power Plants, Regulatory Guide 1.60, Revision 1*. Washington, DC: United States Nuclear Regulatory Commission.

USNRC. (2014). *Design Response Spectra for Seismic Design of Nuclear Power Plants, Regulatory Guide 1.60, Revision 2*. Washington, DC: United States Regulatory Commission.

Wesley, D. A., Kennedy, R. P., and Richter, P. J. (1980). Analysis of the seismic collapse capacity of unreinforced masonry wall structures. *Proc. 7th World Conference on Earthquake Engineering.* Istanbul, Turkey.

Yim, C. K., Chopra, A., and Penzien, J. (1980). Rocking response of rigid blocks to earthquakes. *Earthquake Engineering and Structural Dynamics*, **8**(6), 565–587.

Zhang, J. and Makris, N. (2001). Rocking response of free-standing blocks under cycloidal pulses. *Journal of Engineering Mechanics*, **127**(5), 473-483.

CHAPTER 2 EVALUATION OF ASCE 43-05 SEISMIC DESIGN CRITERIA FOR ROCKING OBJECTS IN NUCLEAR FACILITIES

This chapter has the contents of the following article:

Dar A, Konstantinidis D, El-Dakhakhni WW. "Evaluation of ASCE 43-05 seismic design criteria for rocking objects in nuclear facilities". To be submitted to *ASCE Journal of Structural Engineering*.

2.1 Abstract

Seismic interaction of unanchored objects, such as storage drums, carts, radiation shielding walls, etc., with a seismically qualified safety system or component in a Nuclear Power Plant (NPP) can be detrimental to nuclear safety. Seismic response of unanchored components such as electrical transformers, power supply and cabinets is required in order to assess the seismic risk. The rocking response and toppling vulnerability of unanchored objects is not covered in nuclear standards, guidelines, and reports, except for an approximate method provided in ASCE/SEI 43-05 to estimate the maximum rocking angle in lieu of nonlinear time history analysis. The ASCE/SEI 43-05 method is different from the other methods, having the same purpose, evaluated in the past. In this study, the approximate method adopted by ASCE/SEI 43-05 is evaluated and is found to provide highly unreliable estimates of peak rocking rotations which are not in agreement with the solutions obtained by direct integration of the equation of motion for various earthquake records. It is recommended to use the direct integration method rather than the ASCE/SEI 43-05 method in order to arrive at the correct rocking solution. Since the standard ASCE/SEI 43-05 is focused on the nuclear facilities, its approach

continues to be recognized as the "best-industry-practised" method and is also expected to be adopted in the new revision of ASCE 4. The evaluation of ASCE/SEI 43-05 method is warranted.

2.2 Introduction

The seismic interaction of unanchored objects caused by their rocking and/or sliding has been identified as a contributor to the seismic risk in the seismic margin assessment methodology outlined in the Electrical Power Research Institute Report (EPRI) report NP-6041 (1991). The requirement of rocking analysis is further enhanced in the post-Fukushima environment in the context of Beyond Design Basis (BDB) evaluations where an existing masonry enclosure may be required to be evaluated for a BDB scenario which had never been considered before (EPRI 1025287). More information regarding BDB evaluation can be found in Dar et al. (2014) and the references therein.

According to the standard ASCE/SEI 43-05 *Seismic Design Criteria for Structures, Systems, and Components in Nuclear Facilities* (hereinafter referred to as ASCE 43-05), it is generally preferable to anchor components in order to avoid rocking and sliding. However, unanchored components are acceptable if they satisfy the requirements of ASCE 43-05. Examples of some unanchored objects are shown in Figure 1-1, including components and systems such as spent-fuel dry storage casks, scaffolds, and unreinforced masonry (URM) radiation shielding walls. Although modern standards (e.g. ASCE 43-05 and CSA N291, 2008) do not

allow any URM inside a Nuclear Power Plant (NPP) in seismically qualified areas, some of the existing plants (relatively older, constructed more than three decades ago) have existing URM inside the containment (EPRI report NP-6041 1991). The URM inside a NPP has been identified as one of the major contributors to seismic risk (Reed and Kennedy, 1994).

An unanchored rigid body (RB) subjected to base excitation may rock, slide or slide-rock. Criteria for the initiation of these three modes and response were established by Shenton (1996). The problem of sliding objects has been studied at various levels by Shao and Tung (1999), Choi and Tung (2002), Lopez and Soong (2003), Comerio (2005), Chaudhuri and Hutchinson (2005), Hutchinson and Chaudhuri (2006), Konstantinidis and Makris(2005, 2009 and 2010), Konstantinidis and Nikfar (2015), and references reported therein. Slide-rocking has been investigated by Taniguchi (2002) and Jeong et al. (2003). ASCE 43-05 permits the rocking response to be considered without simultaneous occurrence of sliding. Moreover, the standard permits planar rocking analysis. Also, ASCE 43-05 demonstrates its method of obtaining the maximum angle of rotation of a rocking object through an example by considering pure planar rocking response of a rigid rectangular block. Hence in order to evaluate the ASCE 43-05 method, the current study focuses on the pure planar rocking response of a RB. The three-dimensional rocking response of a RB (Konstantinidis and Makris, 2007; Chatzis and Smyth, 2012) is not addressed in the standard.

The first systematic study of a RB in rocking motion (RM) was carried out by Housner (1963), considering it as an inverted pendulum. Housner (1963) obtained the pure planar rocking response of a RB subject to variety of horizontal base excitations, with small angle approximation, as a combination of hyperbolic functions. Yim et al. (1980) conducted dynamic analyses using simulated ground motions to examine the sensitivity of the rocking and overturning response of a RB to system parameters. Hogan (1989) studied the dynamic response of RB in RM subject to harmonic excitation. Makris and Roussos (2000) and Zhang and Makris (2001) investigated the response of rigid blocks subjected to trigonometric pulses and near-source ground motions. All these studies indicated that the response of a RB in RM (in its linearized form) consists of hyperbolic functions. In contrast, it is well known that the oscillating response (not over critically damped) of a single-degree-of-freedom (SDOF) oscillator is governed by trigonometric functions. For this reason, in this paper, a subtle distinction in terminology is made: the term *oscillation* is used for the response of a SDOF oscillator, whereas the term *vibration* is used for the response of a rocking block.

Despite various studies on RB in RM indicating that its behavior is different from that of a SDOF oscillator, attempts have been made to consider a RB as an equivalent SDOF oscillator. Priestley et al. (1978) developed a method to obtain the displacement of a RB based on response spectrum analysis, assuming that a RB in RM can be represented by an equivalent SDOF oscillator with constant damping ratio but whose period depends on the amplitude of the rocking angle. Wesley et al.

(1980) also considered the RB in RM as a SDOF oscillator and obtained its response based on a reserve energy technique given by Blume (1960). Efforts to replace rocking blocks by equivalent SDOF oscillators were revisited later in the literature. Makris and Konstantinidis (2003) introduced the concept of a *rocking spectrum* and showed it to be a distinct intensity measure for ground motions. The study concluded that the response of a RB in RM cannot be obtained by using an equivalent SDOF oscillator. The standard ASCE 41-06 (2006) refers to their work, cautioning the design professional against the use of a response-spectrum-based approach. Dar et al. (2013) conducted a preliminary evaluation of the methodology proposed by Wesley et al. (1980) and pointed out that its predictions are inaccurate.

Design criteria in ASCE 43-05 are based on a 'best estimate' value for rocking angle. This rocking angle is to be used with a safety factor of 2.0 to ensure that it is less than the 'instability angle' $\alpha = \tan(b/h)$, where for b is half the width and h is half the height of a rectangular object, or to provide sufficient clearance around the object. According to ASCE 43-05, the best estimate of the maximum rocking angle may be computed either through nonlinear time history analysis with a minimum of 5 ground motions or through an approximate method that is prescribed in detail in the standard. The method leans on the assumption that a rocking block can be represented by an 'equivalent' SDOF oscillator with constant damping, but whose period depends on the amplitude of the rocking.

In NPPs, used fuel is stored in large pools of water called fuel bays where it remains for a considerable period of time (around 15 years) before being sent to dry

storage facility. Storage of spent fuel in unanchored fuel casks in a dry storage facility is another area of application of rocking principles.

Luk et al. (2005) used 3D finite element analysis to evaluate the seismic response of freestanding spent fuel dry cask storage systems. The study provided best-fitted power-law curves for estimating the peak rotation or displacement of a cask as a function of various intensity measures (such as, peak ground velocity or pseudo-acceleration at 1Hz) based on selected earthquake records. However, the results of that study are limited to two specific cask designs and are not amenable to generalized application. Furthermore, the data exhibited substantial scatter, and the fitted curves were in some cases of poor quality. The available literature pertaining to nuclear industry applications of rocking and sliding analysis of unanchored objects, ranging from a simplified energy method to detailed time-history methods, including probabilistic analyses, was surveyed by Jensen and Gurbuz (2011). The study provides an overview of new guidance to be adopted in the next edition of ASCE 4 (*ASCE 4 –Rev. 2 Seismic Analysis of Safety-Related Nuclear Structures: Standard and Commentary*). According to Jensen and Gurbuz (2011), the approximate method in ASCE 43-05, which is based on a reserve energy technique, will be adopted in ASCE 4 Rev. 2. Therefore, evaluation of this methodology is still very relevant.

Comparison between the rocking criteria and methods adopted in the European (EN 1990 and EN 1998), German (KTA 2201.1 and 2201.4) and US (ASCE 43-05) standards was drawn by Schau and Johannes (2013) assuming that an unanchored

rigid rocking object can be represented by an SDOF system with a torsional spring. This study found the implicit FE programs to be suitable to study rocking and sliding problems and expressed doubts about the ASCE 43-05 being sufficiently conservative for all geometries of rigid bodies. No detailed investigation of rocking response obtained by the ASCE 43-05 method was reported.

Looking at various examples in Figure 1-1 requiring estimation of rocking response and its importance in evaluation of seismic risk (Reed and Kennedy, 1994), rocking analysis can neither be ignored in NPPs, nor can it be based on approximated methods without any evidence of their evaluation or verification. Also, as seen later, the inconsistent conservatism of the ASCE 43-05 method, over the solution obtained by (numerically) solving equations of motion, is not desirable for computation of seismic risk. An approximate method with less conservatism than the numerical solution cannot be used. However excess conservatism is also not suitable in SPRA since it artificially amplifies the seismic risk resulting in diversion of financial, technical and other resources of a NPP from high-risk components to low-risk ones. Despite ample evidence being available in the literature that a rocking block cannot be represented by a SDOF oscillator, the ASCE 43-05 approach continues to be recognized as the "best-industry-practised" method and is expected to be adopted in ASCE 4 (Jensen & Gurbuz, 2011). Considering these facts, evaluation of the ASCE 43-05 method is warranted. In this paper, the ASCE 43-05 approximate method for estimating maximum rocking rotation of objects in NPPs is evaluated. The evaluation is conducted by comparing

the predictions of the approximate procedure with the solutions obtained by direct integration of the equation of motion of the rocking block for various ground motions. This evaluation also includes identifying the inherent problems in the ASCE 43-05 method.

2.3 Review of the Rocking Response of a Rigid Block

The discussion begins with a brief review of the rocking block problem. Figure 2-1 shows the details of a rectangular RB having width $2b$ and height $2h$ subjected to the horizontal acceleration $\ddot{x}$ at its base. The equations of RM for this block are (Yim et al. 1980):

$$I_o\ddot{\theta} + mgR\sin(-\alpha-\theta) = -m\ddot{x}R\cos(-\alpha-\theta)\,,\ \ \theta < 0 \tag{1}$$

$$I_o\ddot{\theta} + mgR\sin(\alpha-\theta) = -m\ddot{x}R\cos(\alpha-\theta)\,,\ \ \theta \geq 0 \tag{2}$$

where, m is the mass of the block, g is the acceleration of gravity, R is the distance from the pivot point to the center of gravity, angle α is the measure of block stockiness, and I_o is the mass moment of inertia of the rigid block about pivot point O. Substituting $I_o = (4/3)mR^2$ for a rectangular block and rewriting the above equations, leads to

$$\ddot{\theta} = -p^2\left\{\sin[\alpha\ \mathrm{sgn}(\theta)-\theta] + \frac{\ddot{x}}{g}\cos[\alpha\ \mathrm{sgn}(\theta)-\theta]\right\} \tag{3}$$

where $\mathrm{sgn}(\cdot)$ is the *signum* function and $p = \sqrt{(3g)/(4R)}$ for a rectangular block; the larger the block, the smaller p.

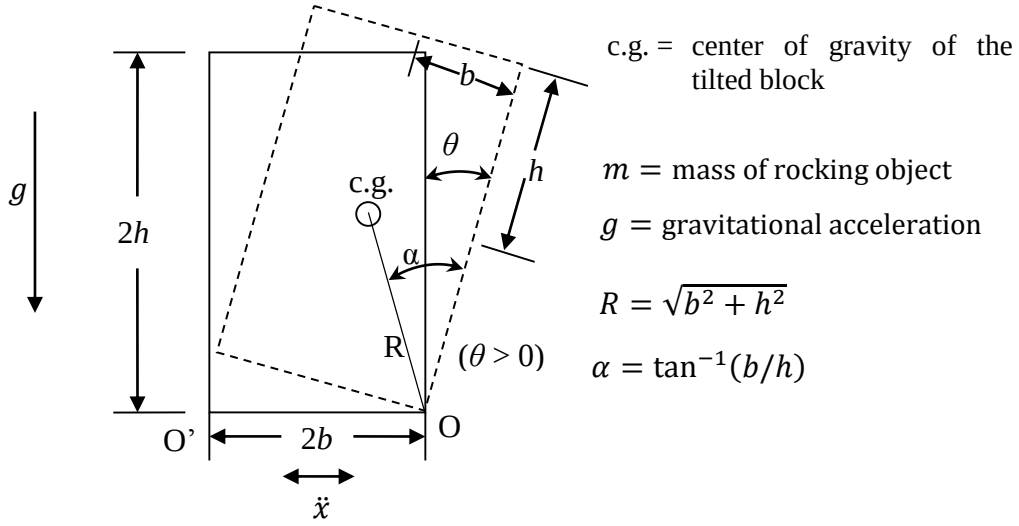

Figure 2-1: Schematic of a freestanding rigid block in rocking motion**.**

The rocking response of a RB subjected to base acceleration is computed numerically via a state space formulation, as discussed later in the paper. The coefficient of restitution r given by Houser (1963) can be utilized to take into account the energy loss due to impact. For the velocity after impact, $\dot{\theta}_2$, and the pre-impact velocity, $\dot{\theta}_1$, the reduction in kinetic energy is:

$$\left(\frac{\frac{1}{2}I_o\theta_2^2}{\frac{1}{2}I_o\theta_1^2}\right) = \frac{\theta_2^2}{\theta_1^2} = r^2$$

where

$$r = 1 - \frac{3}{2}\sin^2\alpha \tag{4}$$

The value of r given by equation (4), obtained through conservation of angular momentum before and after impact, depends only on the geometry of the block, and

it is the maximum value of the coefficient of restitution for which a block of stockiness α will undergo rocking motion. Since $r < 1$, the impacts have to be inelastic, i.e. energy must be lost upon impact in order to maintain smooth rocking motion (*no bouncing*).

The fundamental difference between the dynamic response of a rocking block and a SDOF oscillator can be seen upon piecewise linearization of Equation (3). For slender blocks (say, $\alpha < 20°$ as considered by Housner, 1963),

$$\ddot{\theta} - p^2\theta = -p^2\alpha \,\mathrm{sgn}(\theta) \tag{5}$$

The above equation is easily integrated analytically to obtain closed form solution in terms of hyperbolic functions contrary to the response of a SDOF oscillator, which is described by trigonometric functions (Makris and Roussos 2000). Another notable difference between the two dynamical systems is that the period of free vibration of a SDOF oscillator is constant, whereas, as pointed out by Housner (1963), the duration of a half response cycle of RB in RM depends on the initial rocking angle amplitude; hence the term *apparent period* is used herein. Nevertheless, when two geometrically similar blocks (same α) of different size (different p) experience free vibrations, the response cycle of the larger of the two blocks will be longer. Therefore, the quantity p is itself a measure of the dynamic characteristics of the rocking block.

A detailed discussion on the fundamental differences between the dynamics of a SDOF oscillator and of a rocking block is presented in Makris and Konstantinidis (2003).

2.4 Design Response Spectrum in Nuclear Power Plants

The response spectrum in USNRC Regulatory Guide 1.60 (1973, 2014), specified as the design spectrum for NPPs, was developed by Newmark, Blume and Kapur (1973) and is popularly known as the NBK spectrum. Since the NBK spectrum is the design spectrum of many NPPs in the United States (McGuire, Silva, and Constantino, 2001) and Canada (Dar and Hanna, 2012), and it is also chosen in Appendix B of ASCE 43-05 to illustrate an example of how to apply the methodology, it is considered the most suitable design response spectrum to carry out this study. This response spectrum has control points at 0.1, 0.25, 2.5, 9 and 33 Hz with a Peak Ground Displacement (PGD) of 914 mm and Peak Ground Acceleration (PGA) of 1.0 g. The response spectrum is made of straight lines between these control frequencies on log-log scale which are scaled to the PGA of the site to obtain the site specific design response spectrum (USNRC, 1973, 2014). The peak acceleration of the NBK spectrum occurs at 2.5Hz frequency. The NBK spectrum between two control points at f_{D}= 0.25 Hz and f_{C}=2.5 Hz is of more interest than the rest, as explained later. The equation of straight line on log-log scale between f_{D} and f_{C} takes the form:

$$\log\left(\frac{S_A}{S_A^{\mathrm{C}}}\right) = \log\left(\frac{f}{f_{\mathrm{C}}}\right)^{s}$$

where, S_A and S_A^{C} are the spectral accelerations in g at frequency f and f_{C}, respectively, and s is the slope of the line. The intercept constant and the slope derived from the control points are given in Newmark et al. (1973) and repeated in Appendix A for the reader's convenience. The equation of spectral acceleration S_A between the control points at 0.25Hz and 2.5Hz resolves to the following:

$$S_A = S_A^{\mathrm{C}} \left(\frac{f}{2.5}\right)^{\log\left(\frac{S_A^{\mathrm{C}}}{S_A^{\mathrm{D}}}\right)} PGA$$

where f is in Hz and S_A^{D} is the acceleration at 0.25 Hz. The values for S_A^{C} and S_A^{D} for any damping can be obtained from the equations given in Newmark et al (1973).

The vertical spectral accelerations are obtained by multiplying the horizontal spectral acceleration by 2/3 in ASCE 43-05 for frequencies below 2.5Hz. Hence the same is adopted in the sections (*2.5.2* and *2.5.3*) below related to the ASCE 43-05 example. However, the effect of vertical excitation is not found to be significant by ASCE 43-05. For the purpose of comparing the solutions obtained by various methods, in the sections below, only horizontal excitation is considered unless otherwise noted in some specific cases.

2.5 The ASCE 43-05 Method for estimating maximum rocking angle

2.5.1 Damping in the ASCE 43-05 Method

Since the ASCE 43-05 method is based on representing the rocking block as a viscously damped linear SDOF oscillator, the ASCE 43-05 approximate method requires damping ratio values and equivalent natural frequency. This section

presents ASCE 43-05's approach to determining the former, while determination of the latter is discussed in the following section. First, the ratio between the two successive displacement peaks, u_n and u_{n+1}, of an SDOF oscillator under free vibration is considered, as given in ASCE 43-05,

$$\frac{u_{n+1}}{u_n} = e^{-\gamma} \tag{6}$$

where

$$\gamma = \frac{2\pi\beta}{\sqrt{[1-\beta^2]}} \tag{7}$$

and β is the damping ratio.

ASCE 43-05 then equates the ratio given by Equation (6) with the square (since two impacts occur during each cycle) of the coefficient of restitution given by Equation (4), which leads to

$$\gamma = -2\ln\left(1 - \frac{3}{2}\sin^2\alpha\right) \tag{8}$$

Then, from Equation (7), the equivalent damping β_e in ASCE 43-05 is given by

$$\beta_e = \frac{\gamma}{\sqrt{4\pi^2 + \gamma^2}} \tag{9}$$

with γ computed from Equation (8). This is different from damping by Priestley et al. (1978) approximated in Makris and Konstantinidis (2003) as:

$$\beta_p = -0.34\ \ln\left(1 - \frac{3}{2}\sin^2\alpha\right)^2$$

The above equation predicts much higher value of damping in comparison with Equation (9): e.g. for $\alpha = 0.35$, $\beta_e = 6.2\%$ and $\beta_p = 13.2\%$.

2.5.2 Estimation of maximum rocking angle

Appendix B of ASCE 43-05 provides an approximate method for estimating the maximum rocking angle of a rectangular RB undergoing pure planar RM. This method is based on the dependence of the apparent period of a rocking block on the maximum angle of rotation; hence, the method uses an SDOF oscillator with an *equivalent* period (or frequency), the amplitude of which depends on the maximum rocking angle of the corresponding rocking block.

This method starts with the equation of motion presented in Yim et al. (1980) which includes both horizontal and vertical ground accelerations, $\ddot{x}$ and $\ddot{y}$ respectively. For $\theta > 0$,

$$I_o\ddot{\theta} + m(g + \ddot{y})Rsin(\alpha - \theta) = -mRF_H cos(\alpha - \theta))\ddot{x} \tag{10}$$

where the term $F_H = \frac{m_L h_L}{mh}$, (with h_L being the center of gravity height of the lateral mass m_L, and h being the center of gravity height of resisting mass m) is introduced to account for non-uniform mass distribution. For a block with uniformly distributed mass, $F_H = 1$.

It can be shown that Equation (10) can be written as (ASCE 2005)

$$C_I\ddot{\theta} + \frac{g}{h}f_2(\theta) = -f_1(\theta)F_H\frac{\ddot{x}}{h} - f_2(\theta)\frac{\ddot{y}}{h} \tag{11}$$

where, for a rectangular block with uniformly distributed mass, $C_I = \frac{4}{3}(1 + a^2)$ with $a = \tan\alpha = b/h$, and functions $f_1(\theta)$ and $f_2(\theta)$ are defined by

$$f_1(\theta) = \cos\theta + a\sin\theta \tag{12}$$

$$f_2(\theta) = a\cos\theta - \sin\theta \tag{13}$$

Equation (11) can be re-written as

$$\ddot{\theta} + \frac{g}{C_I h} f_2(\theta) = \frac{-f_1(\theta)F_H\ddot{x} - f_2(\theta)\ddot{y}}{C_I h} \tag{14}$$

At this point ASCE 43-05 makes an assumption that the rocking block nonlinear dynamical system can be replaced by a linear SDOF oscillator and replaces the $\frac{g}{C_I h} f_2(\theta)$ term by ${\omega_e}^2\theta$, where the equivalent natural frequency ω_e is established through the reserve energy method. According to this method, the work required to rotate a block from $\theta = 0$ to $= \theta_o$, i.e.,

$$\int_0^{\theta_o} WR\sin(\alpha - \theta)\, d\theta = Wh[f_1(\theta_o) - 1] \tag{15}$$

is equated to the work done to deform a rotational spring of stiffness K_R by θ_o, i.e., $\frac{1}{2}K_R\theta_o^2$. Recalling $I_o = (4/3)mR^2$, leads to

$$\omega_e = \left[\frac{K_R}{I_o}\right]^{\frac{1}{2}} = \left[\frac{2(f_1(\theta_o) - 1)g}{C_I\theta_o^2 h}\right]^{\frac{1}{2}} \tag{16}$$

Based on an assumption that much more time is spent at θ near zero than is spent at $\theta = \theta_o$. ASCE43-05 simplifies the right hand side of Equation (14) using the time average values of $f_1(\theta) \approx 1$ and $f_2(\theta) \approx a$, giving:

$$\ddot{\theta} + {\omega_e}^2\theta = \frac{-F_H\ddot{x} - a\ddot{y}}{C_I h} \tag{17}$$

Equation (17) is based on an assumption that ignores the fundamentally different nature of the rocking block and SDOF oscillator dynamical systems. This can be easily seen for a slender block (small α), by considering no vertical excitation $(\ddot{y} = 0)$, $F_H = 1$, $f_1(\theta) = \frac{\cos(\alpha-\theta)}{\cos(\alpha)} \approx \frac{R}{h} \approx 1$ and $f_2(\theta) = (\alpha - \theta)$. Substituting these in Equation (11) leads to Equation (5) with forcing function added on right hand side. As discussed earlier, the eigenfunctions corresponding to the ODE in Equation (5) are hyperbolic, while those corresponding to Equation (17) are trigonometric. Moreover, as seen later, the assumption in ASCE 43-05 that much more time is spent near $\theta = 0$ than at $\theta = \theta_o$ is incorrect.

Assuming that the horizontal spectral acceleration SAH and vertical spectral acceleration SAV are randomly phased with respect to each other, and ω_e (Equation (16)) depending on maximum angle of rotation θ_o, ASCE 43-05 obtains the following expression from Equations (16) and (17):

$$C_I h\omega_e^2\theta_o = [F_H^2(SAH^2) + a(SAV^2)]^{\frac{1}{2}} \tag{18}$$

Combining Equations (16) and (18) gives

$$\frac{2g[f_1(\theta_o) - 1]}{\theta_o} = F_H SAH\left[1 + \left(\frac{a\ SAV}{F_H SAH}\right)^2\right]^{\frac{1}{2}} \tag{19}$$

Since θ_o is the maximum angle of a half-cycle (because of two impacts in one cycle), the horizontal spectral acceleration capacity is found from the above in the following equation:

$$SAH_{CAP} = \frac{2g[f_1(\theta_o) - 1]}{F_H F_V \theta_o} \tag{20}$$

where,

$$F_V = \left[1 + \left(\frac{a\ SAV}{F_H SAH}\right)^2\right]^{\frac{1}{2}} \tag{21}$$

It can be seen from Equation (21) that the contribution of the vertical component is negligible. For example, for a relatively stocky uniform rectangular block with $\alpha = 0.5$ and $SAV/SAH = 2/3$, the capacity is reduced by only 1.3%. Consequently, according to ASCE 43-05 the contribution of the vertical ground motions is often ignored.

2.5.3 The ASCE 43-05 Procedure

The procedure adopted by ASCE 43-05 is summarized in Table 2-1 with all equations recast in terms of p and α. The set of equations in this table include the equation for evaluating the minimum value of the maximum angle at the frequency corresponding to the peak spectral acceleration explained in the following section.

Table 2-1: Steps of ASCE 43-05 procedure

1	Calculate damping exponent γ.	$\gamma(\alpha) = -2\ln\left(1 - \frac{3}{2}\sin^2\alpha\right)$
2	Calculate the damping ratio β_e. Obtain the response spectrum corresponding to β_e.	$\beta_e(\alpha) = \frac{\gamma(\alpha)}{\sqrt{4\pi^2 + \gamma(\alpha)^2}}$
3	Calculate the minimum of the maximum rocking angle, θ_{om}, at f_{em}= frequency corresponding to the maximum spectral acceleration of the response spectrum.	$\theta_{om}(p, \alpha, f_{em}) = \frac{2\sin\alpha}{\left(2\pi\frac{f_{em}}{p}\right)^2 + \cos\alpha}$
4	Create a table of various values of θ_o, ranging from θ_{om} up to α with a selected step $\Delta\theta_o$	$\theta_o = \theta_{om},\ \theta_{om} + \Delta\theta_o, \cdots\ , \alpha$
5	Calculate $f_1(\theta_o, \alpha)$ for first value from step 4.	$f_1(\theta_o, \alpha) = \cos\theta_o + \tan\alpha\sin\theta_o$
6	Calculate vertical component factor. If neglecting vertical component, $F_V = 1$.	$F_V(\alpha) = \sqrt{1 + \left(\frac{2\tan\alpha}{3\,F_H}\right)^2}$
7	Calculate horizontal spectral acceleration capacity. (in this paper, $F_H = 1$).	$SAH_{CAP}(p, \alpha) = \frac{2g[f_1(\theta_o, \alpha) - 1]}{F_H F_V(\alpha)\theta_0}$
8	Calculate effective frequency	$f_e = \frac{p}{2\pi\theta_o}\sqrt{2\cos\alpha\,[f_1(\theta_o, \alpha) - 1]}$
9	Create a table or plot a curve for various values of $SAH_{CAP}(p, \alpha)$ and f_e corresponding to the different values of θ_o.	If a curve is plotted, define it as *capacity* curve.
10	Find out spectral acceleration demand for various values of f_e.	Read from the response spectrum. Call it $SAH_{DEM}(f_e)$. Create a table or plot a curve.
11	Compare spectral acceleration in 10 with the capacity acceleration in 7 for every θ_o.	Check if $\lvert SAH_{DEM}(f_e) - SAH_{CAP}(p, \alpha)\rvert <$ acceptable tolerance. This may be true for more than one values of θ_o. The lowest value of θ_o is the solution. This can also be achieved from the intersection of the capacity curve and the response spectrum.

.

Considering $F_H = 1$ (for a rectangular object with uniformly distributed mass), $F_V = 1$, and $f_1(\theta_o) - 1 \approx \theta_o\left(a - \frac{\theta_o}{2}\right)$ for small θ_o (up to approximately 0.4),

$$SAH_{CAP} = 2g\left(a - \frac{\theta_o}{2}\right) = g(2\tan\alpha - \theta_o) \tag{22}$$

For small α, the frequency and acceleration equations simplify as

$$SAH_{CAP} = \alpha g\left(2 - \frac{\theta_o}{\alpha}\right) \tag{23}$$

$$f_e = \frac{\omega_e}{2\pi} = \frac{p}{2\pi}\left[\frac{2}{\frac{\theta_o}{\alpha}} - 1\right]^{\frac{1}{2}} \tag{24}$$

ASCE 43-05 derives the minimum value of θ_o from Equation (16) by substituting $f_1(\theta_o) - 1 \approx \theta_o\left(a - \frac{\theta_o}{2}\right)$,

$$\theta_{om} = \frac{2a}{\frac{C_I}{g}(2\pi f_{em})^2 + 1} \tag{25}$$

where f_{em} is the frequency at Peak Spectral Acceleration (PSA), which is 2.5 Hz for the NBK spectrum. However some other design spectrum may have different shape than the NBK spectrum. Hence the capacity spectrum should be independent of the peak frequency. Minimum and maximum accelerations and frequencies at θ_o/α= 1 and 0 are given by the following equations for small α

$$SAH_{CAP\,min} = \alpha g, \quad SAH_{CAP\,max} = 2\alpha g \tag{26}$$

$$\omega_{e\,min} = p\,, \quad \omega_{e\,max} = \infty \tag{27}$$

Observations with regard to minimum and maximum capacities are given in section 2.6.4.

2.6 Inherent Problems of the ASCE 43-05 Method

This section identifies various problems with the ASCE 43-05 method by revisiting the example illustrated in ASCE 43-05 Appendix B. The RB of interest has the geometric and physical characteristic given in Table 2-2. To begin this investigation, first, the solution given by the ASCE 43-05 is considered.

Table 2-2. Details of rocking block example in Appendix B of ASCE-43-05

h (mm)	b (mm)	*Stockiness* $\alpha = \tan^{-1}(\frac{b}{h})$	$R = \sqrt{b^2 + h^2}$ (mm)	$p = \sqrt{\frac{3g}{4R}}$ (rad/s)	$\frac{2\pi}{p}$ (s)	$r = 1 - \frac{3}{2}(\sin\alpha)^2$
1067	457	0.405	1161	2.517	2.496	0.767

The example block in Table 2-2 is solved in ASCE 43-05, with $F_V = 1.04$ and $F_H = 1$. Following the procedure in Table 2-1, the *capacity curve* is plotted in Figure 2-2(a) together with the NBK spectrum for 8.4% damping, obtained from Equation (9), and PGA $= 0.41\ g$. The equation for the demand horizontal spectral acceleration SAH_{DEM} (NBK spectrum) at 8.4% damping turns out to be the following:

$$SAH_{DEM} = 2.49\left(\frac{f}{2.5}\right)^{0.78} PGA \tag{28}$$

The intersection point of the NBK spectrum with the capacity curve in Figure 2-2(a) (or, alternatively, the third row of Table 2-3) provide the solution. In this case, the 'effective rocking frequency' (ASCE 2005) of the rocking block $f_e = 1.78$ Hz (corresponding to angle of rotation $\theta_o = 0.038$ rad) for the prescribed demand. As seen later, this frequency is not in agreement with the vibration frequency of the

block (in the half cycle pertaining to the maximum rotation) observed in the rotation time history obtained from Non-linear Time History (NLTH) analysis. Points C and D in Figure 2-2(a) correspond to frequencies 0.25 Hz and 2.5 Hz respectively. Since at the point of intersection, $SAH_{DEM} = SAH_{CAP}$, the PGA of a response spectrum suitable to any frequency $f = f_e$ corresponding to a SAH_{CAP} can be calculated by replacing SAH_{DEM} with SAH_{CAP} in Equation (28). Hence, for each value of θ_o, the PGA of a corresponding NBK spectrum which would intersect with the capacity curve at the corresponding frequency f_e can be calculated. This is referred to as PGA_{CAP} in ASCE 43-05 and calculated by

$$PGA_{CAP} = \frac{SAH_{CAP}}{\left[2.49\left(\frac{f_e}{2.5}\right)^{0.78}\right]} \tag{29}$$

For the ASCE 43-05 example, PGA_{CAP} is listed in the last column of Table 2-3.

Table 2-3: Solution for RB in Table 2-2 ($F_V = 1.04, F_H = 1$)

Row	θ_o	f_e	SAH_{CAP}	PGA_{CAP}
1	0.0198	2.497	0.805	0.323
2	0.02	2.485	0.805	0.324
3	0.038	1.783	0.787	0.411
4	0.05	1.543	0.776	0.454
5	0.1	1.056	0.727	0.572
6	0.15	0.832	0.677	0.643
7	0.2	0.693	0.627	0.687
8	0.24	0.612	0.587	0.708
9	0.3	0.518	0.526	0.723
10	0.35	0.456	0.474	0.721
11	0.4	0.403	0.423	0.708
12	0.4049	0.398	0.418	0.706

2.6.1 Assumption that rocking block can be represented by SDOF oscillator

Whereas the stiffness of the SDOF oscillator described in Equation (17) is clearly positive, the appearance of Equation (14) obfuscates the fact that the stiffness of the rocking block is negative away from the equilibrium point $\theta = 0$. Expanding out the restoring term in Equation (14) gives

$$\frac{g}{C_I h} f_2(\theta) = p^2 \sin(\alpha - \theta) = p^2[\sin\alpha - \cos\alpha\, \theta + \cdots]$$

The negative sign attached to the term of θ in the above equation is a clear indication of negative stiffness which is not an attribute of a SDOF oscillator.

2.6.2 Uplift even for PGA< $g\ tan\ \alpha$

In order to demonstrate contradictions in the ASCE 43-05 method, three values of PGA_{CAP} from the last column of Table 2-3 are considered; 0.323g, 0.572g and 0.708g in rows 1, 5 and 8, respectively. The NBK response spectra for these PGA values are shown in Figure 2-2 (b) together with the capacity curve (third and fourth columns of Table 2-3). Here, the capacity curve is divided into three zones: zone 1, to the right of the peak; zone 2, to the left of and including the peak; and zone 3, to the left of and away from the peak. The ASCE 43-05 method considers the solution to the rocking problem to be the first intersection of the demand response spectrum and the capacity curve *to the left of, and including, the peak* (which for the NBK spectrum is at 2.5 Hz). Hence if there are three intersections (i.e. one in each zone), zone 1 and zone 3 are not considered. As shown in Figure 2-2(b), the 0.323g PGA

spectrum intersects with the capacity curve only at 2.5Hz, which corresponds to $\theta_o = 0.0198$ rad, as shown in the first row of Table 2-3. However, 0.323g PGA is less than the minimum required ground acceleration (i.e., $g \tan \alpha = 0.429g$) to initiate rocking. In other words, the ASCE 43-05 method predicts a finite rotation even for ground motions that are not potent enough to induce uplift of the RB.

2.6.3 ASCE 43-05 predicts the less conservative of two solutions

Figure 2-2(b) shows that, to the left of the 2.5 Hz peak, the NBK design response spectrum for 0.572g PGA and 8.4% damping intersects the capacity curve at only one point, at 1.056 Hz (fifth row of Table 2-3). However, Figure 2-2(c) shows that, for frequencies less than 2.5 Hz, the NBK spectrum for 0.708g PGA intersects the capacity curve at two frequencies (0.612 Hz and 0.403 Hz), in zones 2 and 3, respectively. This is due to the reverse curvatures of the capacity curve and the response spectrum. According to Table 2-3 (rows 8 and 11), these two frequencies correspond to $\theta_o = 0.24 \; and \; 0.40$ rad respectively. According to the ASCE 43-05 method, the solution is the first intersection to the left of the peak, i.e., $\theta_o = 0.24$ rad, at frequency of 0.612 Hz (in zone 2); therefore, ASCE 43-05 predicts the less conservative value of the two as the solution for seismic hazard represented by the 0.708g PGA response spectrum.

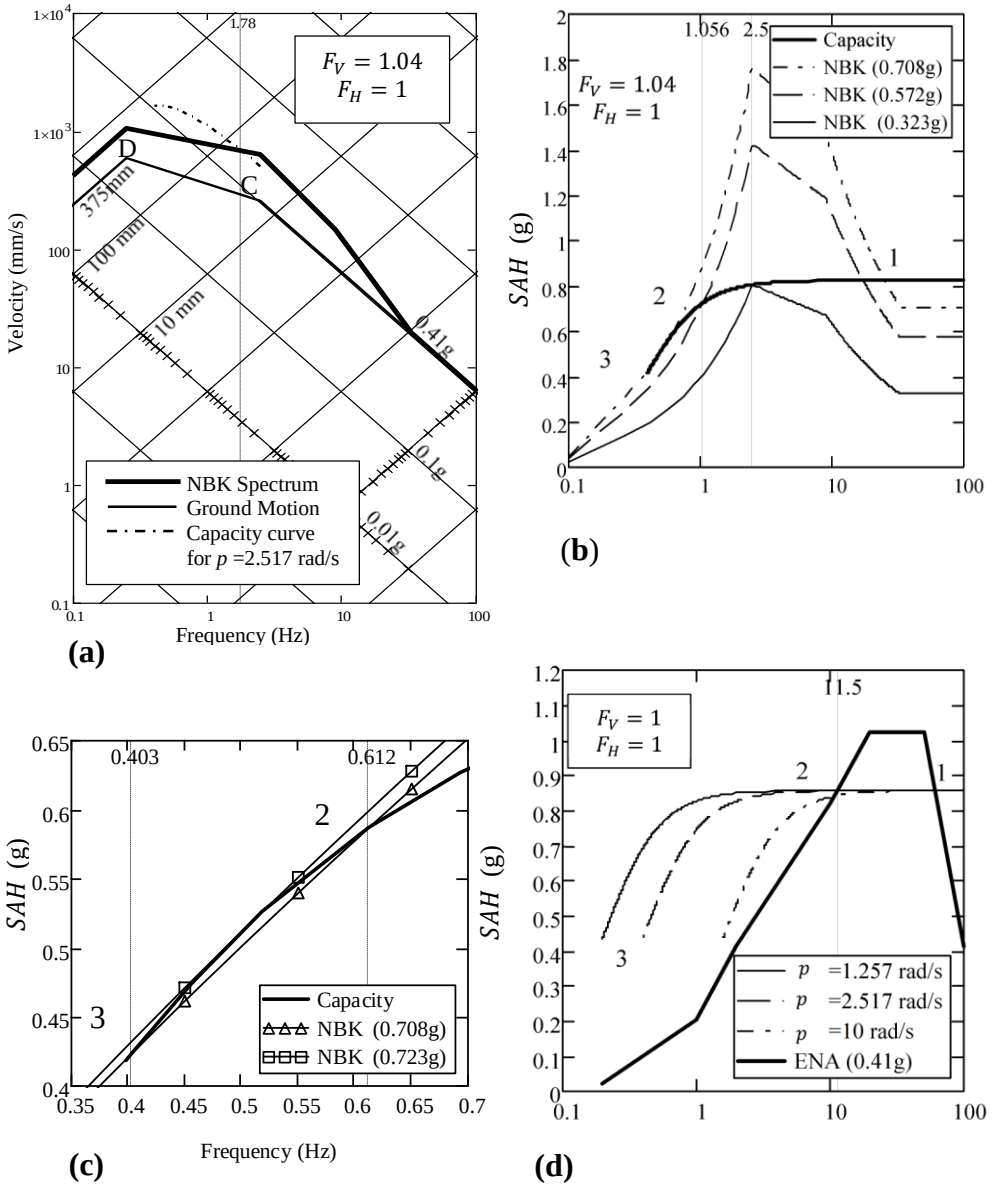

Figure 2-2: Response spectra and capacity curve(s): **(a)** For the example in Table 2-2, on tripartite log-log scale with $F_V = 1.04$. The capacity curve intersects the NBK response spectrum (8.4% damped with 0.41g PGA) at 1.78 Hz **(b)** Intersection of the capacity curve, plotted up to 100 Hz with three 8.4% damped NBK response spectra on log-normal scale **(c)** Enlarged view of this capacity curve in zones 2 and 3 **(d)** ENA spectrum and three capacity curves for three values of p and constant value of $\alpha = 0.405$ at log-normal scale with $F_V = 1$.

Figure 2-2 (c) gives the maximum PGA (of the NBK spectrum) which the RB can sustain. According to Figure 2-2(c) and row 9 of Table 2-3, the solution for 0.723g PGA_{CAP} is a frequency of 0.518 Hz and rotation $\theta_o = 0.3$ rad. Per ASCE 43-05, when subjected to the seismic excitation represented by 0.723g PGA response spectrum, 'the rocking becomes unstable and overturning occurs because θ_o increases unbounded at this angle' (ASCE 2005). This conclusion on stability has nothing to do with the dynamics of a rocking block, and it is entirely an artifact of the shape of the capacity curves. As can be seen in Figure 2-2 (c), due to the reverse curvature of the intersecting response spectrum, every RB will have two solutions (in zone2 and zone 3) and will never witness the maximum rotation ($\theta_o = \alpha$) before overturning. However, referring to Figure 2-2(c) and assuming that a RB in RM can be represented by a SDOF oscillator, depending on the time history of the earthquake record, the block may in fact overturn for the 0.706g PGA earthquake (at its intersection with the capacity curve in zone 3) rather than the 0.723g PGA earthquake (which has a single intersection point with the capacity curve).

2.6.4 *Maximum capacity and minimum capacity contradiction*

The example discussed above used the NBK spectrum with the peak spectral acceleration at 2.5Hz. However, the design ground or floor response spectrum in a different application may have other characteristics, e.g., the high-frequency ENA spectrum (Atkinson and Elgohary, 2007) for some east-coast NPPs. Therefore, it might be necessary to consider a peak at a much higher frequency than the 2.5 Hz

of the NBK spectrum. Consequently, it may also be necessary to consider the capacity curve at high frequencies. For large values of frequency (thus low values of θ_o), SAH_{CAP} in Equation (20) attains a maximum, given by

$$MaxSAH_{CAP} = \frac{2g\ \tan\alpha}{F_H\, F_V}$$

For $F_H = 1$ and $F_V = 1$,

$$MaxSAH_{CAP} = 2g\ \tan\alpha$$

The above would be $2\alpha g$ as given in Equation (26) for small angle approximation. Figure 2-2(d) shows capacity curves for three blocks with the same α but varying p for $F_H = 1$ and $F_V = 1$. The three curves asymptote to a maximum capacity $2g\tan\alpha$ at large frequency. For the high-frequency ENA spectra of some of the east-coast NPPs, the PSA occurs at 25Hz (Dar and Hanna, 2012). Figure 2-2(d) shows the generic ENA spectrum, given by Atkinson and Elgohary (2007), anchored at 0.41g. The intersection to the left side of the peak occurs at 11.5 Hz for the top two capacity curves. The minimum acceleration required to initiate rocking is $g\tan\alpha$. However, for the high-frequency east-coast spectrum, per ASCE 43-05, it would require more than $2g\tan\alpha$ ground acceleration to induce rocking rather than $g\tan\alpha$. This is a contradiction in the ASCE 43-05 method.

At maximum rotation, $\theta_o = \alpha$, the RB is highly vulnerable to overturning and hence has practically zero capacity. Yet the ASCE 43-05 method gives $g\tan\alpha$ (or αg with small angle approximation as given in Equation (26)) as minimum capacity at this rotation. This is another contradiction in the ASCE 43-05 method.

2.6.5 Assumption that much more time is spent near $\theta = 0$ than $\theta = \theta_o$

The free vibration period of the rocking block with initial rotation θ_0, was given by Housner (1963) as

$$T_H = \frac{4}{p} f\left(\frac{\theta_0}{\alpha}\right)$$

where

$$f\left(\frac{\theta_0}{\alpha}\right) = \cosh^{-1}\left[\frac{1}{1-\left(\frac{\theta_0}{\alpha}\right)}\right]$$

Although Housner's period is applicable for small α, say up to 0.35, a

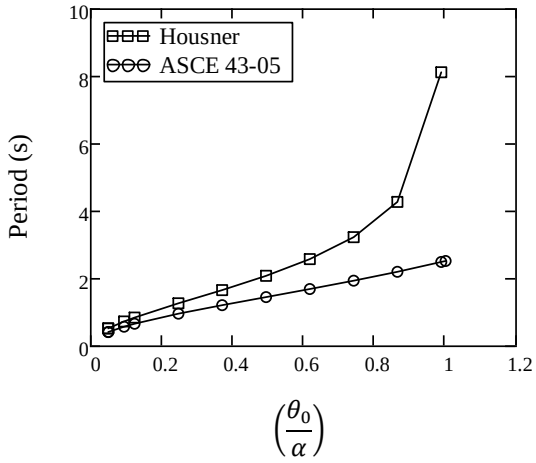

Figure 2-3: Comparison of ASCE 43-05 period with Housner's period

comparison is made with the example in ASCE 43-05 (see Table 2-2) with $\alpha = 0.405$ rad, considering the small difference between the two values. Figure 2-3 shows the difference between Housner's period and the ASCE 43-05 period for the example in Table 2-2 corresponding to the frequency values listed in Table

2-3. It is evident from Figure 2-3 that the free vibration period (per Housner) increases rapidly beyond $\theta_o/\alpha = 0.5$, while the value predicted by ASCE 43-05 does not. The difference between the two grows very large as θ_o/α approaches 1. This means that as the block becomes more vulnerable to overturning), the block spends much more time away from the zero rotation than near it. The assumption in the ASCE 43-05 method that the block spends more time close to zero rotation is not right for relatively larger values of θ_o/α. This is also demonstrated in a later example.

The methodology by Priestley et al. (1978) considers the Housner's period as the period of the SDOF oscillator (Makris and Konstantinidis, 2003). This is another difference between the ASCE 43-05 method and the one given by Priestley et al. (1978).

2.7 Response of RB in RM to Earthquake Records

The original study by Newmark et al. (1973) considered 64 records with PGA ranging from 1.25g to 0.036g from 16 earthquakes, most of them in California. For evaluation of the ASCE 43-05 approximate method, eight records have been selected with varying PGAs ranging from 1.226g to 0.173g (downloaded from PEER = http://peer.berkeley.edu/smcat/). These records are listed in Table 2-4.

The rocking response of the RB is obtained numerically (herein referred to as the Nonlinear Time History (NLTH) analysis) for the selected earthquake records

by direct integration of the equations of motion, expressed in state-space form (Makris and Konstantinidis, 2001):

$$\mathbf{y} = \begin{Bmatrix} \theta \\ \dot{\theta} \end{Bmatrix} \tag{30}$$

with the following time-derivative vector

$$\dot{\mathbf{y}} = \mathbf{f}(\mathbf{y}, t) = \begin{Bmatrix} \dot{\theta} \\ -p^2 \left\{ \sin[\alpha \operatorname{sgn}(\theta) - \theta] + \frac{\ddot{u}_g}{g} \cos[\alpha \operatorname{sgn}(\theta) - \theta] \right\} \end{Bmatrix} \tag{31}$$

The above equations were solved by utilizing the hybrid solver AdamsBDF (PTC, 2012). This hybrid solver utilizes the Adams-Bashforth method but switches to the Backward Differentiation Formula (BDF) method for the stiff system of equations. The energy lost upon impact is taken into account by modifying the angular velocity of the block immediately after impact using the coefficient of restitution given by Equation (4). It is to be noted that in order to calculate equivalent damping of an equivalent SDOF oscillator (Equations (8) and (9)), ASCE 43-05 utilizes Equation (4) and hence the same is used in the NLTH analysis.

Figure 2-4(a) shows the response of a RB, obtained using NLTH analysis, with $2\pi/p = 3$ s ($p = 2.09$ rad/s) and $\alpha = 0.35$ rad subject to the Pacoima Dam 164 motion recorded during the 1971 San Fernando, California, earthquake. The NLTH analysis (Figure 2-4 (a)) yields an apparent period of 1.5 s for the cycle during which the RB experiences the maximum rotation of $\theta_o/\alpha = 0.25$.

Table 2-4: Details of earthquake records used in this study

Group	PGA (g)	Earthquake	Year	Station	Component	PEER records PGA (g)	Record
1	≥0.4	San Fernando, Calif.	1971	Pacoima Dam	S74°W	1.16	PCD 254
		San Fernando, Calif.	1971	Pacoima Dam	S16°E	1.226	PCD 164
		Parkfield, Calif.	1966	Cholame-Shandon No. 2	N65°E	0.476	C02065
		Parkfield, Calif.	1966	Cholame-Shandon No. 5	N85°E	0.442	C05085
2	<0.4 ≥0.3	Imperial Valley, Calif.	1940	El Centro	NS	0.313	I-ELC180
3	<0.3 ≥0.2	Imperial Valley, Calif.	1940	El Centro	EW	0.215	I-ELC270
4	<0.2	Hollister, Calif.	1961	Hollister	N89°W	0.195	B-HCH271
	≥0.1	Helena, Calif.	1935	Helena	EW	0.173	A-HMC270

Applying the ASCE 43-05 method to the response spectrum of this record yields an estimated period of 0.61 s (frequency = 1.64Hz) and normalized rotation $\theta_o/\alpha = 0.078$, Therefore, the ASCE 43-05 method predicts less than half the normalized rotation and less than half the period predicted by the NLTH analysis. Applying the ASCE 43-05 approximate method to the NBK response spectrum corresponding to the PGA of this ground motion results in overturning of the RB considered above, which corresponds to more than 12 times the rotation given by the NLTH analysis. Figure 2-4 (b) shows the response of a RB with $2\pi/p = 3.6$ s ($p = 1.745$ rad/s) and $\alpha = 0.25$ rad. As evident from the figure, for the large normalized rotation (around 0.625), the block spends much more time away from the proximity of zero rotation, i.e., less than 0.25 normalized rotation, considered here as a reasonable limit of proximity. The ASCE method's assumption that a RB spends more time close to

zero rotation than away from it is not valid for relatively larger normalized rotation (>0.25, for the case under consideration).

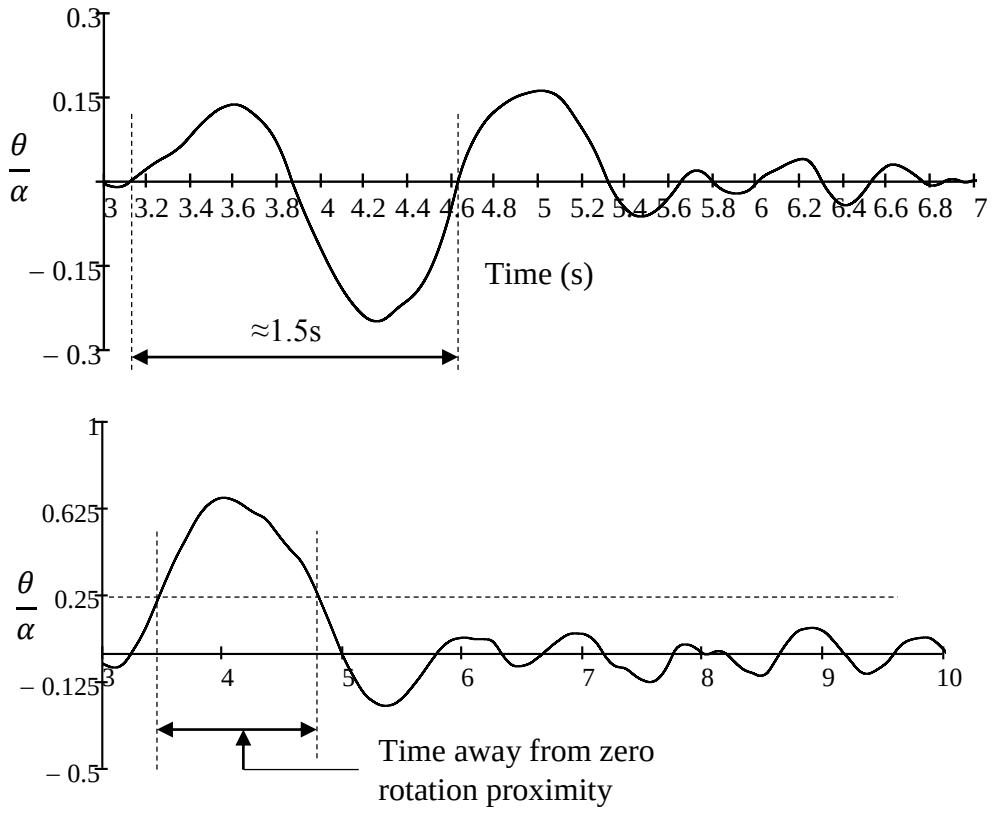

Figure 2-4: Normalized rotation response of RBs obtained by NLTH analysis when subjected to the Pacoima Dam 164 record of the 1971 San Fernando (1971) earthquake. (a) with $2\pi/p = 3$ s ($p = 2.09$ rad/s) and $\alpha = 0.35$ rad (b) with $2\pi/p = 3.6$ s ($p = 1.745$ rad/s) and $\alpha = 0.25$ rad

Table 2-5: Details of analysis and RB geometry

Shape	Rectangular Block (Figure 2-1)
Stockiness (Figure 2-1)	$\alpha = 0.15;\ \ 0.25;\ \ 0.35;\ \ 0.405$ rad
Damping for values of α considered in ASCE 43-05 method	$\beta_e = 1.08\%; 3.06\%;\ 6.16\%; 8.41\%$
Size	$0.186\text{ m} < R \leq 11.92\text{ m}$ $(\text{i.e.}, 1 < 2\pi/p \leq 8\text{ s})$
Overturning condition	$\theta = \alpha$
Excitation direction	horizontal, unidirectional
Other parameters from ASCE 43-05	$m_L = m_H;\quad F_H = 1;\ \ F_V = 1$

NLTH analyses were conducted for blocks with various values of α and p (see Table 2-5) subjected to the ground motions shown in Table 2-4, and the results were collected and presented as rocking spectra (Makris and Konstantinidis 2003), i.e., plots of normalized maximum rotation θ_o/α versus $2\pi/p$ for geometrically similar blocks (same α). The rocking spectra obtained by NLTH analysis are compared with the ones obtained by the ASCE 43-05 method applied to the NBK design response spectrum corresponding to the PGA of the selected earthquake records, as listed in Table 2-4. Rocking spectra are also obtained for the actual response spectra of the selected records by the ASCE 43-05 method. Rocking spectra obtained by these three methods are compared with one another for the four values of α listed in Table 2-5.

Following ASCE 43-05, the block is considered overturned if $\theta = \alpha$, although it is known that in certain cases, a rocking block can survive rotations that exceed this limit (Makris & Zhang, 1999).

The ground acceleration histories of the earthquake records listed in Table 2-4 are shown in Figure 2-5. According to the ASCE 43-05 method, the equivalent damping ratio β_e depends on α and is given by Equation (9). Table 2-5 lists the values of β_e corresponding to the selected α. For these damping ratios, the response spectra for the selected earthquake records were generated. Figure 2-6 to Figure 2-9 show the earthquake response spectra side-by-side with the PGA-scaled NBK design response spectra for the first four selected earthquake records. These response spectra were necessary to generate rocking spectra by the ASCE 43-05 method.

Figure 2-10 to Figure 2-17 compare rocking spectra corresponding to the ground motions listed in Table 2-4 obtained in three different ways:

1. By NLTH analysis, i.e., integrating Equation (31) by utilizing the AdamsBDF hybrid solver (PTC, 2012). Energy lost upon impact is taken into account through the coefficient of restitution given by Equation (4), relating the angular velocity of the block immediately before and immediately after impact. The rocking spectra derived by this solution are denoted as 'NLTH'.

2. By the ASCE 43-05 (or code) approximate method applied to the NBK design spectrum scaled to the PGA of the earthquake record. These rocking spectra are denoted as 'Code NBK'.

3. By the ASCE 43-05 (or code) approximate method applied to the response spectrum of the earthquake record. These rocking spectra are denoted as 'Code RS'.

Figure 2-10 shows the difference between the rocking spectra obtained by the three methods described above for the Pacoima Dam 164 record of the 1971 San Fernando, California, earthquake. It is obvious from the figure that there is a large disparity between the Code NBK and the NLTH rocking spectra. For all four values of α, the Code NBK curve is excessively conservative in all cases. For example, it can be seen that, regardless of α, the ASCE 43-05 method using the NBK spectrum predicts overturning for any block with $2\pi/p < 4$ s, which corresponds to blocks smaller than approximately $R = 3$ m. Contrary to the Code NBK rocking spectra, the Code RS rocking spectra, are in most cases unconservative. The disparity between the Code RS curve and the NLTH rocking spectra is in several cases quite significant. For instance, for an electrical cabinet with height 2 m and width 0.73 m (i.e., $\alpha = 0.35$ rad and $p = 2.63$ rad/s), $2\pi/p = 2.39$ s, and from Figure 2-10 (bottom-left), the maximum θ_o/α predicted by the Code RS curve is less than one-third the value predicted by NLTH analysis. For a geometrically similar smaller cabinet, e.g. 1.4 m tall by 0.51 m wide ($2\pi/p = 2$ s), the former method predicts that θ_o/α is less that 0.2, while NLTH analysis predicts overturning. Of interest here, is the Code RS response for $\alpha = 0.35$ ($\cong 20^o$). This response is entirely different from the response predicted by the method by Priestley et al. (1978), for $\alpha = 20^o$, for San Fernando PCD 164 record given in Makris and Konstantinidis

(2003). At $2\pi/p \cong 3$s, the method given by Priestley et al. (1978) predicts overturning (Makris and Konstantinidis, 2003), whereas the Code RS curve in Figure 2-10 predicts the normalized rotation to be less than 0.1.

Figure 2-11 shows that for the Pacoima Dam 254 record of the 1971 San Fernando earthquake, the ASCE 43-05 method applied to the NBK spectrum (Code NBK) provides the most conservative results for all values of α, whereas the same method applied to the response spectrum (Code RS) for this record leads to inconsistent degree of conservatism. The Code RS curve is more conservative than the NLTH curve for α = 0.25 rad but less conservative for α = 0.15 rad.

Figure 2-12 shows the rocking spectra for the Cholame-Shandon No. 2 record of the 1966 Parkfield, California, earthquake. It can be seen from this figure, that the Code NBK curve predicts overturning for a wide range of blocks with α = 0.15 and α = 0.25 rad, whereas the NLTH curves predicts rocking response that is well within safe levels. On the other hand, for α = 0.35, the Code NBK curve is less conservative than the NLTH curve. This shows that the ASCE 43-05 method does not always provide more conservative results than the NLTH analysis. Figure 2-12 also shows that the NLTH rocking spectrum predicts maximum response that deviates significantly from that of the Code RS rocking spectra. For α = 0.405 rad, the Code NBK and Code RS curves predict appreciable rotations (especially for smaller blocks), whereas the solution obtained by NLTH analysis shows no uplift at all for any value of $2\pi/p$ between 1 and 8 s.

Figure 2-13 shows the rocking spectra for the Cholame-Shandon No. 5 record of the 1966 Parkfield earthquake. In this figure, the Code RS curve is found to be in the middle of the other two curves for all values of α except for α = 0.15 rad. Thus for the two Parkfield earthquake records, significant difference is found between the solutions obtained by the NLTH analysis and the ASCE 43-05 method. For instance, for the block in the example illustrated in Appendix B of ASCE 43-05, and revisited herein (Table 2-2), both the Code NBK and Code RS curves predict finite rotations at 0.41g PGA, whereas the NLTH analysis predicts no uplift for both the Parkfield records with the PGA > 0.41g.

Figure 2-14 and Figure 2-15 depict rocking spectra due to the NS (180) and EW (270) components of the El Centro Array #9 record of the 1940 Imperial Valley, California, earthquake. Even though neither of these motions is strong enough to induce uplift for blocks with α = 0.35 and 0.405 rad, Figure 2-11 shows that the ASCE 43-05 method when applied to the NBK spectrum (Code NBK) predicts rocking of very small blocks with α = 0.405 rad and of blocks with a wide range of $2\pi/p$ values for α = 0.35 rad. The Code RS curve follows the same trend. Here, for both records the Code NBK and the Code RS are found to be more conservative than the NLTH curve.

Figure 2-16 and Figure 2-17 show rocking spectra corresponding to motions recorded during the 1961 Hollister and 1935 Helena earthquakes, respectively. These motions have low PGA values compared with the records discussed above. Of interest here is the response to Helena record in Figure 2-17, where the solution

by equations of motion (NLTH) results in no uplift whatsoever for all values of α, whereas the Code NBK curve predicts overturning at $2\pi/p = 1\ s$ for $\alpha = 0.25$ and at $2\pi/p = 2.8\ s$ for $\alpha = 0.15$.

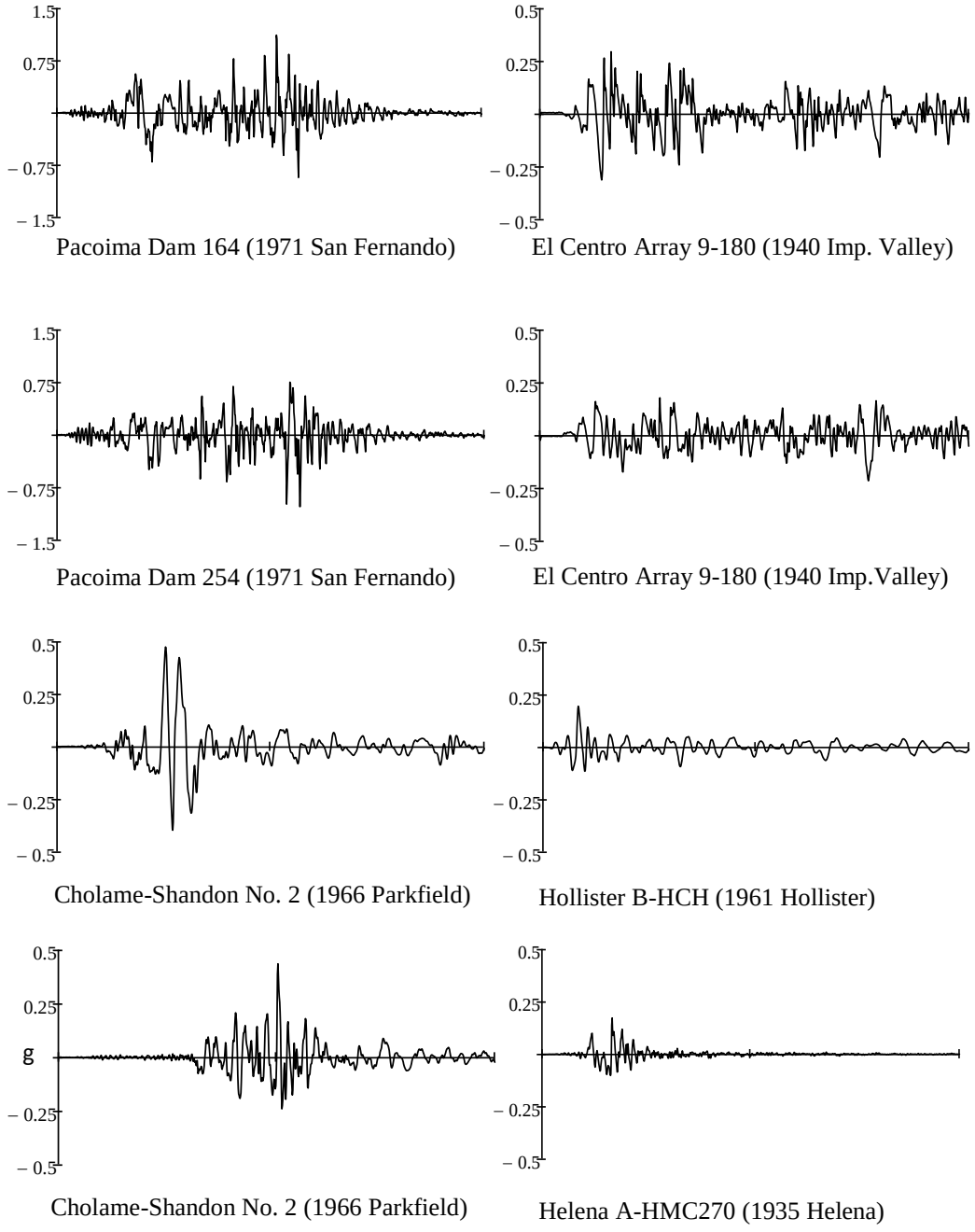

Figure 2-5: Ground acceleration time histories of the earthquake records used in this study.

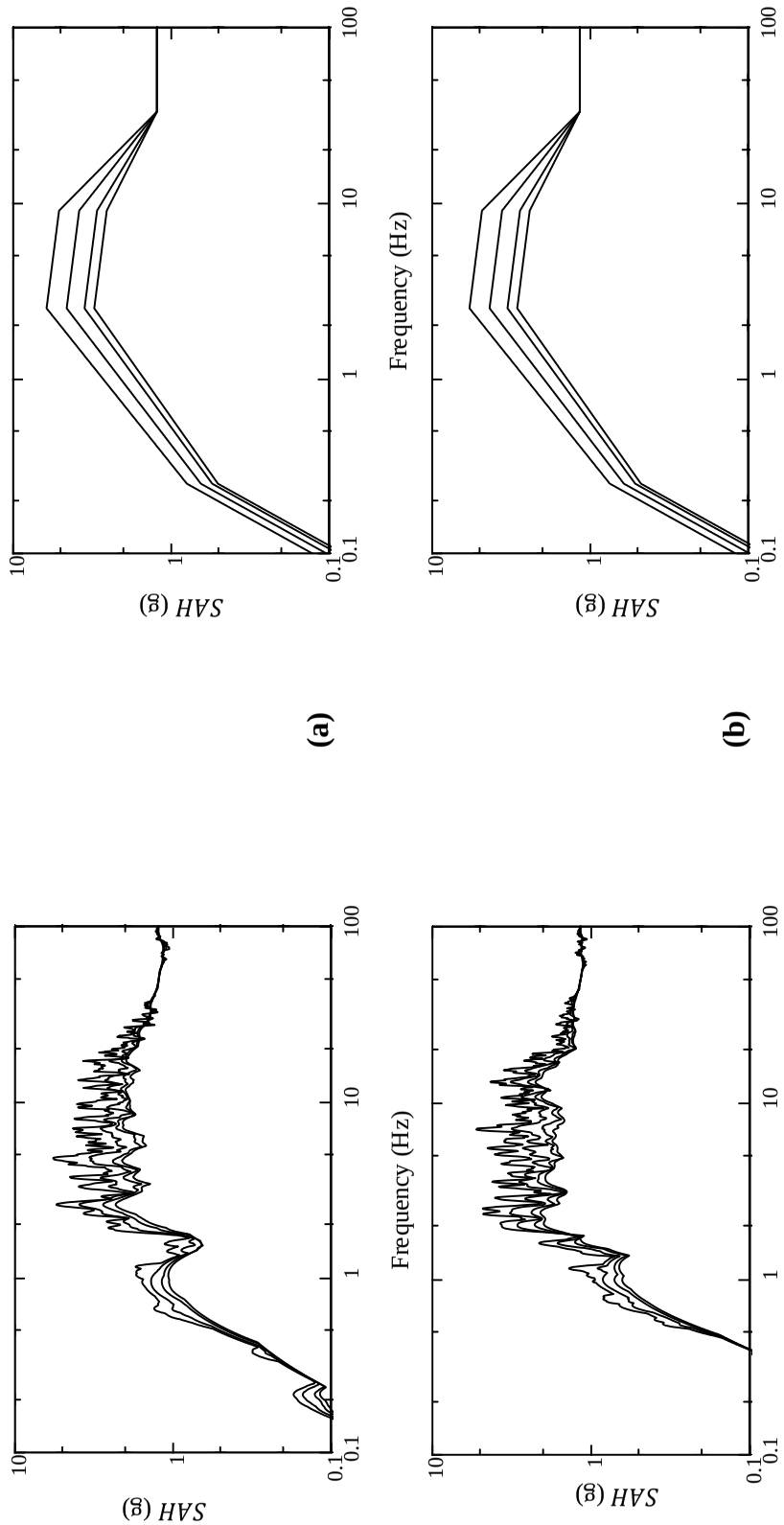

Figure 2-6: Response spectra (left column) for the damping ratios in Table 2-5 and the NBK spectra (right column) for the corresponding PGAs of 1971 San Fernando earthquake records: (a) Pacoima Dam 164, (b) Pacoima Dam 254. The response spectra curves for the individual records are in the increasing order of damping from the top curve to the bottom curve.

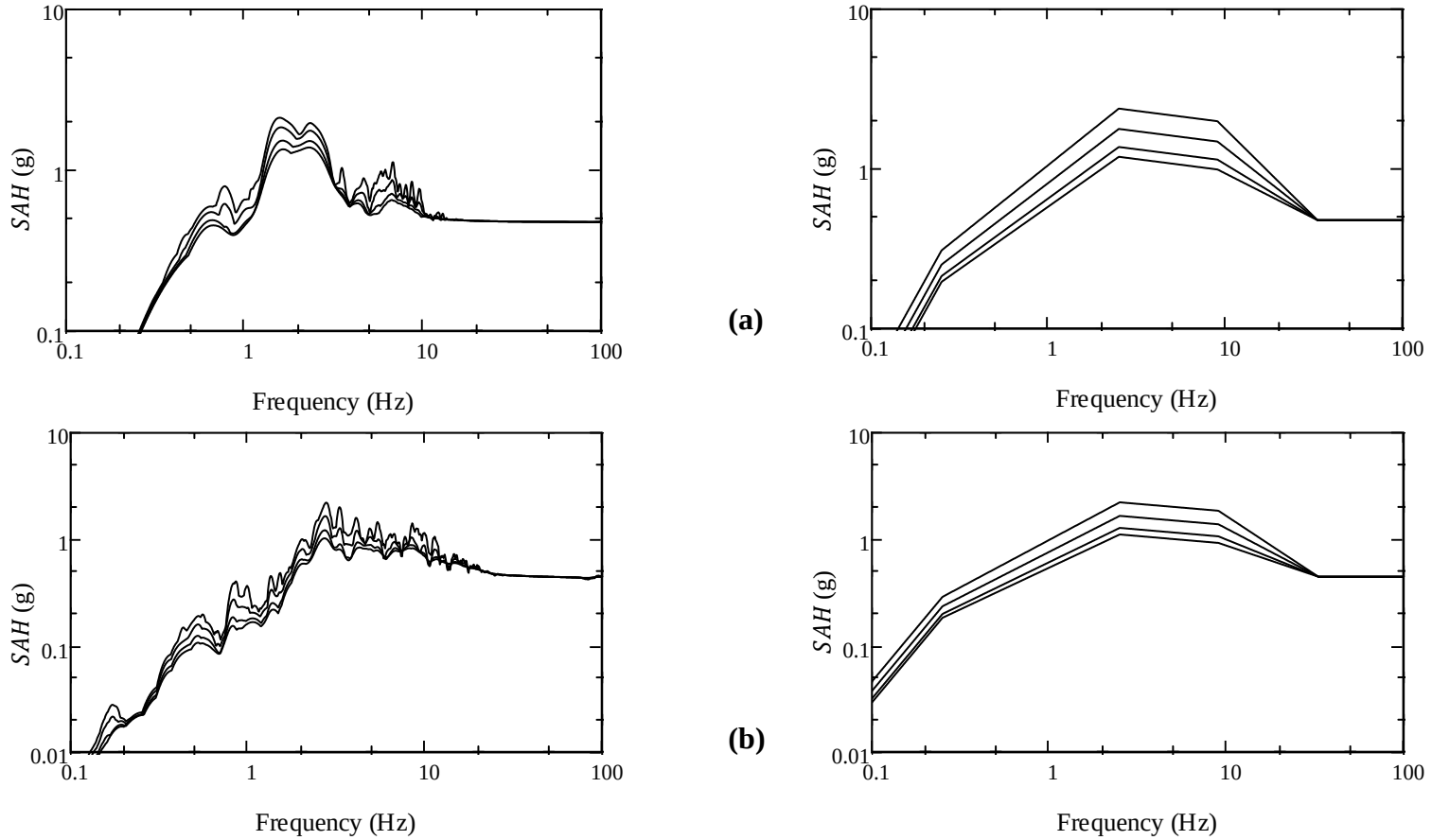

Figure 2-7: Response spectra (left column) for the damping ratios in Table 2-5 and the NBK spectra (right column) for the corresponding PGAs of 1966 Parkfield, California, earthquake records: (a) Cholame-Shandon No. 2 and (b) Cholame-Shandon No. 5. The response spectra curves for the individual records are in the increasing order of damping from the top curve to the bottom curve.

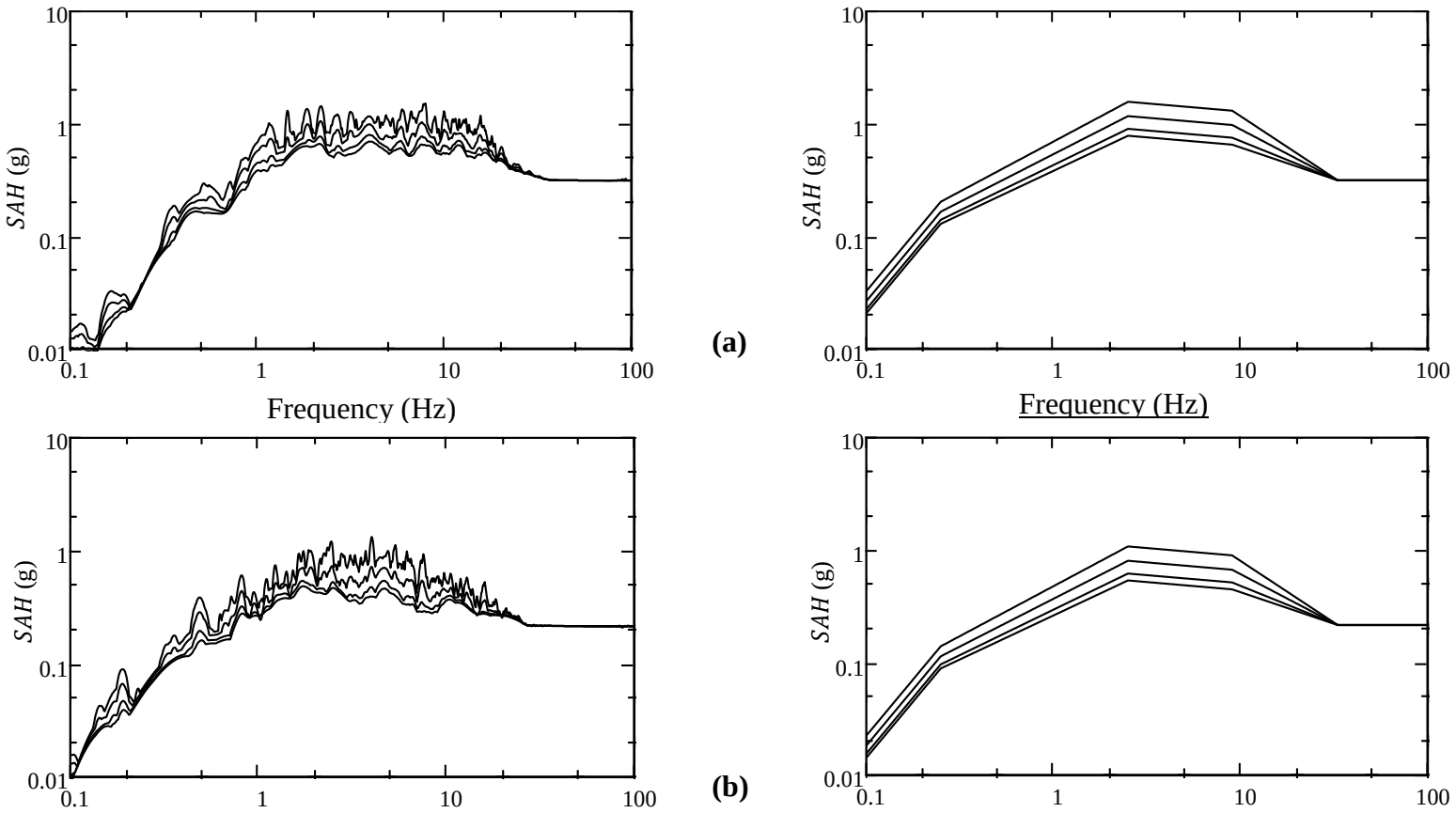

Figure 2-8: Response spectra (left column) for the damping ratios in Table 2-5 and the NBK spectra (right column) for the corresponding PGAs of 1940 Imperial Valley, earthquake El Centro array #9 records: **(a)** NS (180) and **(b)** EW (270). The response spectra curves for the individual records are in the increasing order of damping from the top curve to the bottom curve.

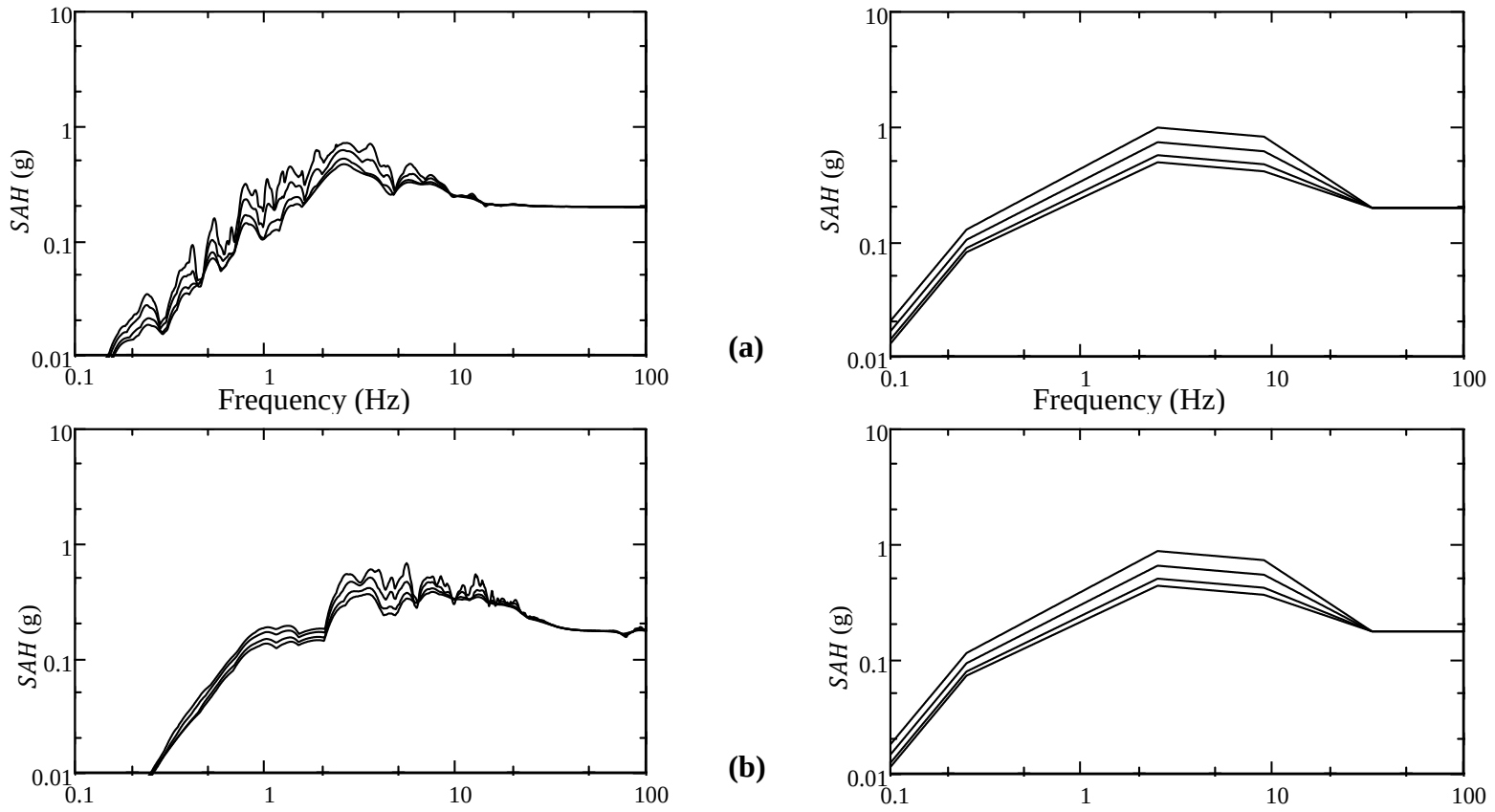

Figure 2-9: Response spectra (left column) for the damping ratios in Table 2-5 and the NBK spectra (right column) for the corresponding PGA of the earthquake records: **(a**) 1961 Hollister B-HCH 271 and (**b)** 1935 Helena A-HMC 270. The response spectra curves for the individual records are in the increasing order of damping from the top curve to the bottom curve.

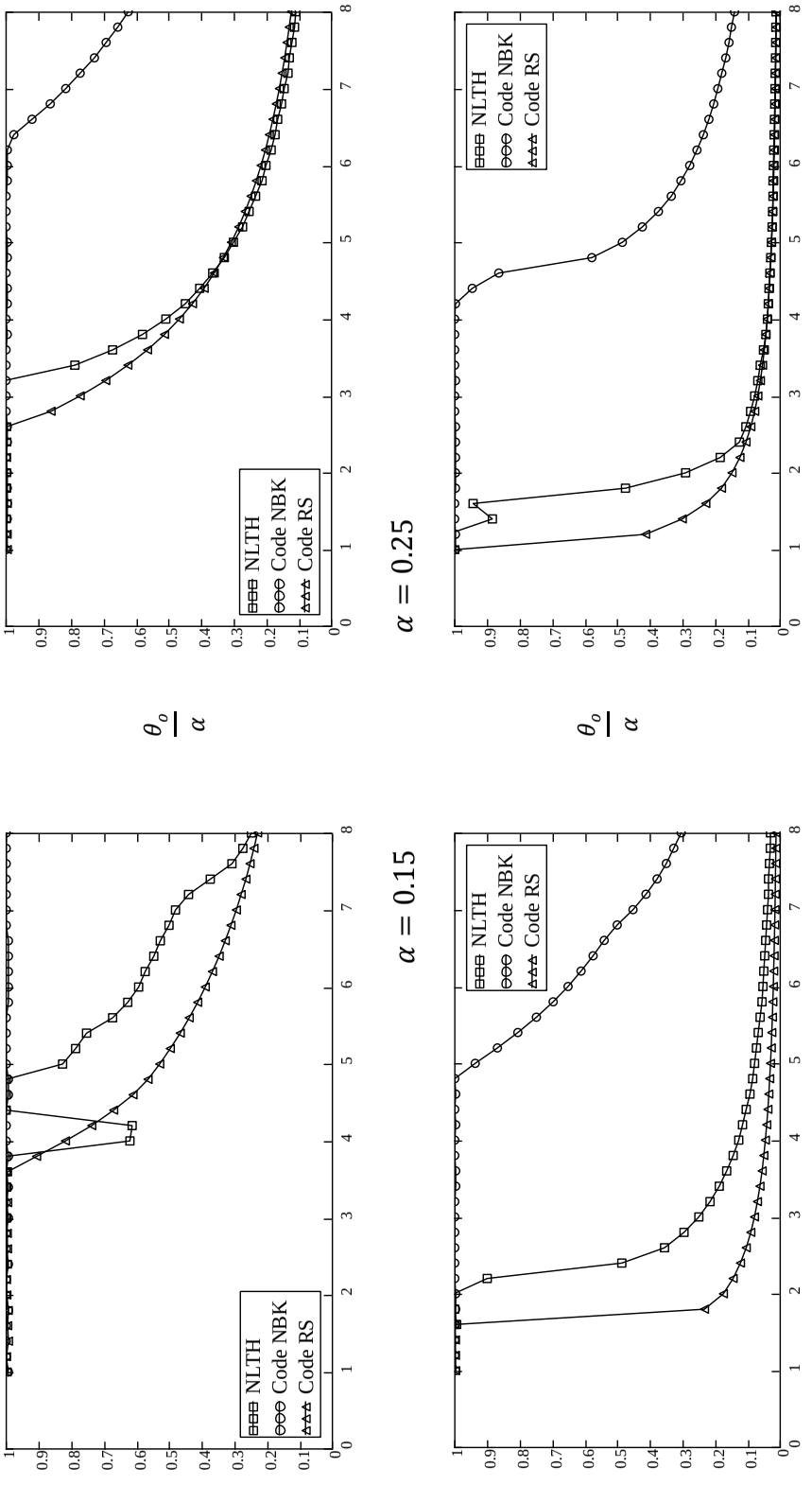

Figure 2-10: Comparison of rocking spectra for 1971 San Fernando earthquake Pacoima Dam 164 record by NLTH analysis, ASCE43-05 method with NBK spectrum (code NBK) and ASCE43-05 method with actual response spectrum (code RS).

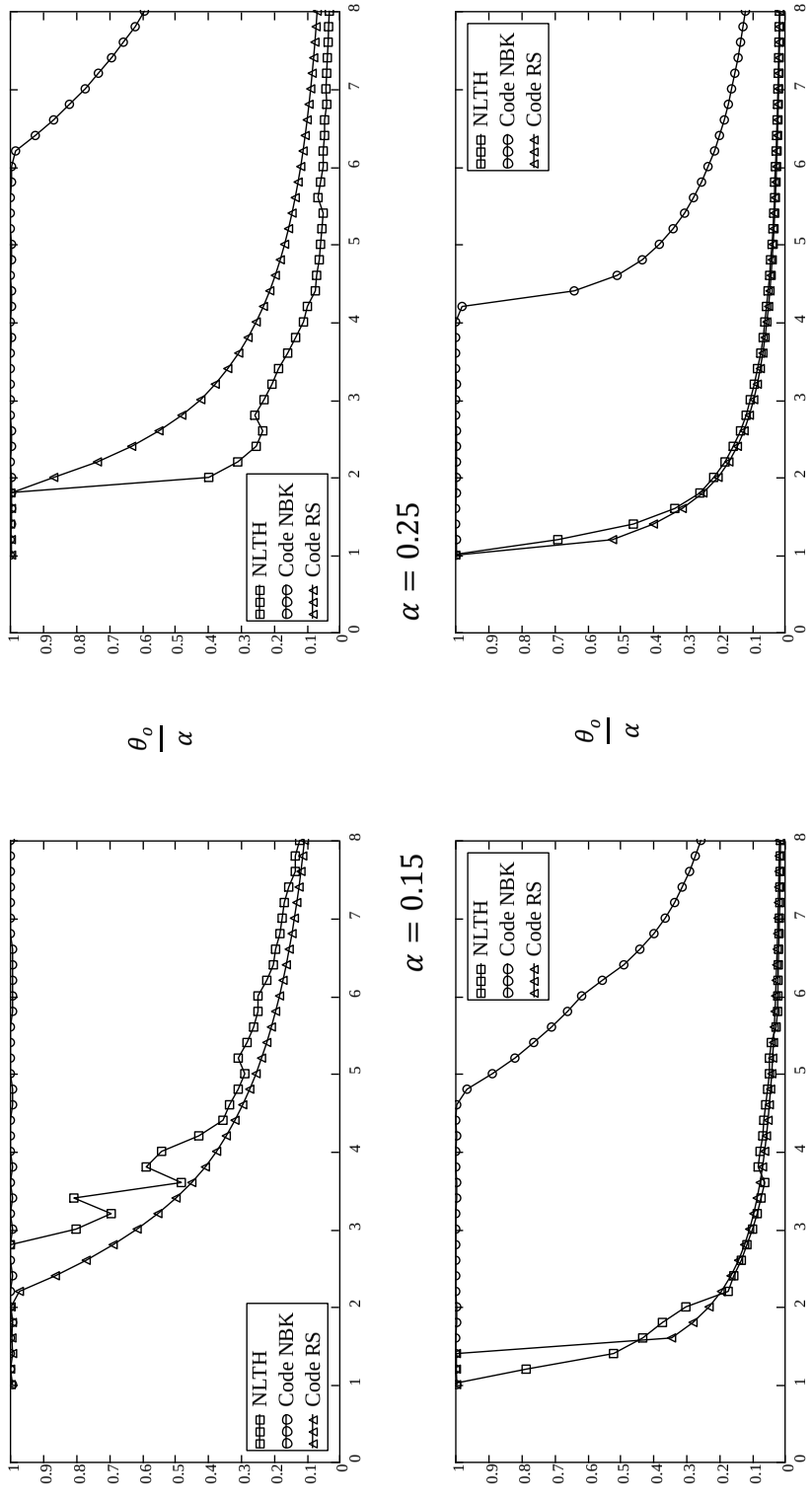

Figure 2-11: Comparison of rocking spectra for 1971 San Fernando earthquake Pacoima Dam 254 record by NLTH analysis, ASCE43-05 method with NBK spectrum (code NBK) and ASCE43-05 method with actual response spectrum (code RS).

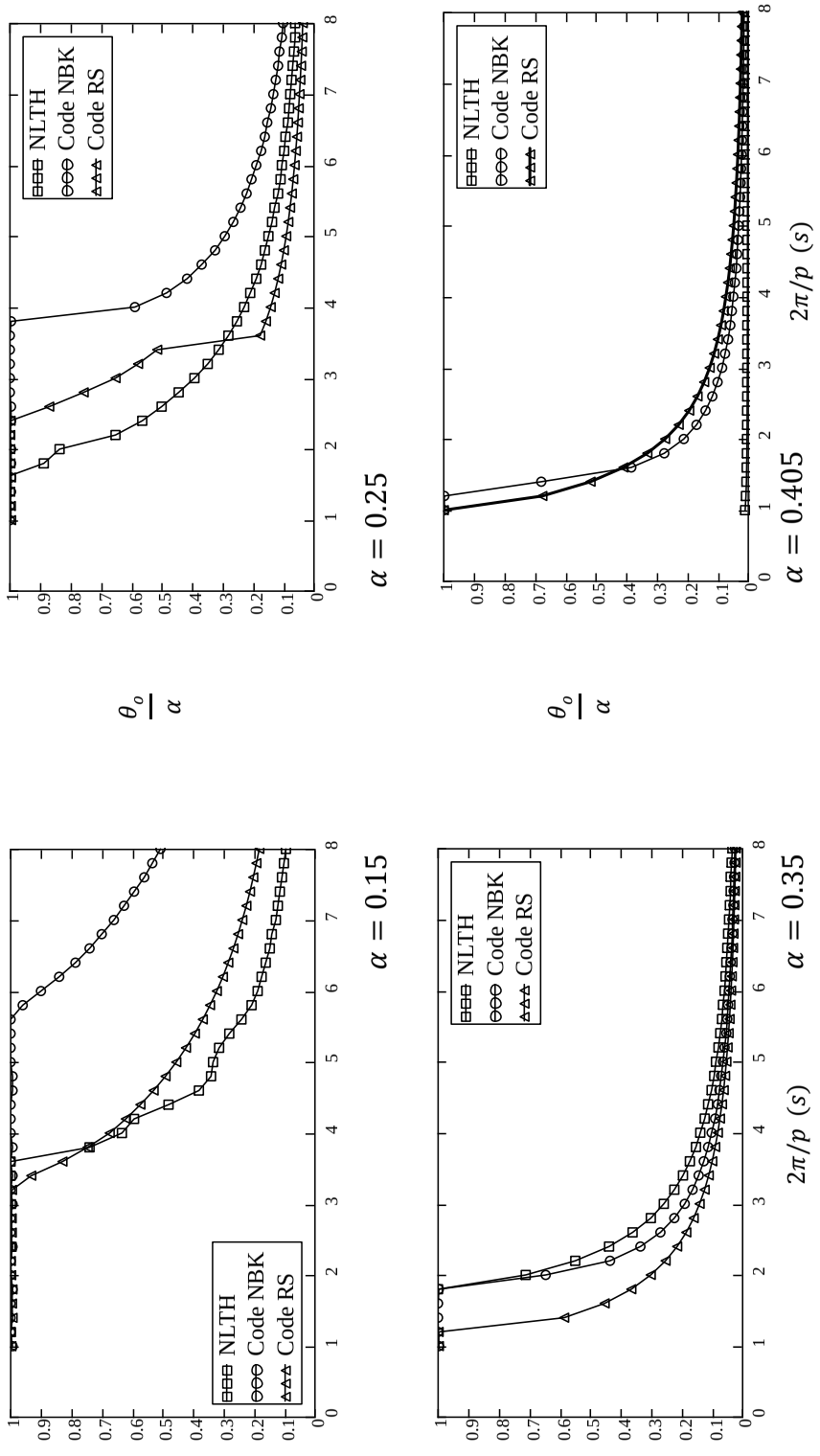

Figure 2-12: Comparison of rocking spectra for 1966 Parkfield, California, earthquake Cholame-Shandon No. 2 record by NLTH analysis, ASCE43-05 method with NBK spectrum (code NBK) and ASCE43-05 method with actual response spectrum (code RS).

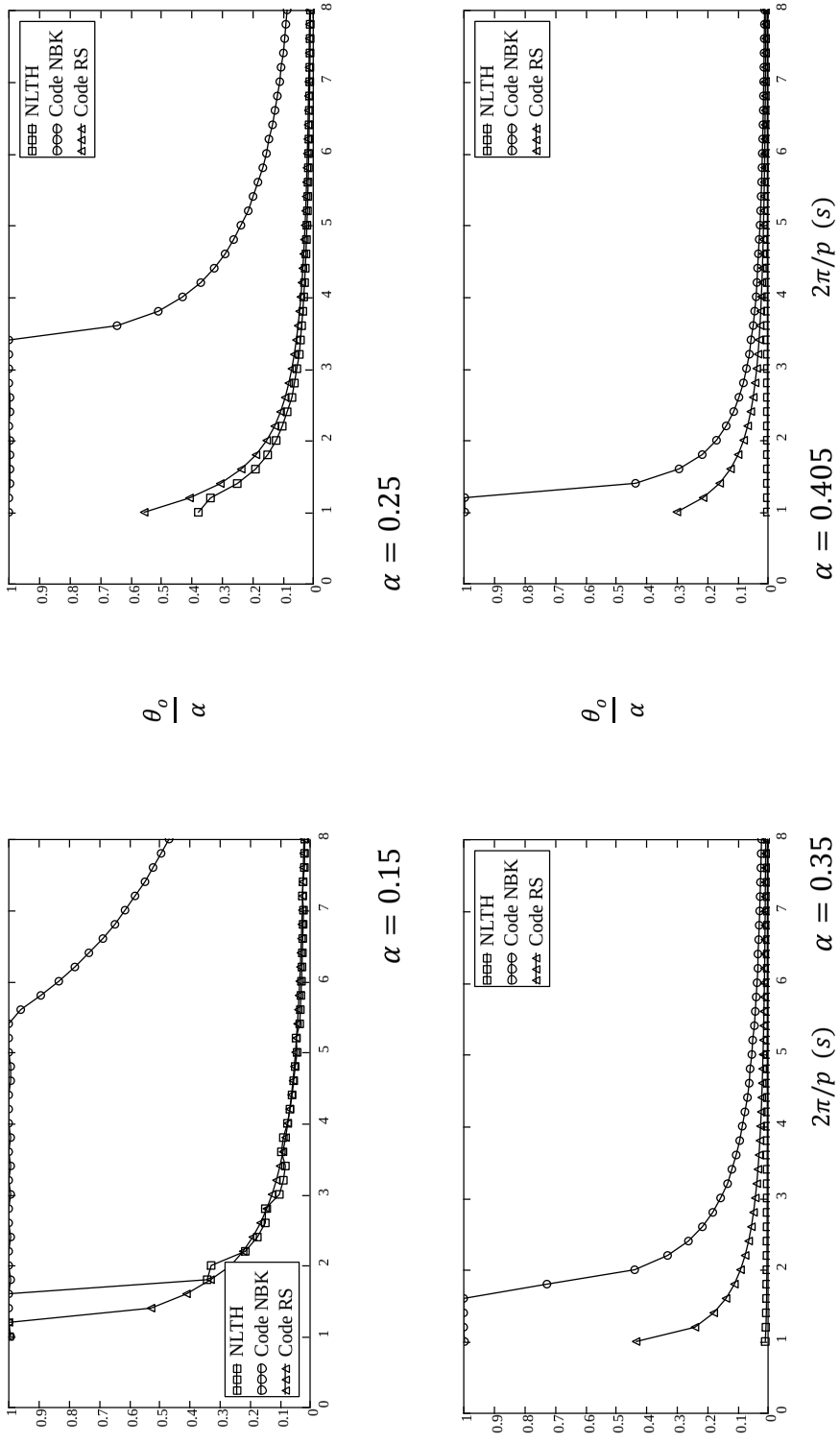

Figure 2-13: Comparison of rocking spectra 1966 Parkfield, California, earthquake Cholame-Shandon No. 5 record by NLTH analysis, ASCE43-05 method with NBK spectrum (code NBK) and ASCE43-05 method with actual response spectrum (code RS).

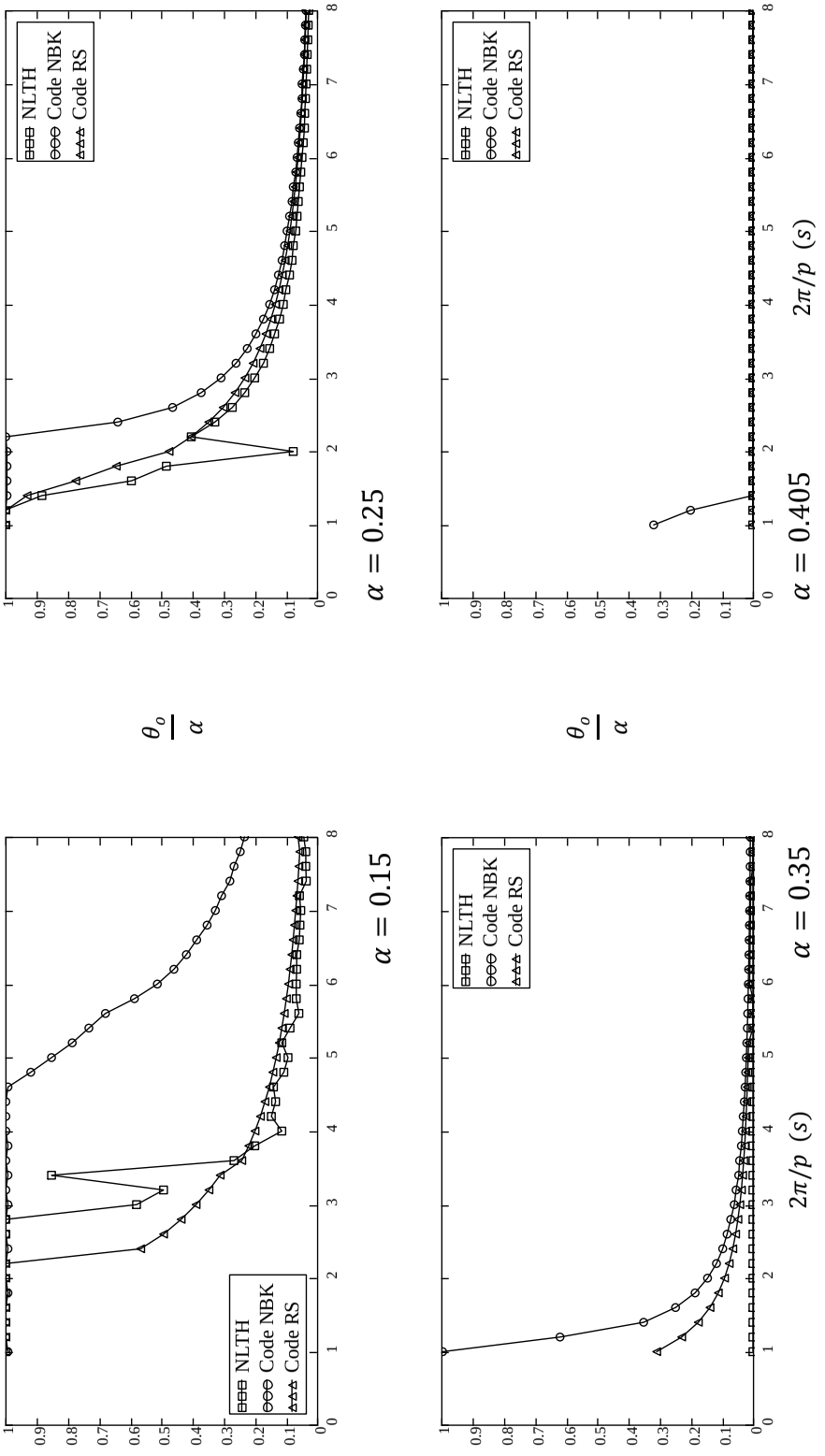

Figure 2-14: Comparison of rocking spectra for Imperial Valley earthquake El Centro array #9 NS (180) record by NLTH analysis, ASCE43-05 method with NBK spectrum (code NBK) and ASCE43-05 method with actual response spectrum (code RS).

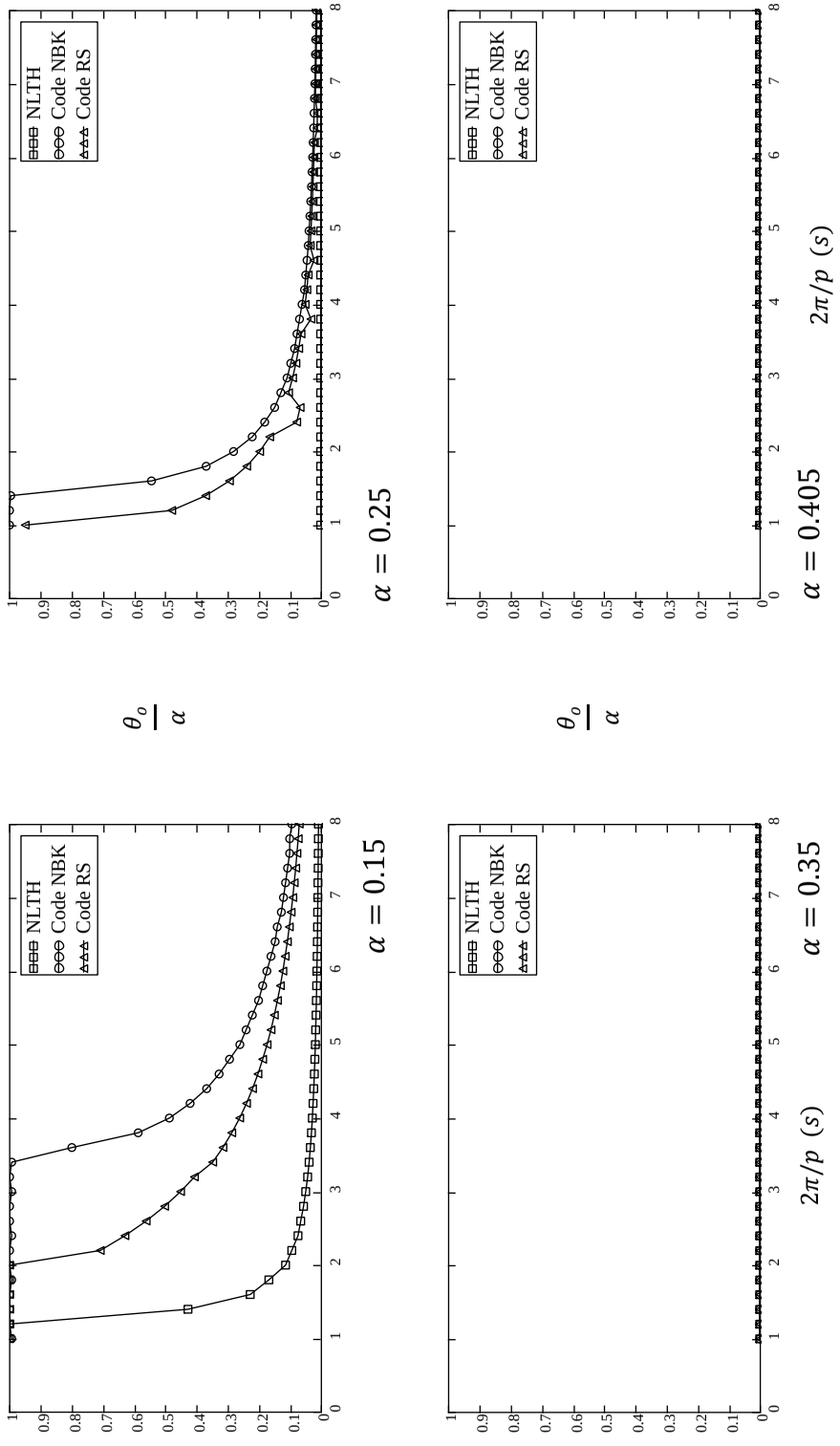

Figure 2-15: Comparison of rocking spectra for Imperial Valley earthquake El Centro array #9 EW (270) record by NLTH analysis, ASCE43-05 method with NBK spectrum (code NBK) and ASCE43-05 method with actual response spectrum (code RS)

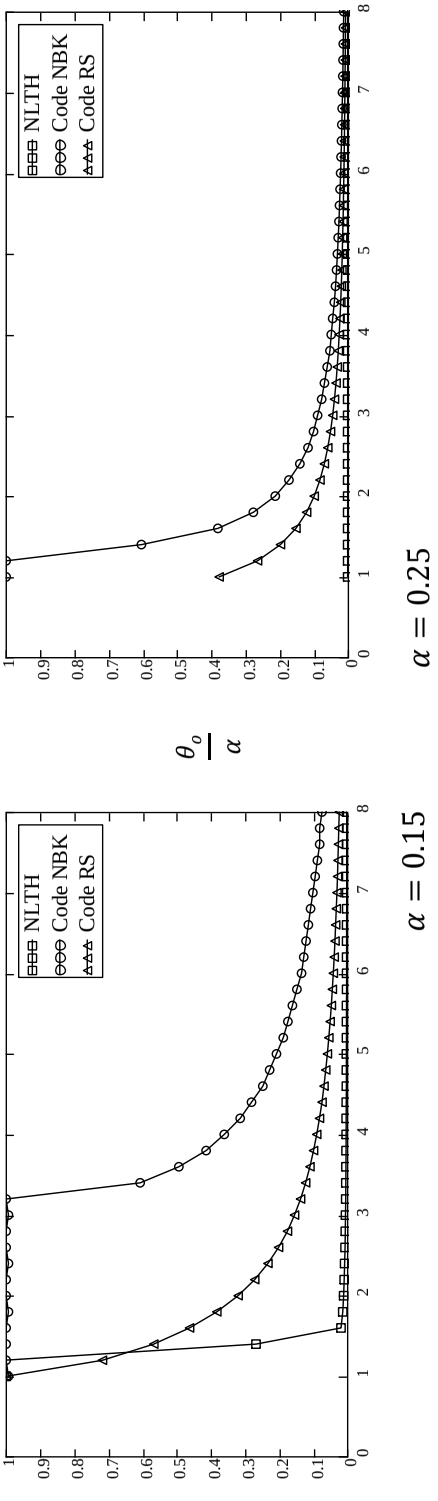

Figure 2-16: Comparison of rocking spectra for 1961 Hollister, California earthquake B-HCH271 record by NLTH, ASCE43-05 method with NBK spectrum (code NBK) and ASCE43-05 method with actual response spectrum (code RS).

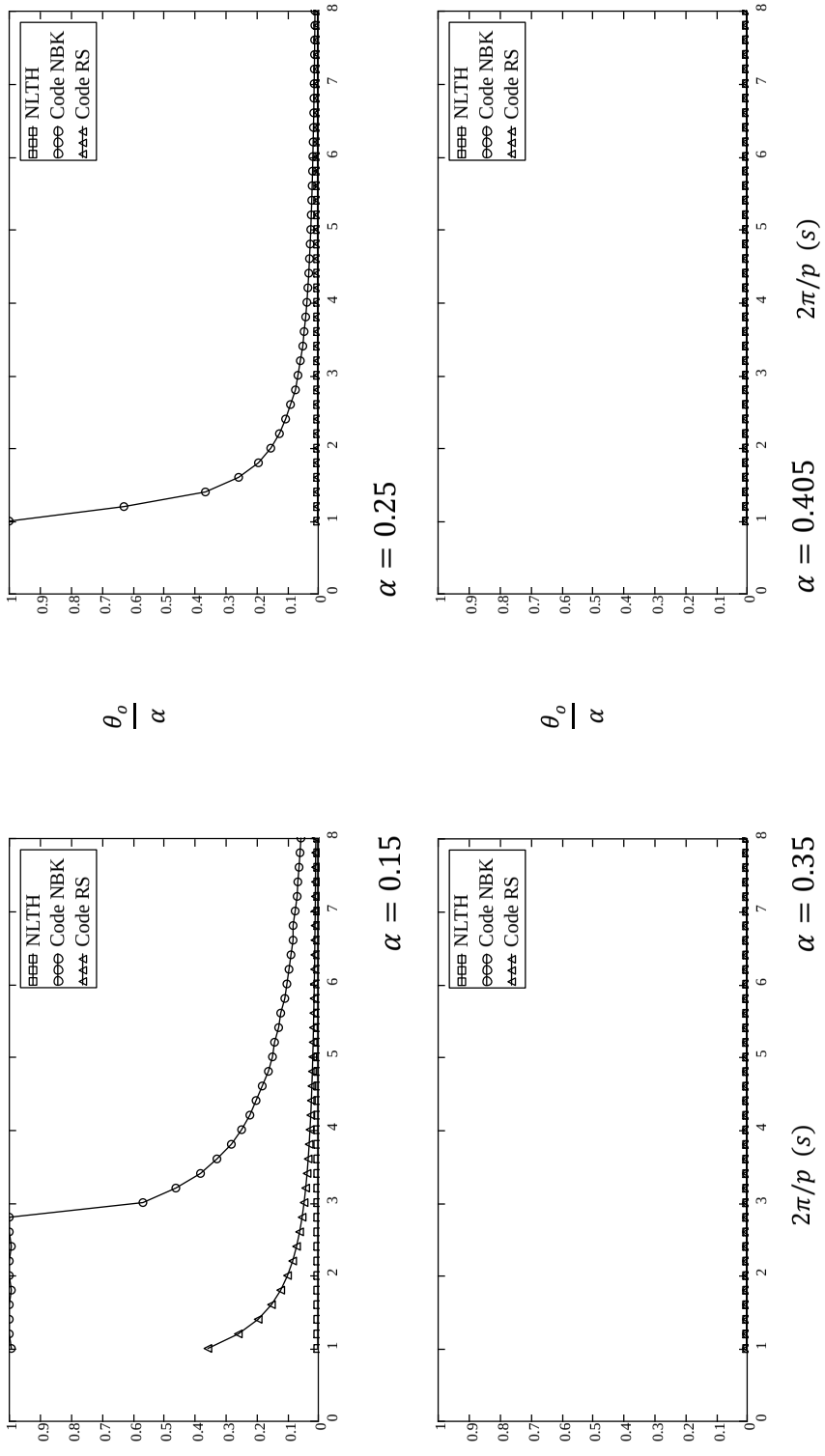

Figure 2-17: Comparison of rocking spectra for 1935 Helena Earthquake A-HMC 270 record by NLTH, ASCE43-05 method with NBK spectrum (code NBK) and ASCE43-05 method with actual response spectrum (code RS) given in columns

2.8 Summary, Conclusions and Recommendations

This study evaluates the ASCE 43-05 seismic design criteria for rocking objects in nuclear facilities. ASCE 43-05 provides an approximate method for estimating the maximum uplift rotation of a rocking object in lieu of time history analysis. The method leans on the erroneous assumption that a rocking block can be represented by an 'equivalent' SDOF oscillator with constant damping, but whose period depends on the amplitude of the rocking. The study first exposes several inherent inconsistencies of the method. Subsequently, using a suite of ground motions, the study compares the predictions of the ASCE 43-05 method with the solutions obtained by direct integration of the nonlinear equations of motion of the rocking block. It is also found that the ASCE 43-05 method is different from the method given by Priestley et al. (1978) in terms of the period and damping of an equivalent SDOF oscillator, and the total response. There are significant differences between the evaluation of the ASCE 43-05 method carried out in this paper and the evaluation of the method by Priestley et al. (1978) in Makris and Konstantinidis (2003).

It is concluded that for the pure planar rocking response subject to horizontal excitation, the approximate method given in the standard ASCE 43-05 provides highly unreliable estimates of peak rocking rotation and thus cannot be used to assess the overturning vulnerability of unanchored objects. The predictions of the ASCE 43-05 method for a wide range of block geometries under various levels of excitation were found to deviate, often significantly, and in many cases

unconservatively, from the predictions obtained by numerically solving the nonlinear equation of motion for the rocking block. Considering the significant level of effort required to implement the ASCE 43-05 method, its inherent contradictions, and its inconsistent conservatism in estimating the seismic demands on rocking objects, it is concluded that the results obtained by nonlinear time history analysis are more accurate, reliable and less time consuming than those by the ASCE 43-05 method. The use of nonlinear dynamic analysis is recommended to obtain the pure planar rocking response of unanchored objects in nuclear facilities.

Presently, rocking spectra are not used in the nuclear industry. The current standard of practice in nuclear facilities for estimating the rocking response of an unanchored object is to deal with them on a case by case basis using approximate methods, such as that in ASCE 43-05. The level of effort in generating design rocking spectra for each elevation within a nuclear power plant would be much lower than the cumulative effort required to solve the rocking problem every time it is encountered, within the lifetime, of the plant. It is therefore recommended that the nuclear industry adopts the concept of rocking spectra, generated by nonlinear dynamic analysis. The models used should acknowledge the fact that the dynamics of rocking structures are inherently different from those of oscillatory structures.

2.9 References for Chapter 2

American Society of Civil Engineers. (2005). *ASCE 43-05 – Seismic Design Criteria for Structures, Systems and Components in Nuclear Facilities.* Reston, Virginia, USA.

American Society of Civil Engineers. (2006). *ASCE 41-06 – Seismic Rehabilitation of Existing Buildings.* Reston, Virginia, USA.

Atkinson, G. M. and Elgohary, M. (2007). Typical uniform hazard spectra for eastern North American sites at low probability levels. *Canadian Journal of Civil Engineering,* **34**, 12-18.

Blume, J. (1960). A reserve energy technique for the earthquake design and rating of structures in the inelastic range. *2nd World Conference on Earthquake Engineering.* Tokyo and Kyoto, Japan.

Chatzis, M. N. and Smyth, A. W. (2012). Modeling of the 3D rocking problem. *International Journal of Non-Linear Mechanics,* **47**(4), 85–98.

Chaudhuri, S. R. and Hutchinson, T. C. (2005). Characterizing frictional behavior for use in predicting the seismic response of unattached equipment. *Soil Dynamics and Earthquake Engineering,* **25**, 591–604.

Choi, B. and Tung, C. D. (2002). Estimating sliding displacement of an unanchrored body subjected to earthquake. *Earthquake Spectra,* **18**(4), 601–613.

Comerio, M. C. (editor) (2005). *Testbed study on a laboratory building: exercising seismic performance assessment. Report No. 2005/12.* Berkeley, CA: Pacific Earthquake Engineering Research Center (PEER) University of California, Berkeley.

CSA (2008). *CSA N291.Requirements for Safety-Related Structures for CANDU Nuclear Power Plants.* Rexdale, Ontario, Canada: Canadian Standards Association.

Dar, A. and Hanna, J. D. (2012). Beyond design basis seismic evaluation of nuclear power plants at Bruce site. *Proc. of the 3rd International Structural Specialty Conference*. Edmonton, Alberta: Canadian Society for Civil Engineering.

Dar, A., Konstantinidis, D., and El-Dakhakhni, W. (2013). Requirement of rocking spectrum in Canadian nuclear standards. *Transactions, 22nd International Structural Mechanics in Reactor Technology Conference (SMiRT22).* San Francisco, CA.

Dar, A., Konstantinidis, D., and El-Dakhakhni, W. W. (2014). Station challenges on seismic qualification of structures, systems and components in Canadian nuclear power plants. *Proceedings of the 10th National Conference in Earthquake Engineering.* Earthquake Engineering Research Institute, Anchorage, AK.

EPRI (1991). *NP-6041-SL-Revision 1. A Methodology for Assessment of Nuclear Power Plant Seismic Margin.* Palo Alto, CA: Electric Power Research Institute.

Hogan, S. (1989). On the dynamics of rigid-block motion under harmonic forcing. *Proceedings of the Royal Society of London*, Series A 1989; **425**: 441– 476.

Housner, G. W. (1963). The behavior of inverted pendulum structures during earthquakes. *Bulletin of the Seismological Society of America,* **53**(2), 403–417.

Hutchinson, T. C. and Chaudhuri, S. R. (2006). Bench-shelf system dynamic characteristics and their effects on equipment and contents. *Earthquake Engineering and Structural Dynamics,* **135**(13), 1631–165.

Jensen, S. R. and Gurbuz, O. (2011). Chapter 7.6 ASCE 4 Revision 2. : Sliding and Rocking of Unanchored Components and Structures. *Structures Congress 2011* (pp. 2178-2189). Las Vegas: American Society of Civil Engineers.

Jeong, M. Y., Suzuki, K., and Yim, S. C. (2003). Chaotic rocking behavior of freestanding objects with sliding motion. *Journal of Sound and Vibration,* **262**(5), 1091–1112.

Konstantinidis, D. and Makris, N. (2005). *Experimental and analytical studies on the seismic response of freestanding and anchored laboratory equipment, Report No. 2005/07.* Berkeley, CA: Pacific Earthquake Engineering Research Center (PEER); University of California, Berkeley.

Konstantinidis, D. and Makris, N. (2007). The dynamics of a rocking block in three dimensions. *Proc. 8th Hellenic Society for Theoretical and Applied Mechanics International Congress on Mechanics.* Patras, Greece.

Konstantinidis, D. and Makris, N. (2009). Experimental and analytical studies on the response of freestanding laboratory equipment to earthquake shaking. *Earthquake Engineering and Structural Dynamics,* **38**(6), 827–848.

Konstantinidis, D. and Makris, N. (2010). Experimental and analytical studies on the response of 1/4-scale models of freestanding laboratory equipment subjected to strong earthquake shaking. *Bulletin of Earthquake Engineering,* **8**(6), 1457–1477.

Konstantinidis, D. and Nikfar, F. (2015). Seismic response of sliding equipment and contents in base-isolated buildings subjected to broad-band ground motions. *Earthquake Engineering and Structural Dynamics*, (in press).

Lopez, G. D. and Soong, T. (2003). Sliding fragility of block-type non-structural components. Part 1: unrestrained components. *Earthquake Engineering and Structural Dynamics,* **32**(1), 111–129.

Luk, V. K., Spencer, B. W., Lam, I. P., and Dameron, R. A. (2005). *NUREG/CR-6865. Parametric evaluation of seismic behavior of freestanding spent fuel dry cask storage systems. Sandia National Laboratories.* U.S. Nuclear Regulatory Commission.

Makris, N. and Konstantinidis, D. (2003). The rocking spectrum and the limitations of practical design methodologies. *Earthquake Engineering and Structural Dynamics,* **32**(2), 265–289.

Makris, N., and Roussos, Y. (2000). 'Rocking response of rigid blocks under near-source ground motions. *Géotechnique,* **50**(3), 243–262.

Makris, N., and Zhang, J. (1999). *Rocking response and overturning of anchored equipment under seismic excitations. Report No. 1999/06.* Berkeley: Pacific Earthquake Engineering Research Center (PEER), University of California.

McGuire, R. K., Silva, W. J., and Constantino, C. J. (2001). *NUREG/CR-6728: Technical Basis for Revision of Regulatory Guidance on Design Ground*

Motions: Hazard- and Risk-consistent Ground Motion Spectra Guidelines. United States Regulatory Commission.

Newmark, N. M., Blume, J. H., and Kapur, K. K. (1973). Seismic Design Spectra for Nuclear Power Plants. *Journal of the Power Division, ASCE*, **99**(2), 287-303.

Nigam, S. C. and Jennings, P. C. (1969). Calculation of Response Spectra from Strong-Motion Earthquake Records. *Bulletin of the Seismological Society of America,* **59**(2), 909-922.

Priestley, M., Evison, R., and Carr, A. J. (1978). Seismic response of structures free to rock on their foundations. *Bulletin of the New Zealand National Society for Earthquake Engineering,* **11**(3), 141–150.

PTC. (2012). Mathcad 15.0. Parametric Technology Corporation, 140 Kendrick Street, Needham, MA 02494, USA.

Reed, J. W., and Kennedy, R. P. (1994). *Methodology for Developing Seismic Fragilities EPRI TR-103959.* Palo Alto, California: Electric Power Research Institute.

Schau, H., and Johannes, M. (2013). Rocking and sliding of unanchored bodies subjected to seismic load according to conventional and nuclear rules. *4th ECCOMAS Thematic Conference on Computational Methods in Structural Dynamics and Earthquake Engineering (COMPDYN).* Kos Island, Greece.

Shao, Y. and Tung, C. (1999). Seismic response of unanchored bodies. *Earthquake Spectra,* **15**(3):523–536.

Shenton III, H. W. (1996). Criteria for initiation of slide, rock, and slide-rock rigid-body modes. *Journal of Engineering Mechanics (ASCE),* **122**(7), 690–693.

Taniguchi, T. (2002). Non-linear response analyses of rectangular rigid bodies subjected to horizontal and vertical ground motion. *Earthquake Engineering and Structural Dynamics,* **31**(8), 1481–1500.

USNRC. (1973). *Design Response Spectra for Seismic Design of Nuclear Power Plants, Regulatory Guide 1.60, Revision 1.* Washington, DC: United States Nuclear Regulatory Commission.

USNRC. (2014). *Design Response Spectra for Seismic Design of Nuclear Power Plants, Regulatory Guide 1.60, Revision 2.* Washington, DC: United States Regulatory Commission.

Wesley, D. A., Kennedy, R. P., and Richter, P. J. (1980). Analysis of the seismic collapse capacity of unreinforced masonry wall structures. *Proc. 7th World Conference on Earthquake Engineering.* Istanbul, Turkey.

Yim, C. K., Chopra, A., and Penzien, J. (1980). Rocking response of rigid blocks to earthquakes. *Earthquake Engineering and Structural Dynamics,* **8**(6), 565–587.

Zhang, J. and Makris, N. (2001). Rocking response of free-standing blocks under cycloidal pulses. *Journal of Engineering Mechanics*, **127**(5), 473-483.

CHAPTER 3 SUMMARY, CONCLUSIONS, RECOMMENDATIONS AND FUTURE RESEARCH

3.1 Summary

This study evaluates the ASCE 43-05 seismic design criteria for rocking objects in nuclear facilities. ASCE 43-05 provides an approximate method for estimating the maximum uplift rotation of a rocking object in lieu of time history analysis. The method leans on the erroneous assumption that a rocking block can be represented by an 'equivalent' SDOF oscillator with constant damping, but whose period depends on the amplitude of the rocking. The study first exposes several inherent inconsistencies of the method. Subsequently, using a suite of ground motions, the study compares the predictions of the ASCE 43-05 method with the solutions obtained by direct integration of the nonlinear equations of motion of the rocking block. It is also found that the ASCE 43-05 method is different from the method given by Priestley et al. (1978) in terms of the period and damping of an equivalent SDOF oscillator, and the total response. There are significant differences between the evaluation of the ASCE 43-05 method carried out in this paper and the evaluation of the method by Priestley et al. (1978) in Makris and Konstantinidis (2003).

3.2 Conclusions

It is concluded that for the pure planar rocking response subject to horizontal excitation, the approximate method given in the standard ASCE 43-05 provides highly unreliable estimates of peak rocking rotation and thus cannot be used to

assess the overturning vulnerability of unanchored objects. The predictions of the ASCE 43-05 method for a wide range of block geometries under various levels of excitation were found to deviate, often significantly, and in many cases unconservatively, from the predictions obtained by numerically solving the nonlinear equation of motion for the rocking block. Considering the significant level of effort required to implement the ASCE 43-05 method, its inherent contradictions, and its inconsistent conservatism in estimating the seismic demands on rocking objects, it is concluded that the results obtained by nonlinear time history analysis are more accurate, reliable and less time consuming than those by the ASCE 43-05 method. The use of nonlinear dynamic analysis is recommended to obtain the pure planar rocking response of unanchored objects in nuclear facilities.

3.3 Recommendations

Presently, rocking spectra are not used in the nuclear industry. The current standard of practice in nuclear facilities for estimating the rocking response of an unanchored object is to deal with them on a case by case basis using approximate methods, such as that in ASCE 43-05. The level of effort in generating design rocking spectra for each elevation within a nuclear power plant would be much lower than the cumulative effort required to solve the rocking problem every time it is encountered, within the lifetime, of the plant. It is therefore recommended that the nuclear industry adopts the concept of rocking spectra, generated by nonlinear dynamic analysis. The models used should acknowledge the fact that the dynamics of rocking structures are inherently different from those of oscillatory structures.

3.4 Future Research

Seismic design is a onetime process for any structure, component or system in a NPP unless they are modified or altered after their construction or installation, but the risk evaluation is an ongoing process initiated by new requirements emerging from various beyond design basis incidents across the globe. Calculation of risk depends of calculation of capacity. While practicing conservatism in design may enhance redundancy, it may lead to adverse results in determining capacity by artificially amplifying the risk. This undesired amplification of risk shifts the focus from the weak links and directs the financial and other resources of an organization away from the SSCs which are dominate contributors to the seismic risk. Computation of fragilities of rocking objects play an important role in this regard. Some of the rocking objects are found to be significant contributors to the seismic risk in a recent assessment in Canada. Since the Housner's period of a RB in RM increases rapidly for normalized rotation larger than 0.5, an investigation is required in this regard to establish a critical rotation beyond which the block becomes highly susceptible to overturning and to study its impact on the fragility of a RB. Further research is required in this regard to establish the relationship between the critical rotation and fragility of a RB in RM where reaching the critical rotation would be considered as failure of a RB.

Other possible topics of future research are the effect of various factors on response such as block and base flexibilities, vertical acceleration, uneven distribution of mass etc.

APPENDIX A SEISMIC DESIGN BASIS OF NUCLEAR POWER PLANTS

A.1 NBK spectrum

The response spectrum in USNRC Reg. Guide 1.60 (Revision 1 (1973) and Revision 2 (2014)) was given by Newmark, Blume and Kapur (1973) as design spectrum for NPPs, popularly known as the NBK spectrum. The design response spectra in USNRC Reg. Guide 1.60 Revision 1 (1973) for various levels of damping have control points (frequencies) A, B, C and D at 33Hz, 9Hz, 2.5Hz, and 0.25Hz, with the ground motion parameters, 36 inch peak ground displacement (PGD) and 1g peak ground acceleration (PGA). In order to obtain the DBE for a particular site, the USNRC Reg. Guide 1.60 recommends scaling of this spectrum at the desired level of damping to the PGA of the site. For example if the site PGA is 0.5g, the values of the spectrum corresponding to the desired damping ratio would be multiplied by 0.5g/1.0g=0.5. The acceleration value at point A is the site PGA and acceleration values at points B, C and D obtained from Newmark et al. (1973) are given below:

$$S_A^{\mathrm{B}} = 4.25 - 1.02\ln(\beta),$$

$$S_A^{\mathrm{C}} = 5.1 - 1.224\ln(\beta),$$

$$S_A^{\mathrm{D}} = 0.23\big(2.85 - 0.5\ln(\beta)\big)$$

where, β is the damping ratio expressed as percentage number (e.g. 5 for 5% damping), S_A^{B}, S_A^{C}, and S_A^{D} are acceleration in g's. The displacement ordinate at point D has been converted to acceleration from the displacement equation given in Newmark et al. (1973).

The response spectrum is made of straight lines between these control frequencies on log-log scale. Of interest here are only two control points, f_{D}= 0.25Hz and f_{C}=2.5Hz. Since maximum spectral acceleration occurs at 2.5Hz, the equation of straight line on log-log scale between f_{D} and f_{C} takes the form:

$$\log\left(\frac{S_A}{S_A^C}\right) = \log\left(\frac{f}{f_C}\right)^s$$

where, S_A is the required spectral acceleration at frequency f, and s is the slope of the line. Using the values of spectral acceleration at 0.25Hz and 2.5Hz for 8.4% damping (for the example considered in ASCE 43-05), the equation to obtain the demand acceleration SAH_{DEM} reduces to the following:

$$SAH_{DEM} = \left[2.49\left(\frac{f}{2.5Hz}\right)^{0.78}\right] PGA$$

which is the same as Eq B-38 in Appendix B of ASCE 43-05.

A.2 Equation for NBK Spectrum

In order to obtain rocking spectrum by the ASCE 43-05 method, the NBK spectrum is required at a desired level of damping for a given RB. This damping ratio value is generally an uncommon number, such as 8.4%, given above. Hence it is necessary to form a generalized equation for this spectrum. Given below is a generalized equation for constructing the NBK spectrum at any damping with frequency (in Hz) on x-axis and acceleration (in g's) on y-axis simplified from the details given by Newmark et al. (1973). The spectrum obtained from the equation below consists of straight line segments on log-log scale between control points.

$$S_A = I.\left(\frac{f}{f_r}\right)^s$$

Where, S_A is the spectral acceleration in g, f is the frequency variable, f_r is the larger of the two frequencies defining the control point interval ($r =$ D for the first interval, C for the second and so on). Table A-1 below provides values of I and s for the given frequency ranges with the frequencies: f_E=0.1Hz, f_D=0.25Hz, f_C=2.5Hz, f_B=9Hz and f_A=33Hz. For frequencies greater than 33 Hz, the spectral acceleration is equal to the PGA.

Table A-1: Intercepts and slopes for various frequency intervals

	$f_E \le f < f_D$	$f_D \le f < f_C$	$f_C \le f < f_B$	$f_B \le f < f_A$
I	S_A^D	S_A^C	S_A^B	S_A^A=1
s	2	$\log\left(\frac{S_A^C}{S_A^D}\right)$	$1.798 \log\left(\frac{S_A^B}{S_A^C}\right)$	$1.772 \log\left(\frac{1}{S_A^B}\right)$

In order to obtain spectral acceleration at any damping for any frequency, an equation was written in Mathcad 15.0 with spectral acceleration as a function of damping, PGA and frequency. Simplified version of this equation is given below.

Spectral Acceleration at a given frequency = PGA × Amplification factor

Flow chart to calculate the amplification factor in accordance with Table A.1 is:

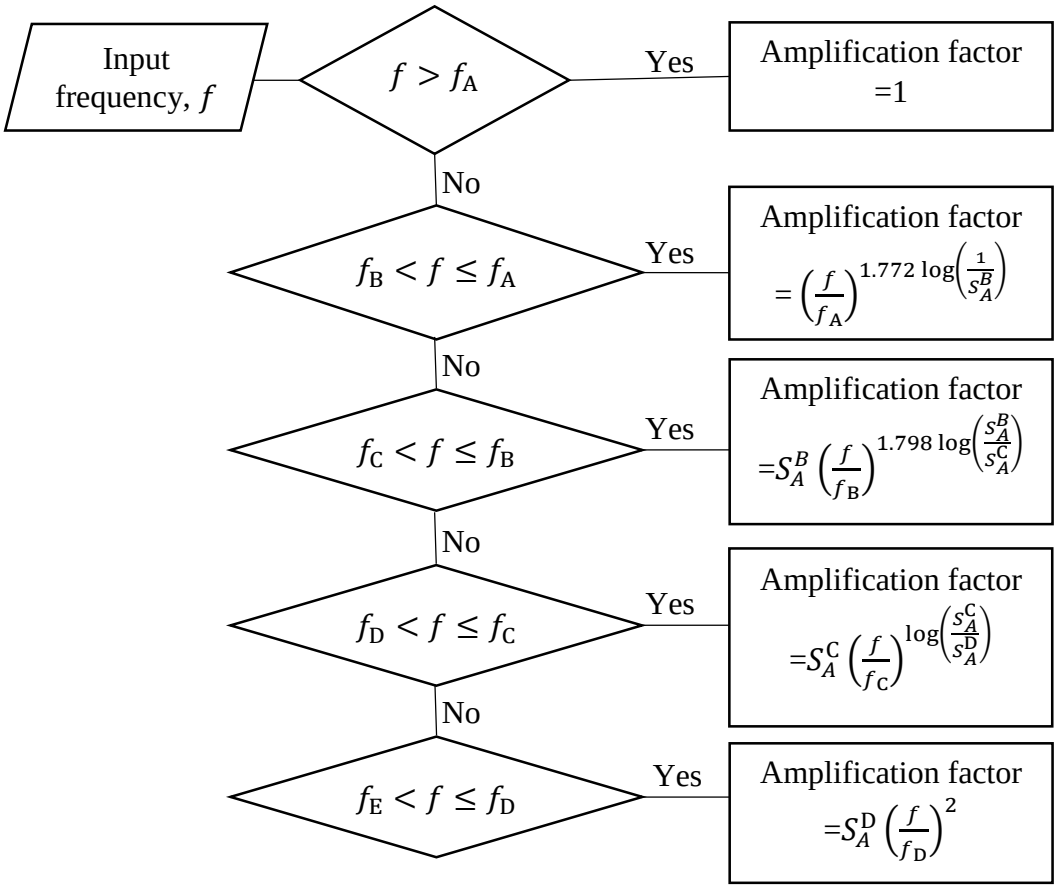

The equation pertaining to the above chart is given below, where f5 corresponds to f_A, f4 corresponds to f_B and so on

$$SA(\beta, PGA, f) := PGA \cdot \begin{cases} 1 & \text{if } f > f5 \\ \text{otherwise} & \\ \quad \left(\frac{f}{f5}\right)^{1.772 \log\left(\frac{1}{B1(\beta)}\right)} & \text{if } f5 \geq f > f4 \\ \quad \text{otherwise} & \\ \quad\quad \left[B1(\beta) \cdot \left(\frac{f}{f4}\right)^{\left(1.798 \cdot \log\left(\frac{B1(\beta)}{C1(\beta)}\right)\right)}\right] & \text{if } f4 \geq f > f3 \\ \quad\quad \text{otherwise} & \\ \quad\quad\quad \left[C1(\beta) \cdot \left(\frac{f}{f3}\right)^{\left(\log\left(\frac{C1(\beta)}{D1(\beta, f2)}\right)\right)}\right] & \text{if } f3 \geq f > f2 \\ \quad\quad\quad \left[D1(\beta, f2)\left(\frac{f}{f2}\right)^2\right] & \text{otherwise} \end{cases}$$

Where, functions (such as B1(β), C1(β) etc.) represent points S_A^B, S_A^C and S_A^D, f is frequency (Hz) and PGA is expressed as a multiple of g. A Mathcad 15 worksheet to obtain and plot the NBK spectrum on tripartite scale was prepared. The response spectra obtained by using the above equation at various levels of damping on tripartite scale are given in Figure A-1. This is in agreement with USNRC Reg. Guide 1.60**.**

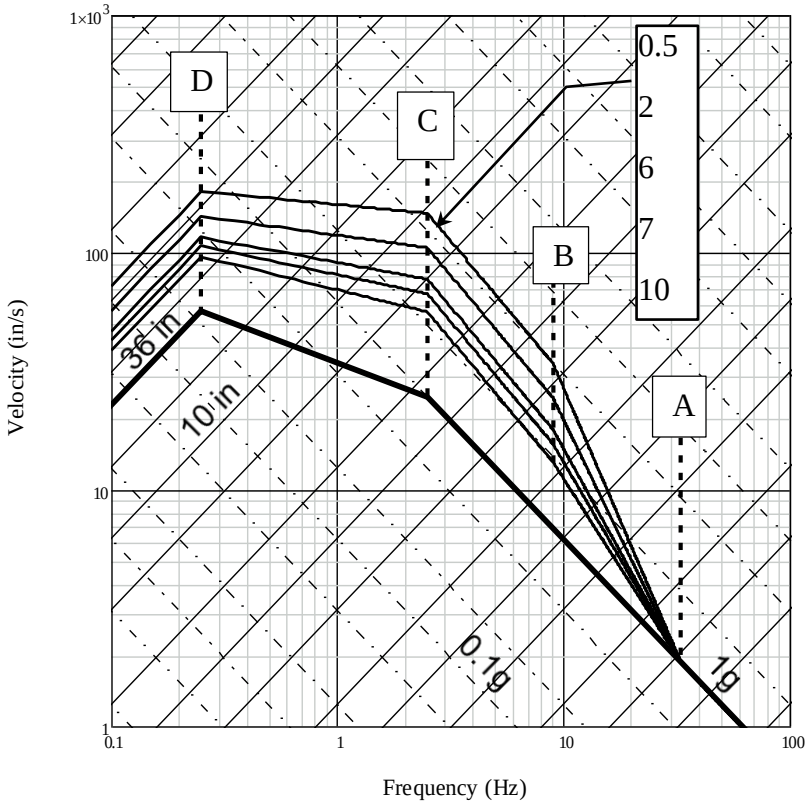

Figure A-1: NBK spectrum obtained at various values of damping. (0.5% to 10%, starting from the top curve). Bottom most line represents ground motion

A.3 Earthquake records considered by Nemark et al (1973)

Table A-1 and A-2 provide the details of the earthquakes and their records respectively considered by Newmark et al (1973). In Table A-2, the earthquake records are divided into five groups in the order of their PGAs based on the four values of α utilized in this study. The selected records have been highlighted in bold letters. From Table A-2, three earthquakes stand out in the first three groups: San Fernando (1971), Parkfield (1966) and Imperial Valley (1940). Hence the records for these three earthquake were selected. Other two earthquakes pertaining to Hollister (1961) and Helena (1935) are selected on the basis of their PGAs being close to the values of α (0.25 and 0.15).

Table A-1: Earthquakes considered by Newmark et al. (1973)

S.No.	Earthquake	Year	Location
1	El Centro	1934	California
2	El Centro	1940	California
3	El Centro	1956	California
4	El Centro	1968	California
5	Eureka	1954	California
6	Ferndale	1951	California
7	Ferndale	1954	California
8	Helena	1935	California
9	Hollister	1961	California
10	Kern county	1952	California
11	Lima	1966	Peru
12	Olympia	1965	Washington
13	Parkfield	1966	California
14	San Fernando	1971	California
15	San Francisco	1957	California
16	Tokachi-Oki	1968	Japan

Table A-2: Details of earthquake records (Newmark et al. (1973)

Group	PGA (g)	Earthquake	Date	Site	Component	PGA (g)	PEER* records PGA	PEER* records Record
1	≥0.4	Parkfield	1966	Cholame-Shandon No. 2, California	S25°W	Not recorded		
		San Fernando	**1971**	Pacoima Dam California	S74°W	1.25	1.16	**PCD 254**
		San Fernando	**1971**	Pacoima Dam California	S16°E	1.241	1.226	**PCD 164**
		Parkfield	**1966**	Cholame-Shandon No. 2, Calif	N65°E	0.51	0.476	**C02065**
		Parkfield	**1966**	Cholame-Shandon No. 5, Calif	N85°E	0.47	0.442	**C05085**
		Lima	1966	Lima, Peru	N8°E	0.42		
2	<0.4 ≥0.3	Parkfield	1966	Cholame-Shandon No. 5, Calif	N5°W	0.4	0.367	C05355

Table A-2: Details of earthquake records (Newmark et al. (1973) Continued…

Group	PGA (g)	Earthquake	Date	Site	Component	PGA (g)	PEER* records PGA	PEER* records Record
2 Contd.	<0.4 ≥0.3	San Fernando	1971	Castaic, ORR, Calif	N21°E	0.34		
		Parkfield	1966	Temblor, Calif.	N25°E	0.33		
		El Centro	**1940**	El Centro, Calif.	NS	0.33	0.313	**I-ELC180**
		Olympia	1949	Olympia, Wash.	S86°W	0.31		
3	<0.3 ≥0.2	San Fernando	1971	Castaic, ORR, Calif	S69°E	0.29		
		Parkfield	1966	Temblor, Calif.	N65°W	0.28		
		San Fernando	1971	V.N. Holiday Inn, Calif.	NS	0.28		
		Lima	1966	Lima, Peru	N82°W	0.27		
		Eureka	1954	Eureka, Calif.	N79°E	0.26		
		El Centro	1934	El Centro, Calif.	NS	0.26		
		Tokachi-Oki	1968	Hachinohe, Japan	EW	0.23		
		San Fernando	1971	Bank of California, Calif.	N11°E	0.23		
		El Centro	**1940**	El Centro, Calif.	EW	0.22	0.215	**I-ELC270**
		Ferndale	1954	Ferndale, Calif.	N46°W	0.209		
		Olympia	1965	Olympia, Wash.	S4°E	0.2		
4	<0.2 ≥0.1	Olympia	1949	Olympia, Wash.	N4°W	0.19		
		Tokachi-Oki	1968	Hachinohe, Japan	NS	0.19		
		Hollister	**1961**	Hollister, Calif.	N89°W	0.189	0.195	**B-HCH271**
		El Centro	1934	El Centro, Calif.	EW	0.18		
		Eureka	1954	Eureka, Calif.	N11°W	0.18		
		Kern County	1952	Taft, Calif.	N21°E	0.18		
		San Fernando	1971	Universal Sheraton, Calif.	NS	0.18		
		Helena	1935	Helena, Mont.	EW	0.16	0.173	**A-HMC270**
		Kern County	1952	Taft, Calif.	S69°E	0.16		

Table A-2: Details of earthquake records (Newmark et al. (1973) Continued…

Group	PGA (g)	Earthquake	Date	Site	Component	PGA (g)	PEER* records PGA	PEER* records Record
4 Contd	<0.2 ≥0.1	Olympia	1965	Olympia, Wash.	S86W	0.16		
		San Fernando	1971	V.N. Holiday Inn, Calif.	EW	0.15		
		Ferndale	1954	Ferndale, Calif.	N44°E	0.146		
		El Centro	1968	El Centro, Calif.	NS	0.142		
		San Fernando	1971	Bank of California, Calif.	N79°W	0.14		
		San Fernando	1971	Universal Sheraton, Calif.	EW	0.13		
		San Francisco	1957	Golden Gate Park, Calif	N80°W	0.13		
		Helena	1935	Helena, Mont.	NS	0.13		
		Ferndale	1951	Ferndale, Calif.	S44°W	0.123		
		Ferndale	1951	Ferndale, Calif.	N46°W	0.12		
		San Francisco	1957	Golden Gate Park, Calif	N10°E	0.11		
5	<0.1	Hollister	1961	Hollister, Calif.	S01W	0.076		
		Kern county	1952	Hollywood age PE Lot, Calif.	NS	0.063		
		Kern county	1952	Hollywood age Basement Calif	NS	0.059		
		El Centro	1968	El Centro, Calif.	EW	0.058		
		El Centro	1956	El Centro, Calif.	EW	0.055		
		Kern county	1952	Hollywood age Basement Calif	EW	0.046		
		Kern county	1952	Hollywood age PE Lot, Calif.	EW	0.043		
		El Centro	1956	El Centro, Calif.	NS	0.036		

*PEER = http://peer.berkeley.edu/smcat/

A.4 References for Appendix A

Mathcad 15.0. (2012). Parametric Technology Corporation, 140 Kendrick Street, Needham, MA 02494, USA.

Newmark, N. M., Blume, J. H., & Kapur, K. K. (1973). Seismic Design Spectra for Nuclear Power Plants. *Journal of the Power Division, ASCE*, 287-303.

USNRC. (1973). *Design Response Spectra for Seismic Design of Nuclear Power Plants, Regulatory Guide 1.60, Revision 1.* Washington, D.C.: United States Nuclear Regulatory Commission.

USNRC. (2014). *Design Response Spectra for Seismic Design of Nuclear Power Plants, Regulatory Guide 1.60, Revision 2.* Washington DC: United States Regulatory Commission.

APPENDIX B RESERVE ENERGY METHOD BY WESLEY et al (1980)

B.1 Reserve Energy Method

This method initially proposed by Wesley et al (1980) remains in practice till date in the nuclear industry. Figure B-1 (a) and (b) demonstrate how the frequency of an equivalent SDOF oscillator is obtained by equating the area under its force-displacement curve to that of a RB in RM.

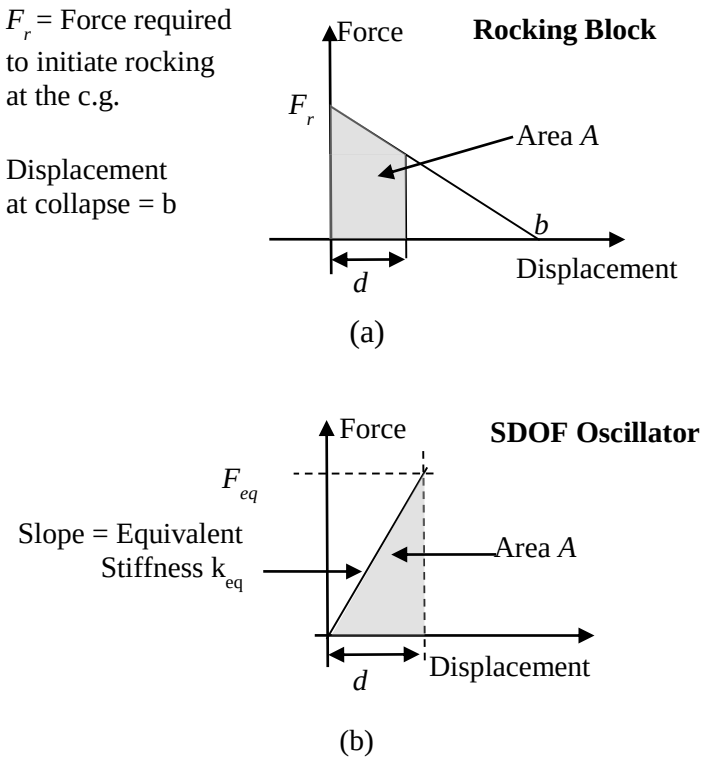

Figure B-1: Equivalent Stiffness of a SDOF oscillator by Wesley et al (1980) based on Reserve Energy Method by Blume (1960).

Critical evaluation of this method and its comparison with the method by Konstantinidis and Makris (2003), is given by Dar et al (2013). According to this method, variation in equivalent frequency of an equivalent oscillator is obtained by varying the displacement at the center of gravity of the rigid block which in turn

depends on the horizontal acceleration. Thus various values of displacement result in unique combination of frequency and acceleration given by the set of equations below:

Required acceleration to cause uplift,

$$a_r = g\tan(\alpha)$$

Equivalent acceleration of a SDOF oscillator,

$$a_{eq} = g\tan(\alpha)\left(2 - \frac{d}{b}\right)$$

Equivalent frequency at this acceleration

$$f_{eq} = \frac{1}{2\pi}\sqrt{\frac{a_{eq}}{d}}$$

Minimum acceleration and minimum frequency at $d = b$ are derived to be

$$a_{min} = g\ tan(\alpha) \quad \text{and} \quad f_{min} = \frac{1}{2\pi}\sqrt{\frac{g\tan(\alpha)}{b}}$$

Similarly maximum acceleration and maximum frequency at $d = 0$ will be

$$a_{max} = 2g\ tan(\alpha) \quad \text{and} \quad f_{max} = \infty$$

For small α, the above leads to,

$$a_{min} = \alpha g \quad \text{and} \quad a_{max} = 2\alpha g$$

$$f_{min} = \frac{1}{2\pi}\sqrt{\frac{\alpha g}{b}} = \frac{1}{2\pi}\sqrt{\frac{g}{R}} = \frac{p}{2\pi}\sqrt{\frac{4}{3}} \cong 1.15\left(\frac{p}{2\pi}\right) \quad \text{and} \quad f_{max} = \infty$$

Since equivalent frequency and acceleration both are functions of displacement, the acceleration-frequency combination curve is plotted along with the capacity curve by the ASCE 43-05 method in Figure B-2 for a rigid rectangular object example from Appendix B of ASCE 43-05. Intersection of this curve with an applicable response spectrum, such as NBK spectrum for example, is considered as a solution to the rocking problem. It is seen from Figure B-2 that the ASCE 43-05 method provides results similar to the reserve energy method. As shown in Figure

B-2, the capacity curves intersect with the 0.41g PGA response spectrum, giving solution to rocking problem (in terms of frequency which is 1.78 Hz for the curve of ASCE 43-05 method) and not with 0.30g PGA response spectrum indicating no rocking for the seismic excitation pertaining to the 0.30g PGA NBK spectrum.

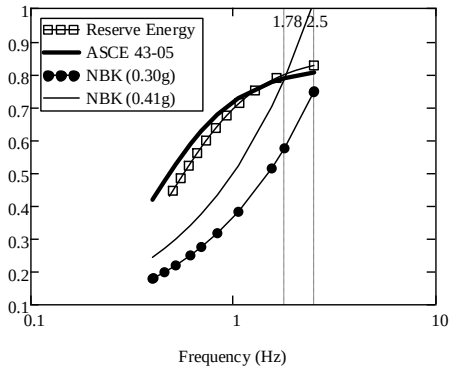

Figure B-2: Frequency–acceleration curves of equivalent SDOF by Reserve Energy and ASCE 43-05 methods along with two NBK response spectra.

B.2 References for Appendix B

American Society of Civil Engineers. (2005). *ASCE 43-05 – Seismic Design Criteria for Structures, Systems and Components in Nuclear Facilities.* Reston, Virginia, USA.

Blume, J. (1960). A reserve energy technique for the earthquake design and rating of structures in the inelastic range. *2nd World Conference on Earthquake Engineering.* Tokyo and Kyoto, Japan.

Dar, A., Konstantinidis, D., and El-Dakhakhni, W. (2013). Requirement of rocking spectrum in Canadian nuclear standards. *Transactions, 22nd International Structural Mechanics in Reactor Technology Conference (SMiRT22).* San Francisco, CA.

Wesley, D. A., Kennedy, R. P., and Richter, P. J. (1980). Analysis of the seismic collapse capacity of unreinforced masonry wall structures. *Proc. 7th World Conference on Earthquake Engineering.* Istanbul, Turkey.

APPENDIX C MATHCAD WORKSHEET ON ASCE 43-05 METHOD

NBK spectrum equation

First, insert the equation of NBK spectrum below in order to utilize it anywhere in the worksheet.

Define control frequencies in Hz.

$f1 := 0.1$

$f2 := 0.25$

$f3 := 2.5$

$f4 := 9$

$f5 := 33$

$A1(\beta) := 1$

for f5 and above

$B1(\beta) := (4.25 - 1.02 \cdot \ln(\beta))$

for f4 to f3

$C1(\beta) := [5.1 - 1.224 \ln((\beta))]$

for f3 to f2

$D(\beta) := 2.85 - 0.5 \cdot \ln(\beta)$

This is for displacement. Convert below to acceleration.

$$D1(\beta, f) := \frac{36in \cdot \left(2 \cdot \pi \cdot \frac{f}{s}\right)^2}{g} \cdot (2.85 - 0.5 \cdot \ln(\beta))$$

for f2 to f1

$$AC(\beta, PGA, f) := PGA \cdot \begin{cases} 1 & \text{if } f > f5 \\ \text{otherwise} & \\ \quad \begin{cases} \left(\frac{f}{f5}\right)^{1.772 \log\left(\frac{1}{B1(\beta)}\right)} & \text{if } f5 \geq f > f4 \\ \text{otherwise} & \\ \quad \begin{cases} \left[B1(\beta) \cdot \left(\frac{f}{f4}\right)^{\left(1.798 \cdot \log\left(\frac{B1(\beta)}{C1(\beta)}\right)\right)}\right] & \text{if } f4 \geq f > f3 \\ \text{otherwise} & \\ \quad \begin{cases} \left[C1(\beta) \cdot \left(\frac{f}{f3}\right)^{\left(\log\left(\frac{C1(\beta)}{D1(\beta, f2)}\right)\right)}\right] & \text{if } f3 \geq f > f2 \\ \left[D1(\beta, f2)\left(\frac{f}{f2}\right)^2\right] & \text{otherwise} \end{cases} \end{cases} \end{cases} \end{cases}$$

ASCE 43-05 method

All equations below are from ASCE 43-05 but converted to p, α format.

Step 1 - Calculate damping to establish the response spectrum.

$$\gamma(\alpha) := -2\ln\left(1 - \frac{3}{2}\cdot\sin(\alpha)^2\right)$$

Maximum α for rocking

At impact maximum energy loss will result in angular velocity to be zero. Equating coefficient of restitution to zero gives:

$$1 - \frac{3}{2}\cdot\sin(\alpha)^2 = 0$$

$$\frac{3}{2}\cdot\sin(\alpha)^2 = 1$$

$$\frac{3}{2}\cdot\sin(\alpha)^2 = \sin(\alpha)^2 + \cos(\alpha)^2$$

$$\tan(\alpha) = \sqrt{2}$$

$\alpha = 0.9553$

If α is more than the above value, there will be no rocking.

$F_H := 1$

$$\beta_e(\alpha) := \frac{\gamma(\alpha)}{\left(4\cdot\pi^2 + \gamma(\alpha)^2\right)^{\frac{1}{2}}}$$

ASCE 43-05 in the table on page 37 provides equivalent damping values β for various values of C_R which is basically the co-efficient of restitution. In order to compare the results, calculate angle alpha from the given C_R and then reverse calculate C_R.

Coeff of restitution CR is

$$e(\alpha) := 1 - \frac{3}{2}\cdot\sin(\alpha)^2$$

From the above calculate the value of alpha for the CR given in the table in ASCE 43-05. Try four values.

$$\alpha_a(E) := \operatorname{asin}\left[\sqrt{(1 - E)\cdot\frac{2}{3}}\right]$$

$\alpha_a(0.5) = 0.615$

$\alpha_a(0.6) = 0.543$

$\alpha_a(0.7) = 0.464$

$\alpha_a(0.8) = 0.374$

Corresponding C_R values are given below:

$e(0.615) = 0.501$

$e(0.543) = 0.6$

$e(0.464) = 0.7$

$e(0.374) = 0.8$

Corresponding damping is obtained as:

$\beta_e(0.615) = 0.215$

$\beta_e(0.543) = 0.161$

$\beta_e(0.464) = 0.113$

$\beta_e(0.374) = 0.071$

Step 2 - Calculate minimum of maximum angle

ASCE 43-05 defines the minimum of max angle corresponding to the frequency of 2.5Hz in Eq (B-36).

Maximum frequency with max acceleration

$f_{em} := 2.5Hz$

$$\theta_{om} = \frac{2 \cdot a}{\left[\frac{C_I \cdot h}{g} \cdot \left(2 \cdot \pi \cdot f_{em}\right)^2\right] + 1}$$

$$\theta_{om} = \frac{2 \cdot b}{\left[\frac{\frac{I_B}{M \cdot h^2}}{g} \cdot \left(2 \cdot \pi \cdot f_{em}\right)^2\right] + h}$$

$$\theta_{om} = \frac{2 \cdot (R \cdot \sin(\alpha))}{\left[\frac{4 \cdot R^2}{3 \cdot g} \cdot \left(2 \cdot \pi \cdot f_{em}\right)^2\right] + h}$$

$$\theta_{om} = \frac{2 \cdot (\sin(\alpha))}{\left[\frac{4 \cdot R}{3 \cdot g} \cdot \left(2 \cdot \pi \cdot f_{em}\right)^2\right] + \cos(\alpha)}$$

$$\theta_{om}(p,\alpha,f_{em}) := \frac{2\cdot(\sin(\alpha))}{\left[\left(2\cdot\pi\cdot\frac{f_{em}}{p}\right)^2\right] + \cos(\alpha)}$$

Step 3 - Calculate capacity acceleration by ASCE method for a given maximum angle.

Define a vector of angle, starting at minimum angle and increasing to maximum = α. The RB overturns at α

$$inc := 0.001$$

$$\theta_o(p,\alpha,f_{em}) := \left|\begin{array}{l} i \leftarrow 0 \\ \theta_i \leftarrow \theta_{om}(p,\alpha,f_{em}) \\ \text{while } \theta_m \le \alpha \\ \quad \left|\begin{array}{l} \theta_{i+1} \leftarrow \theta_i + inc \\ \theta_m \leftarrow \theta_{i+1} \\ i \leftarrow i + 1 \end{array}\right. \\ \theta \end{array}\right.$$

Step 4 - Calculate capacity acceleration by ASCE method for a given maximum angle.

Vary this angle in order to get freq-acceleration combination.

Define

$$f1 = \cos(\theta_o) + \tan(\alpha)\cdot\sin(\theta_o)$$

As a function of θ_o, α:

$$F1A(\theta_o,\alpha,f_{em}) := \cos(\theta_o) + \tan(\alpha)\cdot\sin(\theta_o)$$

As a function of p, α:

$$f_{1a}(p,\alpha,f_{em}) := \cos(\theta_o(p,\alpha,f_{em})) + \tan(\alpha)\cdot\sin(\theta_o(p,\alpha,f_{em}))$$

$$F_{V1}(\alpha) := \left[1 + \left(\frac{\tan(\alpha)}{F_H} \cdot \frac{2}{3}\right)^2\right]^{\frac{1}{2}}$$

$$F_{V1}(0.405) = 1.04$$

OK for the given example in ASCE 43-05.

As a function of θ o, α:

$$SAH1_{CAP}(\theta_o, \alpha, f_{em}) := \frac{2 \cdot g \cdot \left(F1A(\theta_o, \alpha, f_{em}) - 1\right)}{F_H \cdot F_{V1}(\alpha) \cdot \theta_o}$$

Maximum Capacity:

Maximum capacity with F_V =1 and F_H = 1

$$\lim_{\theta_o \to 0} \frac{2 \cdot g \cdot \left(F1A(\theta_o, \alpha, f_{em}) - 1\right)}{\theta_o} \text{ simplify } \to 2 \cdot g \cdot \tan(\alpha)$$

$$MSAH2_{CAP}(\alpha) := 2 \cdot g \cdot \tan(\alpha)$$

In order to calculate maximum capacity find the limit as θ o approaches zero.

Since Fv(α) and F_H are constants for a given α , maximum capacity including Fv and F_H is given as:

$$MSAH_{CAP}(\alpha) := \frac{2 \cdot g \cdot \tan(\alpha)}{F_H \cdot F_{V1}(\alpha)}$$

As a function of p, α:

$$SAH_{CAP}(p, \alpha, f_{em}) := \frac{2 \cdot g \cdot \left(f_{1a}(p, \alpha, f_{em}) - 1\right)}{F_H \cdot F_{V1}(\alpha) \cdot \theta_o(p, \alpha, f_{em})}$$

Step 5 - Calculate corresponding frequency

For each p, the frequency and acceleration capacities vary with θ_o.

As a function of θo, α:

$$\omega 1_{ea}(\theta_o, \alpha, p, f_{em}) := \left[\frac{2 \cdot p^2 \cdot \cos(\alpha) \cdot (F1A(\theta_o, \alpha, f_{em}) - 1)}{\theta_o^2} \right]^{\frac{1}{2}}$$

$$f1_{ea}(\theta_o, \alpha, p, f_{em}) := \frac{\omega 1_{ea}(\theta_o, \alpha, p, f_{em})}{2 \cdot \pi}$$

As a function of p, α:

$$\omega_{ea}(p, \alpha, f_{em}) := \left[\frac{2 \cdot p^2 \cdot \cos(\alpha) \cdot (f_{1a}(p, \alpha, f_{em}) - 1)}{\theta_o(p, \alpha, f_{em})^2} \right]^{\frac{1}{2}}$$

$$f_{ea}(p, \alpha, f_{em}) := \frac{\omega_{ea}(p, \alpha, f_{em})}{2 \cdot \pi}$$

For the given example with p=2.517/s and; p=10/s with α =0.405, the following values are obtained.

The length of the vector depends on increment inc in θ function above.

$$f_{ea}\left(\frac{2.517}{s}, 0.405, f_{em}\right) =$$

	0
0	2.499918
1	2.437521
2	2.37944
3	2.325196
4	2.274381
5	2.226647
6	2.181692
7	2.139254
8	2.099105
9	2.061044
10	2.024896
11	1.990503
12	1.957728
13	1.926444
14	...

$\frac{1}{s}$

$$f_{ea}\left(\frac{10}{s}, 0.405, f_{em}\right) =$$

	0
0	2.487
1	2.479
2	2.472
3	2.464
4	2.457
5	2.45
6	2.443
7	2.435
8	2.428
9	2.421
10	2.414
11	2.407
12	2.4
13	2.393
14	...

$\frac{1}{s}$

Note –The first frequency value in both frequency vectors is 2.5Hz since that corresponds to the peak spectral acceleration of the NBK spectrum. θ varies from θ_{min} to α corresponding to the first frequency (2.5Hz) and last frequency respectively. For NBK spectrum, it is to be noted that the first frequency will always be 2.5Hz irrespective of p since this frequency corresponds to θ_{min}

For the example in ASCE 43-05, the values of θ come out to be the following:

$$\theta_o\left(\frac{2.517}{s}, 0.405, f_{em}\right) =$$

	0
0	0.01976714
1	0.02076714
2	0.02176714
3	0.02276714
4	0.02376714
5	0.02476714
6	0.02576714
7	...

However, define the maximum angle of rotation exactly as in ASCE43-05 and obtain the corresponding frequencies and capacity accelerations:

$$\theta 1_o := \begin{pmatrix} 0.0198 \\ 0.02 \\ 0.038 \\ 0.05 \\ 0.1 \\ 0.15 \\ 0.2 \\ 0.25 \\ 0.3 \\ 0.35 \\ 0.4 \\ 0.4049 \end{pmatrix}$$

$$f1_{ea}\left(\theta 1_o, 0.4049, \frac{2.517}{s}, f_{em}\right) = \begin{pmatrix} 2.497 \\ 2.485 \\ 1.783 \\ 1.543 \\ 1.056 \\ 0.832 \\ 0.693 \\ 0.595 \\ 0.518 \\ 0.456 \\ 0.403 \\ 0.398 \end{pmatrix} \frac{1}{s}$$

This frequency table is same as in the ASCE 43-05 example.

Define frequencies as independent vector same as in ASCE 43-05 example.

$$Fr := \begin{pmatrix} 2.497 \\ 2.485 \\ 1.783 \\ 1.543 \\ 1.056 \\ 0.832 \\ 0.693 \\ 0.595 \\ 0.518 \\ 0.456 \\ 0.403 \\ 0.398 \end{pmatrix}$$

$SAH1_{CAP}\left(\theta 1_o, 0.4049, f_{em}\right) =$

	0
0	0.805
1	0.805
2	0.787
3	0.776
4	0.727
5	0.677
6	0.627
7	0.576
8	0.526
9	0.474
10	0.423
11	0.418

$\cdot g$

The above values match with Table B-3 of ASCE 43-05.

Calculate PGA cap table for frequencies in ASCE example. Matches with the table in ASCE 43-05.

$$\overrightarrow{AC1 := AC(8.4, 1, Fr)}$$

$$PGAR1 := round\left(\frac{\overrightarrow{SAH1_{CAP}\left(\theta 1_o, 0.4049, f_{em}\right)}}{AC1 \cdot g}, 2\right)$$

$$PGAR := \frac{\overrightarrow{SAH1_{CAP}\left(\theta 1_o, 0.4049, f_{em}\right)}}{AC1 \cdot g} =$$

	0
0	0.323
1	0.324
2	0.411
3	0.454
4	0.572
5	0.643
6	0.687
7	0.711
8	0.723
9	0.721
10	0.708
11	0.706

Step 6 - Calculate response spectrum acceleration for the frequency in step 5.

$AC(\beta, PGA, f)$

Step 7 - Compare the above acceleration with the capacity acceleration.

Check if

$$SAH_{CAP}\left(\theta_o, \alpha\right) = ACC(\beta, f, PGA)$$

If true, then θ o is the solution. If not then increase θ o and repeat the step.

ASCE example

$H := 84in$

$B := 36in$

$h := \frac{H}{2}$

$b := \frac{B}{2}$

$PGA1(\alpha 1) := \frac{\tan(\alpha 1)}{F_H \cdot F_{V1}(\alpha 1)}$

$R := \sqrt{b^2 + h^2}$

$R = 45.695\,in$

$a := \frac{b}{h}$

$a = 0.429$

$p := \sqrt{\frac{3 \cdot g}{4 \cdot R}}$

$p = 2.517 \frac{1}{s}$

$\alpha := \operatorname{atan}(a)$

$\alpha = 0.405$

Superimpose acceleration frequency curve from reserve energy principle

Define displacement between the freq ranges of 0.4 to 2.5Hz

$d1 := 1.3in, 1.4in .. b$

$$f_{eq}(b, h, d) := \frac{1}{2\pi} \cdot \sqrt{\frac{b \cdot g \cdot \left(2 - \frac{d}{b}\right)}{h \cdot d}}$$

$$a_{eq}(b, h, d) := \begin{cases} \left[\frac{b}{h} \cdot g \cdot \left(2 - \frac{d}{b}\right)\right] & \text{if } 0 \le d \le b \\ 0 & \text{otherwise} \end{cases}$$

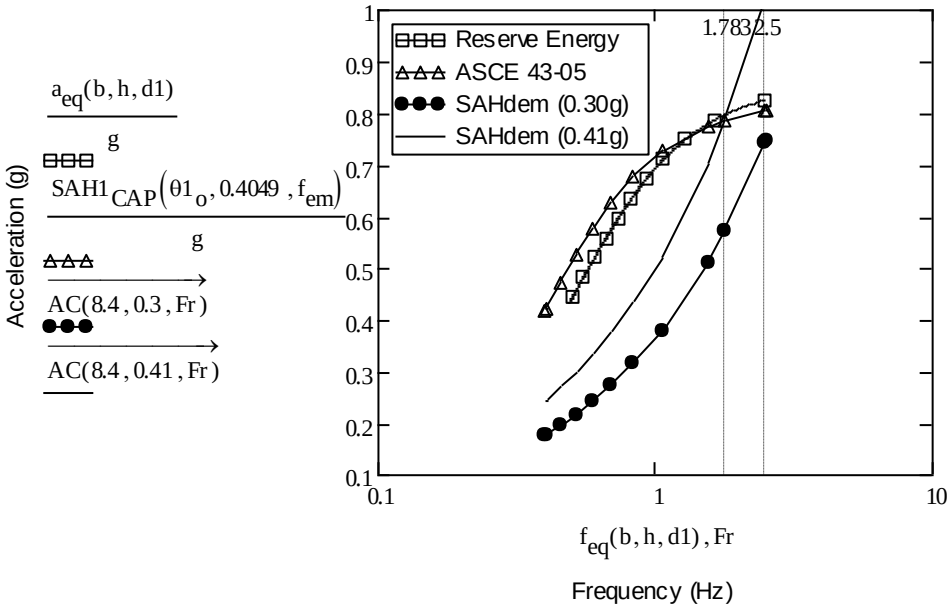

ASCE 43-05 example: Comparison of capacity with two demand spectra at PGAs of

0.70g and 0.72g

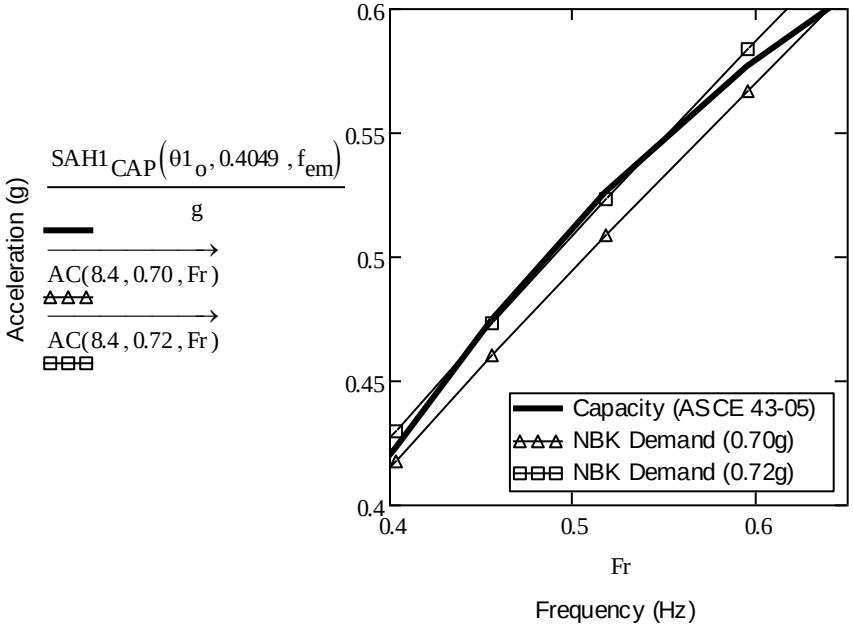

Contradiction in ASCE 43-05 method: As seen in the above diagram, the capacity curve intersects with the higher PGA (0.72g) demand curve at higher frequency

(higher rotation) than the lower PGA (0.70g) curve, The higher PGA leads to lower rotation which should not be the case in this method.

In order to establish the above fact further the same level of accuracy is achieved as for the example in ASCE 43-05 by using the same formula for spectral acceleration as in Eq B-38 in Appendix B of ASCE 43-05. .

$\theta 2_o := 0.001, 0.002 .. 0.404$

$f_1(\theta_o) := \cos(\theta_o) + \tan(\alpha)\cdot\sin(\theta_o)$

$SAH2_{CAP}(\theta_o) := \dfrac{2\cdot g\cdot(f_1(\theta_o) - 1)}{F_H\cdot F_{V1}(\alpha)\cdot\theta_o}$

$SAH_{DEM}(\theta_o, PGA) := 2.49\left(\dfrac{f1_{ea}(\theta_o, \alpha, p, f_{em})}{2.5Hz}\right)^{0.78}\cdot PGA$

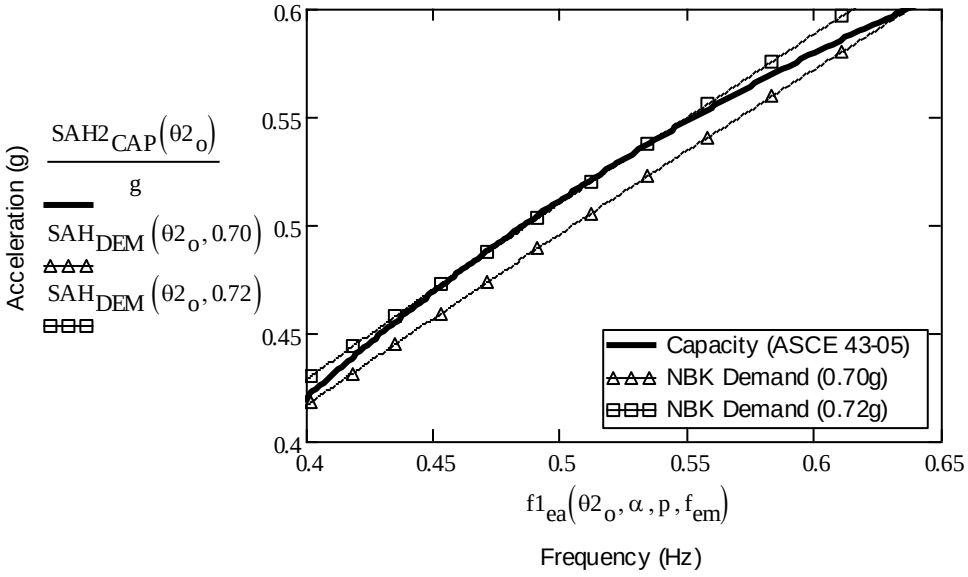

Comparison of capacity curves of three blocks with different values of parameter p:

For full capacity curve, consider maximum frequency up to 100 Hz. The demand spectrum is NBK spectrum at 0.41g PGA.

Maximum capacity of all curves = 2tan(α) for Fv=1.

$f_{em} = 100\frac{1}{s}$

Construct a diagram below by multiplying the capacity curves by Fv(α). They all merge to the asymptote 2tan(α).

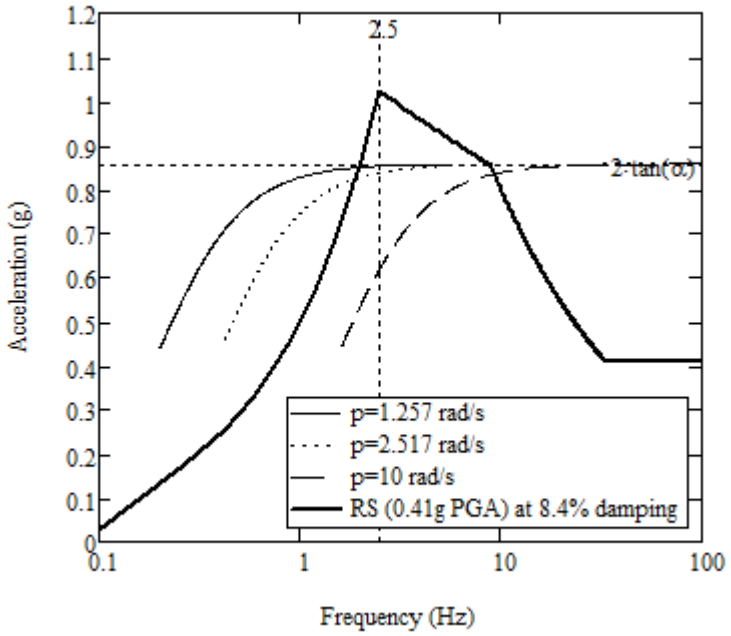

Capacities with Fv = 1.04

Considering capacity curves including Fv = 1.04 and comparing results

with NBK spectrum at PGAs of 0.41g and 0.323g gives the following diagram. The capacity curve for the example considered intersects with the peak of 0.323 g curve at 2.5Hz.

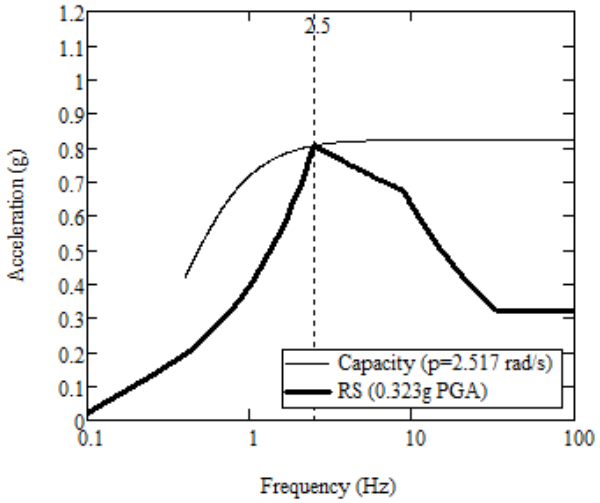

The curve with 0.323g PGA provides a solution of rotation angle for the example under consideration, however, there will not be any rocking initiated at this acceleration even after considering the vertical acceleration. The minimum capacity of the rocking block in example is 0.418g at maximum rotation (at overturning) where it should have practically zero capacity.

$\theta 1_o =$

	0
0	0.0198
1	0.02
2	0.038
3	0.05
4	0.1
5	0.15
6	0.2
7	0.25
8	0.3
9	0.35
10	0.4
11	0.4049

$SAH1_{CAP}\left(\theta 1_o, 0.4049, f_{em}\right) =$

	0
0	0.805
1	0.805
2	0.787
3	0.776
4	0.727
5	0.677
6	0.627
7	0.576
8	0.526
9	0.474
10	0.423
11	0.418

$\cdot g$

$$f1_{ea}\left(\theta 1_o, 0.4049, \frac{2.517}{s}, f_{em}\right) = \begin{array}{|c|c|}\hline & 0 \\ \hline 0 & 2.497 \\ \hline 1 & 2.485 \\ \hline 2 & 1.783 \\ \hline 3 & 1.543 \\ \hline 4 & 1.056 \\ \hline 5 & 0.832 \\ \hline 6 & 0.693 \\ \hline 7 & 0.595 \\ \hline 8 & 0.518 \\ \hline 9 & 0.456 \\ \hline 10 & 0.403 \\ \hline 11 & 0.398 \\ \hline \end{array} \frac{1}{s}$$

SIMPLIFICATION OF ASCE 43-05 METHOD

The long and complicated method given in the ASCE 43-05 can be summarized into two simple equations considering small angle approximations up to $\alpha = 0.4$:

$$SAH_{CAP} = \frac{\alpha g}{F_H F_V}\left(2 - \frac{\theta_o}{\alpha}\right)$$

$$f_e = \frac{\omega_e}{2\pi} = \frac{p}{2\pi}\left[\frac{2}{\frac{\theta_o}{\alpha}} - 1\right]^{\frac{1}{2}}$$

For large angles, a RB is more likely to respond by sliding rather than rocking. F_H, and F_V are generally considered as 1. If at all someone is interested in following the ASCE 43-05 method, considering the above expressions leads to quick and conservative results by varying θ_o/α from very small value (0.001 for example) to 1, rather than following the complicated expressions given in ASCE 43-05 and varying θ_o from its minimum to maximum values. The capacity curve can be plotted with accelerations computed at the corresponding frequencies for various values of θ_o/α . Intersection of such capacity curve with the applicable response spectrum at the highest frequency on the left of the peak would be the solution to the rocking problem. However, this would not be the right solution because the ASCE 43-05 method is based on assumptions not applicable to rocking motion. An example is

given below to demonstrate the closeness of approximate equations with the ones given in ASCE 43-05. .

SMALL ANGLE APPROXMATION CAPACITY COMPARISON

$\theta_r := 0.0001, 0.0002 .. 1$

$f2_e(\theta_r, p) := \frac{p}{2\cdot\pi}\cdot\sqrt{\frac{2}{\theta_r} - 1}$

where

$\theta_r = \frac{\theta_o}{\alpha}$

$SAH2_{CAP}(\alpha, \theta_r) := \alpha\cdot g\cdot(2 - \theta_r)$

Two examples are given below with two values of α and p.

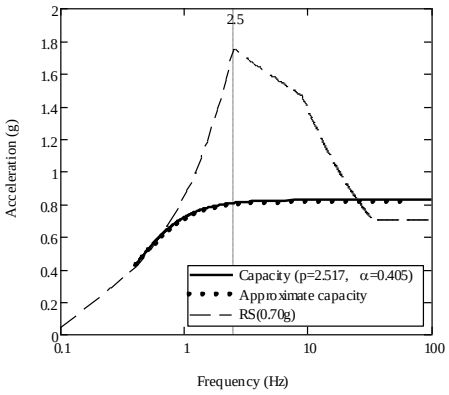

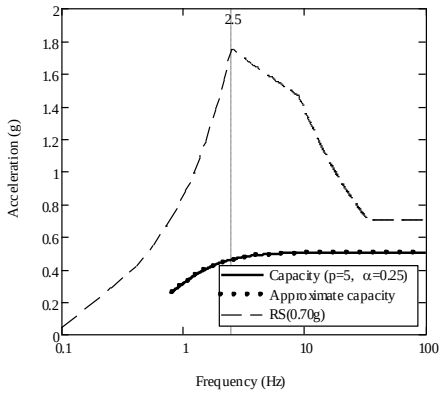

APPENDIX D FLOW CHART FOR ROCKING SPECTRA FROM NBK SPECTRA BY ASCE 43-05 METHOD

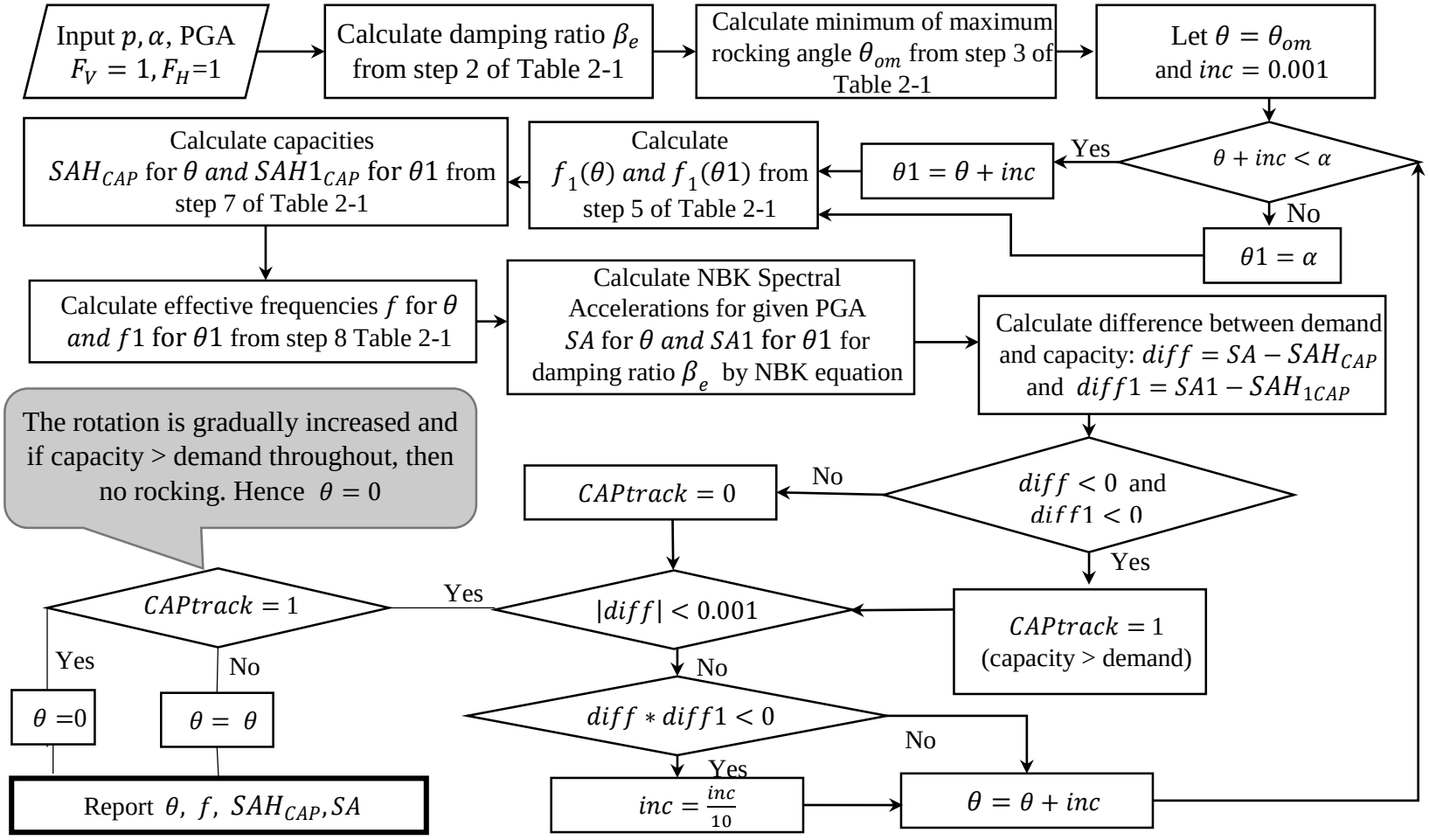

APPENDIX E FLOW CHART FOR ROCKING SPECTRA FROM RESPONSE SPECTRA (ASCE 43-05 METHOD)

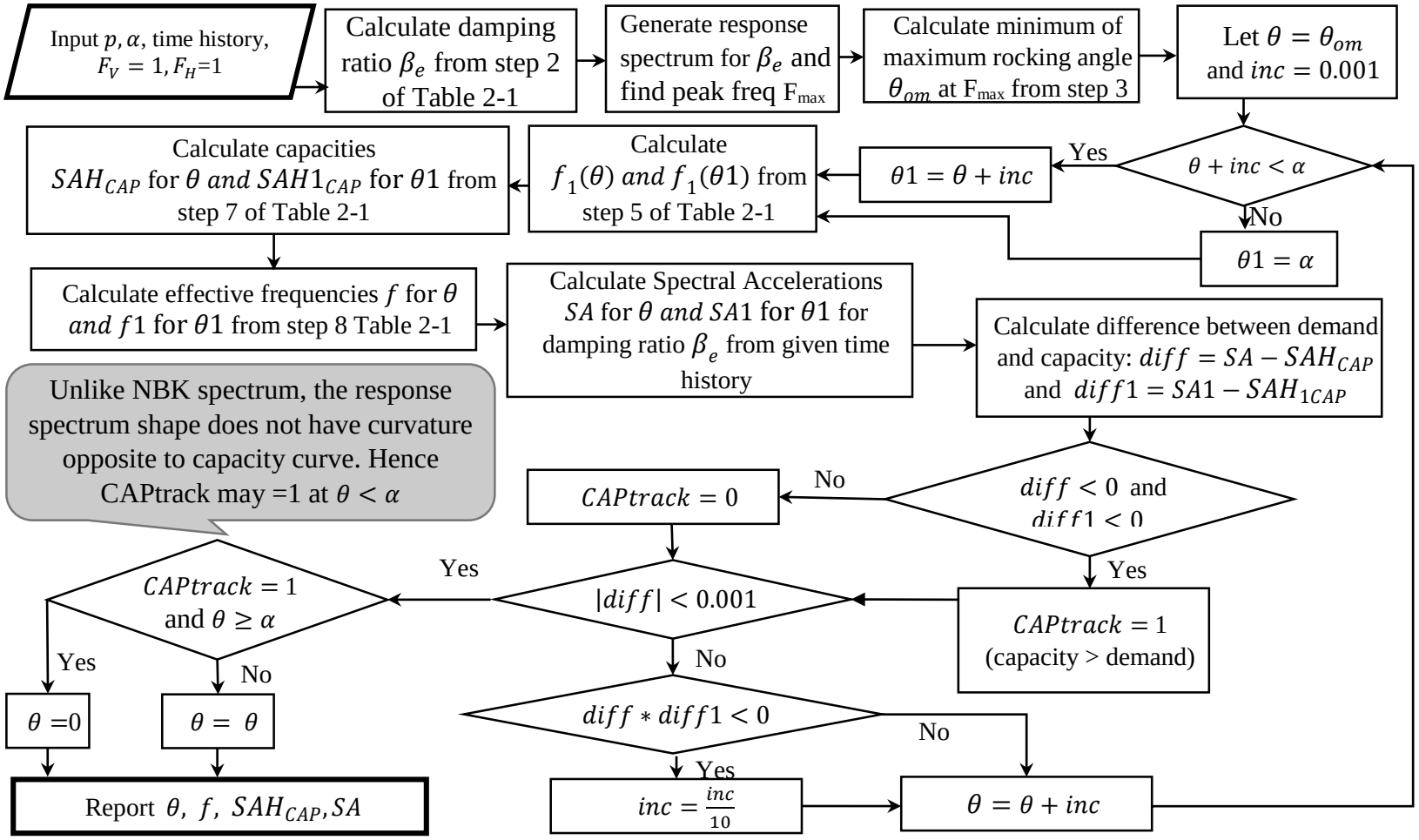

APPENDIX F FLOW CHART FOR ROCKING SPECTRA BY NON LINEAR TIME HISTORY ANALYSIS